University of Nevada, Reno

Regional Water Budget Accounting and Uncertainty Analysis Using a Deuterium-Calibrated Discrete State Compartment Model: White Pine County, Nevada, and Adjacent Areas in Nevada and Utah

A thesis submitted in partial fulfillment of the
requirements for the degree of Master of Science in
Hydrology

by

Kevin William Lundmark

Dr. Greg Pohll / Thesis Advisor

May, 2007

© by Kevin William Lundmark 2007
All Rights Reserved

University of Nevada, Reno
Statewide · Worldwide

THE GRADUATE SCHOOL

We recommend that the thesis
prepared under our supervision by

KEVIN WILLIAM LUNDMARK

entitled

Regional Water Budget Accounting and Uncertainty Analysis Using a Deuterium-Calibrated Discrete State Compartment Model: White Pine County, Nevada, and Adjacent Areas in Nevada and Utah

be accepted in partial fulfillment of the
requirements for the degree of

MASTER OF SCIENCE

Gregory Pohll, Ph.D., Advisor

James Thomas, Ph.D., Committee Member

Ilya Zaliapin, Ph.D., Graduate School Representative

Marsha H. Read, Ph.D., Associate Dean, Graduate School

May, 2007

ABSTRACT

Groundwater budgets for a 12-basin carbonate aquifer study area were evaluated using a steady-state groundwater mass-balance accounting model. The groundwater budgets included components of recharge, evapotranspiration (ET) discharge, and interbasin flow and incorporated previous and recent estimates for recharge and groundwater ET discharge. Deuterium was used as a conservative tracer in the discrete-state compartment (DSC) model and the model optimization algorithm was varied to include either deuterium values or a combination of deuterium values and target groundwater ET rates. Uncertainty of the accounting model predictions was evaluated deterministically by varying model inputs and objective functions and stochastically by performing a series of Monte Carlo simulations using distributions for recharge inputs and target groundwater ET rates. Modeling results suggest that incorporation of target discharge values in the model's objective function is necessary in order to yield basin discharge rates which are realistic for the assumed hydrogeologic constraints and groundwater losses through ET for some basins. Regional groundwater flow systems discharging at varying rates from White River Valley and Snake Valley were predicted by the model for all simulations.

Table of Contents

List of Figures ..... **iv**
List of Tables ..... **vi**
1. INTRODUCTION **1**
2. PURPOSE AND SCOPE **4**
3. BACKGROUND **5**
3.1 Study Area 5
3.1.1 Climate 6
3.1.2 Geologic Setting 6
3.1.3 Hydrostratigraphy 7
3.2 Groundwater Flow Systems 8
3.3 Water Budgets 11
3.3.1 Water Budget Components 12
3.3.2 Previous Water Budget Investigations 13
3.3.3 BARCAS Water Budget Estimates 16
3.4 Groundwater Accounting Models 18
3.4.1 Discrete State Compartment (DSC) Model Background 19
3.4.2 DSC Model Optimization 21
3.5 Deuterium as a Groundwater Tracer 23
4. METHODOLOGY **26**
4.1 Approach 26
4.2 Assumptions 28
4.3 Deuterium Database 29
4.4 Model Inputs 32
4.4.1 Model Cells 32
4.4.2 Cell Connectivity 32
4.4.3 Head Rankings 33
4.4.4 Recharge Rates 34
4.4.5 Recharge δD Values 34
4.5 Calibration Parameters 36
4.5.1 Observed δD Values 36
4.5.2 Observation Weights 36
4.5.3 Groundwater ET Discharge Weights 39
4.5.4 Objective Functions 39
4.6 Uncertainty Analysis 43
4.6.1 Deterministic-Sensitivity Uncertainty Analyses 43
4.6.2 Monte Carlo Uncertainty Analyses 46
5. MODEL RESULTS **57**
5.1 BARCAS DSC Base Model 57
5.1.1 Optimization Scenario C: Concentration 59
5.1.2 Optimization Scenario O: Concentration + Outflow 60
5.1.3 Optimization Scenario O*: Concentration + Modified Outflow 61
5.2 Deterministic-Sensitivity Uncertainty Analyses 62

5.2.1 Recharge δD Estimation Method 63
5.2.2 Optimization Criteria and Objective Functions 68
5.3 Monte Carlo Uncertainty Analyses 72
5.3.1 Water Budget Component Frequency Distributions 76
5.3.2 Stability of Statistics 77
5.4 Uniqueness of Model Solutions 79
6. DISCUSSION 81
7. CONCLUSIONS AND RECOMMENDATIONS 87
8. REFERENCES 91

APPENDICES

A. Deuterium Data for Recharge Samples

B. Deuterium data for Regional / Deep-Intermediate Groundwater Samples

C. Comparison of Optimization Methods for a Discrete-State Compartment (DSC) Groundwater Accounting Model: Uniform Random Search (URS), Shuffled-Complex Evolution (SCE), and Multi-Objective Complex Evolution (MOCOM) Algorithms

List of Figures

1. Study Area
2. Regional Groundwater Flow Systems Identified in the Great Basin Regional Aquifer System Analysis (RASA) Report.
3. Conceptual Model Showing Local, Deep-Intermediate, and Regional Groundwater Flow Systems and Water Budget Components for Accounting Model Cells
4. BARCAS Recharge and Groundwater Evapotranspiration (ET) Discharge Estimates for the Study Area
5. Discrete-State Compartment (DSC) Model Components
6. Recharge Deuterium Sample Locations, Inverse Distance Weighted (IDW) Interpolated Recharge Deuterium Values, and Recharge-Weighted Average Recharge Deuterium Values
7. Regional / Deep-Intermediate Groundwater Deuterium Sample Locations and DSC Model Calibration (Observed) Deuterium Values
8. DSC Model Cell Connectivity and Head Ranks
9. Plot Showing Recharge δD values Versus Latitude
10. Ranges of Recharge Estimates Used for Developing Recharge Distributions for Monte Carlo Uncertainty Analysis Simulations
11. PRISM Map Showing Precipitation Intervals Used for Bootstrap Brute-Force Recharge Method (BBRM) Recharge Calculations
12. Ranges of Groundwater Evapotranspiration (GWET) Estimates Used for Developing GWET Distributions for Monte Carlo Uncertainty Analysis Simulations
13. Summary of Base BARCAS DSC Model Interbasin Groundwater Flow Rates
14. Water Budget Summary for Monte Carlo Uncertainty Analysis Simulations MC-1 through MC-5
15. Water Budget Component Distributions for Spring Valley, Monte Carlo Simulation MC-5

16. Stability of Statistics for Interbasin Inflow to Spring Valley, Monte Carlo Simulation MC-5
17. of Statistics for Interbasin Outflow from Spring Valley, Monte Carlo Simulation MC-5
18. Stability of Statistics for Outflow from the Model Domain from Spring Valley, Monte Carlo Simulation MC-5
19. of Interbasin Groundwater Inflow Rates from Previous Studies and Monte Carlo Simulation MC-2
20. Summary of Interbasin Groundwater Outflow Rates from Previous Studies and Monte Carlo Simulation MC-2

List of Tables

1. Previous Estimates for Groundwater Recharge
2. Previous Estimates for Groundwater Discharge as Evapotranspiration
3. Previous Estimates for Interbasin Groundwater Flow
4. Summary of Groundwater Recharge and Evapotranspiration (ET) Discharge Rate Estimates for the BARCAS Study
5. DSC Model Cell Input Parameters and Calibration Criteria
6. Principle Characteristics for Deterministic-Sensitivity Analyses
7. Summary of DSC Model Cell Recharge δD Values Calculated Using Inverse Distance Weighting (IDW) and Latitude Regression Estimation Methods
8. Principle Characteristics of Monte Carlo Uncertainty Analysis Simulations
9. Summary of δD Values Estimated for Model Cells
10. Model-Predicted δD Values and Outflow Rates and Calculated Objective Function Values for the Base BARCAS DSC Model
11. Basin Water Budget Summary for the Base BARCAS DSC Model
12. Summary of Deterministic-Sensitivity Uncertainty Analysis Simulation Results
13. Summary of Monte Carlo Uncertainty Analysis Results for Simulations MC-1 through MC-7
14. Summary of Monte Carlo Uncertainty Analysis Results for Simulation MC-8

1. INTRODUCTION

As the population of Nevada continues to increase, additional water resources will be required to meet municipal and industrial needs. Groundwater development is a probable source for providing additional water resources. On a basin basis, the amount of groundwater available for appropriation to beneficial uses is based on the water budget for the basin, where the water budget describes the inputs and outputs of water to the basin. Groundwater available for appropriation is determined by the amount of water recharging the aquifer and the amount of groundwater discharged (or "lost") to non-beneficial uses.

Remarkable growth has occurred in the greater Las Vegas area of southern Nevada. As part of its long-term water development plan, the Southern Nevada Water Authority (SNWA) has proposed the Clark, Lincoln, and White Pine Counties Groundwater Development Project which includes the withdrawal of groundwater from basins in White Pine and Lincoln Counties in eastern Nevada for conveyance to Las Vegas via pipeline (SNWA, 2006).

To better understand and evaluate regional ground-water flow systems in Nevada and to initiate long-term studies of potential impacts from future ground-water pumping, Federal legislation was enacted in December 2004 (Section 131 of the Lincoln County Conservation, Recreation, and Development Act of 2004; short title, Lincoln County Land Act). The Lincoln County Land Act states:

> "The Secretary, acting through the United States Geological Survey, the Desert Research Institute, and a designee from the State of Utah shall conduct a study to investigate ground-water quantity, quality, and flow characteristics in the deep carbonate and alluvial aquifers of White Pine County, Nevada, and any groundwater basins that are located in White Pine County, Nevada, or Lincoln County, Nevada, and adjacent areas in Utah."

The Act directs the Secretary of Interior, through the U.S. Geological Survey (USGS), the Desert Research Institute (DRI), and a designee from the State of Utah, to conduct a water resources study of the alluvial and carbonate aquifers in White Pine County Nevada and surrounding areas in Nevada and Utah (USGS, 2005).

The Basin and Range Carbonate Aquifer System (BARCAS) study was initiated by the USGS, in cooperation with the DRI and the Utah State Engineer's Office in response to the Lincoln County Land Act. The BARCAS study includes six separate but coordinated tasks which were identified with the overarching goal of quantifying basin groundwater budgets and developing an improved understanding of regional groundwater flow. Hydrographic areas in White Pine County are the primary focus of the study, covering approximately 90 percent of White Pine County (Figure 1). The study area includes Spring Valley, Snake Valley and Cave Valley where groundwater development is proposed by SNWA. Results from the various components of the BARCAS study are summarized and synthesized in a USGS Special Investigation Report (SIR) being prepared for congress (Welch and Bright, in review).

Task 6 of the BARCAS study includes the estimation of water budgets and the development of a conceptual description of groundwater flow in the study area. To help evaluate basin and regional water budgets, a steady-state mass-balance groundwater accounting model was developed and applied to the BARCAS study area. The groundwater accounting model incorporates recent, independent estimates for groundwater recharge from precipitation and groundwater discharge as evapotranspiration which were developed for the BARCAS study and provides estimates for interbasin groundwater flowrates based on the fluxes of a conservative tracer. The groundwater accounting model developed for the BARCAS study, described in Lundmark et al. (2007), included a set of deterministic model results and an initial limited Monte Carlo uncertainty analysis which evaluated the uncertainty in model predictions resulting from variability in assumed recharge characteristics for the study area.

The work presented in this thesis builds on the groundwater accounting model and uncertainty analysis completed for the BARCAS study by expanding the uncertainty analyses to include additional water budget components and distributions, estimation methods for model inputs, and objective functions for model optimization. Consequently, results from the BARCAS groundwater accounting model are presented along with additional modeling simulations, with the BARCAS groundwater accounting model functioning as a basis for comparison.

2. PURPOSE AND SCOPE

The purpose of this research project is to apply a mass-balance groundwater accounting model to evaluate basin and regional water budgets for the BARCAS study area and estimate uncertainty associated with these water budgets. The groundwater accounting model also provides information regarding potential rates of interbasin groundwater flow between project basins and estimates for rates of groundwater discharge as interbasin flow to outside of the study area based on fluxes of a conservative tracer. Simulated water budget uncertainties are evaluated by varying model inputs and optimization criteria and via Monte Carlo uncertainty analyses. Results from this research project provide additional information on potential regional groundwater flow characteristics for the BARCAS study area, as well as presenting basin water budgets in a probabilistic context where uncertainties are incorporated into estimated rates.

Building on the work completed for the BARCAS study, this research project expands the BARCAS uncertainty analysis to incorporate more water budget components into the uncertainty analysis and evaluate wider distributions for recharge characteristics. The modeling presented within this thesis includes the BARCAS model with supplemental modeling simulations which were developed to elaborate the water budget uncertainty analysis.

3. BACKGROUND

3.1 Study Area

The BARCAS study area is located in White Pine County, Nevada and adjacent areas in Elko, Eureka, Lincoln and Nye Counties in Nevada and Beaver, Iron, Juab, Millard, and Tooele Counties in Utah (Figure 1). The BARCAS study area covers approximately 13,500 square miles (8,550,000 acres) and extends from about 40°23′ to 37°57′ north-south and about 113°25′ to 116°17′ east-west (North American Datum [NAD] 1983). The BARCAS study area comprises twelve distinct hydrographic areas (basins): central and northern portions of Little Smoky Valley, Newark Valley, Long Valley, southern portion of Butte Valley, Steptoe Valley, Spring Valley, Snake Valley, Jakes Valley, White River Valley, Cave valley, and Lake Valley.

The study area is typical of the Basin and Range, where generally north-trending mountain ranges are separated by broad alluvial desert basins (Harrill and Prudic 1998). Mountain ranges in the study area are commonly greater than 10,000 feet above mean sea level (amsl). Valley floor elevations are generally 6,000 feet or less. Major mountain ranges include White Pine Range, Schell Creek Range, Egan Range and the Snake Range. The high point is Mount Wheeler, elevation 13,063 feet in Great Basin National Park. The lowest area is located near Fish Springs in northeastern Snake Valley, Utah where elevation is approximately 4,200 feet.

3.1.1 Climate

The study area is a very dry environment where the atmospheric moisture contents are among the lowest in the United States (NRCS). Average temperatures are about 60 to 70 degrees Farenheit in the summer and about 32 degrees Fahrenheit in the winter. The average annual precipitation is highly variable and dependent on elevation. The lower valleys generally receive less than 10 inches of precipitation annually. Mountainous areas receive much more precipitation due to the orographic effect. Annual precipitation at high elevations in the study area may exceed 30 inches. Snowfall is also variable within the study area; although in general about 20 to 40 inches of annual snowfall occurs in the area. Snowfall amounts at higher elevation are much greater, where annual totals may exceed 70 to 100 inches (NRCS).

3.1.2 Geologic Setting

The BARCAS study area is located within three overlapping provinces: the Basin and Range Province, the Great Basin, and the carbonate-rock province of eastern Nevada (Dettinger *et al.* 1995). The Basin and Range Province is an area characterized by north-trending mountain ranges (horsts) with intermontane basins (grabens) which are filled with alluvium eroded from the mountain blocks. The Great Basin extends from eastern California, through Nevada and into western Utah and includes parts of southern Oregon and Idaho. The Great Basin is a region which is characterized by internally-drained basins in which surface water does not flow to the ocean. The carbonate-rock province of the Basin and Range is informally defined as the portion of the Basin and Range where

groundwater flow is predominantly or strongly influenced by aquifers occurring in Paleozoic-age carbonate formations (Dettinger et al., 1995)

The general geology of the BARCAS study area consists of Tertiary and Quaternary alluvial fill, Tertiary volcanic rocks, and Paleozoic rocks. The alluvial fill comprises primarily clay, silt, sand and gravel with some local deposits of freshwater limestone or evaporite (Eakin, 1966). The exposed rocks occurring within the BARCAS study area generally belong to three groups: Precambrian to Triassic igneous, metamorphic, and sedimentary rocks; Cenozoic sedimentary rocks; and Cenozoic volcanic rocks (Kirk and Campana, 1990). Zones where volcanic rocks are exposed are primarily volcanic tuff and welded tuff or ignimbrite; however, other volcanic rock types and some sedimentary deposits are present. Precambrian rocks are primarily limestone and dolomite; however, quartzite, shale and sandstone may occur locally (Eakin, 1966).

3.1.3 Hydrostratigraphy

The carbonate rocks which compose the aquifer system were deposited between 200 million and 500 million years ago and consist of predominantly limestone and dolomite with interlayers of quartzite or shale. The layers of Paleozoic rocks have total thickness of up to 30,000 feet in some areas (Stewart 1980). Three types of permeability contribute to the movement of water within the formation: primary porosity through the pore spaces of the rocks; permeability through joints, fractures, or bedding planes; and permeability through solution cavities (Mifflin and Hess, 1979). The primary

permeability (porosity) of the carbonates is typically low; therefore, the secondary permeability is largely responsible for the large flows of water associated with the carbonate-rock aquifer.

The valleys overlying the carbonate rock are filled with unconsolidated alluvium, including layers of sands, gravels, silts, and clays, and lake sediments of Pleistocene or younger age (Mifflin and Hess, 1979). In multi-basin flow systems such as in the BARCAS study area, the alluvial aquifers are considered to have a hydraulic connection with the underlying carbonate-rock aquifer (Thomas et al., 1996).

3.2 Groundwater Flow Systems

The BARCAS study area is composed of a network of alluvial (basin-fill) aquifers within 12 hydrographic basins (valleys) and the underlying regional carbonate-rock aquifer. In addition, groundwater may occur within the formations of the recharge areas and be discharged as small or local springs. Groundwater flow systems within the BARCAS study area are classified as local, intermediate, or regional. The definitions for these types of flow systems were proposed by Tóth (1963) who developed a two dimensional model to evaluate groundwater flow within a theoretical small basin. Local systems are characterized by groundwater recharge occurring at topographic highs, groundwater discharge occurring at topographic lows, and adjacent recharge and discharge areas. Intermediate systems are characterized by the presence of one or more topographic highs or lows between recharge and discharge areas. Regional systems are characterized by recharge occurring at a water divide and discharge areas occurring at the

valley bottom of a basin. The general geochemical characteristics of local and regional flow systems of the Great Basin are described in the following paragraphs.

The chemical composition of groundwater evolves as it travels through the subsurface. As recharge water flows through the basin-fill aquifers and the deeper carbonate-rock aquifers, the dominant processes affecting water chemistry include 1) dissolution of minerals and carbon dioxide gas from the soil zone, 2) mineral precipitation, 3) mixing with waters of differing chemical characteristics, 4) ion exchange with clay minerals, and 5) geothermal heating during deep circulation (Thomas et al., 1996).

Local flow systems are considered to be confined to within one topographic or hydrographic basin and have relatively short groundwater flow paths. The short flow paths and short residence time of groundwater within these flow systems indicate that groundwater chemistry is strongly influenced by recharge (precipitation) water chemistry and may be altered through interaction with more soluble minerals, such as evaporites and to a lesser extent, carbonates. Local springs are characterized by cooler temperatures, generally low dissolved solids content, and lower concentrations of sodium, potassium, chloride, and sulfate relative to regional springs (Mifflin, 1968).

Regional flow systems encompass multiple topographic or hydrographic basins, with inter-basin flow playing an important role in groundwater flow. Principle evidence of regional aquifers include large springs occurring in hydrographic basins where recharge to the basin cannot account for the large volume of water discharged, warm

temperatures, and elevated dissolved solids content (Mifflin, 1968; Hershey and Mizell, 1995).

Within the Great Basin, the term "regional groundwater flow system" may imply groundwater flowpaths which traverse multiple basins. One of the first regional multibasin groundwater flow systems identified in the Great Basin is the White River flow system (Eakin, 1966) which comprises fourteen hydrographic basins, four of which are within the BARCAS study area (Long Valley, Jakes Valley, White River Valley, and Cave Valley). Thirty-nine major flow systems in the Great Basin were identified as part of the Great Basin Regional Aquifer-System Analysis (RASA) based on groundwater data (Harrill et al., 1988). Of these regional flow systems, four include hydrographic areas which are part of the BARCAS study area (Figure 2). The Newark Valley regional flow system comprises Newark Valley and the central and northern portions of Little Smoky Valley and discharges to Newark (dry) Lake. The Colorado River regional flow system, of which the White River flow system is a subsystem, includes 34 hydrographic areas and discharges to the Colorado River. Long Valley, Jakes Valley, White River Valley, Cave Valley, and Lake Valley are part of the Colorado River flow system. The Goshute Valley regional flow system includes three hydrographic areas, two of which are in the BARCAS study area (southern portion of Butte Valley and Steptoe Valley). Goshute Valley playa (elevation about 5,585 ft) is terminus of the system; however, significant discharge occurs in upgradient areas. The Great Salt Lake Desert system comprises sixteen hydrographic areas, including Spring Valley, Tippet Valley, and Snake Valley. Discharge of the flow system is to the Great Salt Lake Desert.

For the context of the groundwater accounting model, groundwater will be classified as either "regional/deep-intermediate" or "local". Local, deep-intermediate, and regional groundwater flow systems are shown conceptually on Figure 3. Regional groundwater is defined as having long flow paths spanning multiple hydrographic areas, discharge far from recharge areas, long travel times, and deep mixing (heating). Deep-intermediate groundwater is considered to be groundwater which does not traverse multiple basins; however this water does flow to sufficient depths to allow for heating and/or mixing with regional-type groundwater. Both regional groundwater and deep-intermediate groundwater are important to the study because these are the groundwater types that may be representative of the regional carbonate aquifer. Groundwater occurring as local systems is of importance for the estimation of recharge characteristics.

3.3 Water Budgets

Water budgets (or water balances) are an application of simple mass conservation equations which may be used to establish the basic hydrologic characteristics of a geographical region (Dingman, 2002). A water budget is one of the most basic ways to quantitatively evaluate the movement of groundwater through an aquifer system. Water budgets may be developed for systems of any size and for this study are useful at both basin and regional scales.

3.3.1 Water Budget Components

The fundamental equation for a water budget is the sum of inputs rates (Q, volume per time) minus the sum of output rates equals the change in storage of the system:

$$\sum Q_{Inputs} - \sum Q_{Outputs} = \Delta Storage \tag{1}$$

If the system is assumed to be at steady-state, then the change in storage is zero and the water budget becomes:

$$\sum Q_{Inputs} = \sum Q_{Outputs} \tag{2}$$

For a groundwater system, inputs may include direct recharge from precipitation, indirect recharge of precipitation from surface water runoff, groundwater inflow from outside the system boundary, or recharge from anthropogenic sources. Groundwater outputs may include discharge as springs, discharge to surface water bodies, loss to the atmosphere by evapotranspiration (ET), groundwater outflow to outside the system boundary, and pumping for domestic, agricultural, industrial, and mining uses. Considering that for basins within the BARCAS area the primary groundwater inputs are recharge from precipitation and interbasin groundwater inflow and that the primary outputs are discharge as groundwater ET and interbasin groundwater outflow, a simplified water budget may be expressed as:

$$Recharge_{precip} + GW_{inflow} = Discharge_{GWET} + GW_{outflow} \tag{3}$$

where recharge from anthropogenic sources and pumping for domestic, agricultural, industrial, and mining uses are assumed to be negligible. A conceptual representation of

these water budget components is provided in Figure 3. This simplified water budget also assumes that groundwater discharged from springs recycles back into the shallow water table where subsequent evaporation or transpiration occurs.

3.3.2 Previous Water Budget Investigations

Groundwater investigations of Nevada's basins began in the 1940s with the publication of Nevada Water Resources Bulletins by the USGS in cooperation with the Office of the State Engineer (Epstein, 2004). Legislature passed in 1960 provided for a series of water resources and groundwater appraisals referred to as the Water Resources Reconnaissance Series. The Reconnaissance Series reports provided water budget information on basin basis. Subsequently, most basins within the study area have had one or more additional estimates published for recharge, discharge, and/or interbasin flow rates. Summaries of water budget components for the study area from previous studies are presented for recharge, ET discharge, and interbasin flow on Table 1, Table 2, and Table 3, respectively. A brief summary of the reports and their calculation approaches is provided below.

A variety of methods were used to estimate water budget components for the Reconnaissance Series reports (Eakin, 1960; Eakin, 1961; Eakin, 1962; Rush and Eakin, 1963; Rush and Kazmi, 1965; Hood and Rush, 1965; Rush and Everett, 1966; Eakin et al., 1967; Glancy, 1968; Harrill, 1971; Eakin, 1966). A summary of the water budgets developed for the Reconnaissance Series is provided in State of Nevada Water Planning

Report Part 3: Nevada's Water Resources (Scott et al., 1971). A common method used to estimate recharge in the Reconnaissance Series reports is an empirical technique which uses precipitation zones from the Hardman precipitation map of Nevada (Hardman 1936). This method, referred to as the Maxey-Eakin method was developed by fitting discharge volumes to precipitation volumes for thirteen basins in Nevada (Maxey and Eakin 1949).

Recharge calculations from precipitation zones were revisited by Watson et al. (1976) who examined the Maxey-Eakin method by a comparing calculated recharge rates from the Maxey-Eakin method to results from other simple-linear and multiple-linear regression models which estimate recharge based on precipitation zones. Nichols (2000) presented revised water budgets for selected hydrographic areas within the Great Basin. Water budgets included revised estimates for ET, recharge, and interbasin flow. Recharge estimates were based on a regression model including precipitation zones from the PRISM map (Daly et al., 1994). ET discharge was calculated from plant cover, as determined from satellite imagery, and interbasin flow rates were calculated from the difference between recharge and discharge rates. Epstein (2004) re-evaluated the Maxey-Eakin and Nichols methods for calculating recharge and developed a new model for estimating recharge, the Bootstrap Brute-force Recharge Model (BBRM), in which coefficients are applied to spatially-distributed annual precipitation volumes to estimate annual recharge volume. Epstein also examined the uncertainty associated with the new and re-evaluated recharge models.

Mass-balance type approaches have been completed using chloride and deuterium tracers. Dettinger (1989) presented a chloride mass balance of sixteen hydrographic areas in the Great Basin. The chloride mass balance approach estimates the recharge rate based on an assumed chloride concentration of precipitation and observed chloride concentrations in groundwater. Kirk and Campana (1990) developed a deuterium-calibrated discrete-state compartment (DSC) model of the White River flow system. The calibrated model provided estimates for groundwater recharge and interbasin groundwater flow rates. Thomas et al. (2001) present a deuterium mass balance interpretation of groundwater flow within the White River, Meadow Valley Wash, and Lake Mead area flow systems. The mass balance used deuterium data to evaluate revised recharge estimates and discharge estimates developed by SNWA.

In a series of reports prepared for SNWA (previously Las Vegas Water District), Brothers et al. (1993, 1994) developed finite-difference groundwater flow models for Cave Valley, Spring Valley, and Snake Valley. Recharge, discharge and interbasin flow rates for the basins were from Reconnaissance Series reports. Katzer et al. 2003 presented a revised water budget for Spring Valley prepared for SNWA which included a detailed analyses of surface water within the basin. Recharge efficiency factors were applied to estimate partitioning of precipitation between runoff and recharge was calculated on a mountain block basis

Most recently, Flint et al. (2004) presented a basin characterization model (BCM) for calculating groundwater recharge for hydrographic areas within the Great Basin.

Groundwater recharge was calculated as the sum of potential in-place recharge and an assumed percentage of surface water runoff. Annual totals were calculated from time-series simulations performed on a pixel (grid) basis using climate conditions for the 34-year period of 1956 through 1999. Calculations were performed using average monthly climate conditions, where monthly averages were calculated for the 34-year period, and using time-varying monthly climate conditions.

3.3.3 BARCAS Water Budget Estimates

Work completed for the BARCAS recharge task and discharge task determined rates for recharge from precipitation and discharge by ET from groundwater (Welch and Bright, in review). Recharge estimates included both in-place recharge occurring in the mountain areas as well as infiltration of surface water runoff to become recharge. In-place recharge and surface water runoff rates were computed using BCM methodology at an 886-foot grid resolution and a monthly time step using average climate data from the 30-year period of 1971 to 2000. Total recharge was calculated as the sum of in-place recharge plus 15 percent of the surface runoff. Uncertainty associated with recharge rates was the described in terms of the percentage of surface runoff assumed to infiltrate to become recharge, with basins that receive proportionally more recharge via run-off infiltration having more uncertainty associated with their recharge estimates. The standard deviation for recharge estimates was identified as 10 percent of the runoff.

Groundwater ET discharge was estimated by first calculating the total ET for each basin or sub-basin then subtracting the amount of precipitation to yield the groundwater discharge component of the total ET rate. Total ET rates were calculated by determining the acreage of land cover types (or "ET units") within each basin, multiplying the acreage by a coefficient to generate ET loss, and summing the losses for each ET unit within a basin. The uncertainty associated with the groundwater ET rates was evaluated based on assumed distributions for ET rates, acreage measurements, and precipitation rates.

The estimated recharge rates and groundwater ET discharge rates for basins and sub-basins in the BARCAS area are presented in Table 4. Net (basin) recharge rates are greater than discharge rates for all basins except White River Valley, indicating that groundwater outflow should be occurring from most basins in the study area (Figure 4). This groundwater outflow may occur as interbasin flow to basins within the study area or as groundwater flow out of the study area. Groundwater pumping is another type of groundwater discharge which may occur within the study area, however groundwater pumping was not included in the simplified water budget (see equation 3) due to the temporal nature of pumping (versus a steady-state water budget). The omission of groundwater pumping may have some impact on the water budget for the study area. For example, the omission of groundwater pumping may cause interbasin groundwater outflow rates predicted by the model to be overestimated for basins with recharge rates that are much greater than groundwater ET discharge rates.

3.4 Groundwater Accounting Models

A groundwater accounting model is a tool which can help verify tabulated water budgets and evaluate interbasin groundwater flows. For a basic mass-balance type groundwater accounting model, simplified mass-balance mixing equations are used to account for inputs and outputs to accounting "cells", rather than the standard groundwater flow equation used in typical numerical simulations. The mass-balance model has the same fundamental equation as the water budget; the difference for the mass balance model is that the mass of a tracer moving in and out of the system per unit time is used instead of volumes of water.

Considering that the mass flux of a tracer in water may be calculated as its concentration (mass of tracer per volume of water) times the flow rate (volume of water per time), the mass balance approach may be viewed as a water budget modified to include concentrations. Assuming this system is at steady state, the general equation may be expressed as:

$$\sum_{i=1}^{N_{in}} (Q_{in\,i} \times C_{in\,i}) = \sum_{j=1}^{N_{out}} (Q_{out\,j} \times C_{out\,j}) \qquad (4)$$

where Q_{in} and C_{in} represent the flowrate (volume/time) and concentration (mass/volume) for each of N_{in} inputs and Q_{out} and C_{out} represent the flowrate and concentration for each of N_{out} outputs.

The benefit of this approach is that if characteristic tracer concentrations vary between different model inputs and between different "cells" within the system, then

modeling the movement of the tracer within the system can provide information on magnitudes and directions of water flow. In this way, groundwater chemistry data are used to help constrain the water budget and may provide information on the mixing patterns and source areas for groundwater in the aquifer system.

3.4.1 Discrete State Compartment (DSC) Model Background

The groundwater accounting model developed and applied to the BARCAS study area is a modified Discrete-State Compartment (DSC) model. This accounting-type model uses water budget and environmental tracer values to perform iterative water and mass-balance calculations for a groundwater system which is modeled as a network of interconnected compartments (or "cells"). Both water and tracer movements are governed by a set of recursive conservation of mass equations in which the volumetric flux of water and associated mass flux of a tracer are tracked. The model is calibrated by comparing simulated concentrations of the selected environmental tracer to observed values at each iteration. The DSC model is advantageous for use in the Great Basin because it may be applied to systems lacking sufficient information on aquifer hydraulic properties necessary to define a rigorous finite-difference or finite-element numerical groundwater model. (Carroll et al., 2006).

The DSC model was originally developed by Campana (1975) as a tool to model the mass of any groundwater tracer (i.e., groundwater constituents or environmental isotopes) via mixing cell mass-balance equations. Subsequent use of the DSC model has

occurred in several groundwater studies in the Great Basin (Feeney et al., 1987; Karst et al., 1988; Roth and Campana 1989; Sadler 1990; Kirk and Campana 1990; Campana et al., 1997; Calhoun 2000; Earman and Hershey, in review).

Whereas the original DSC model allowed for transient simulations and the use of non-conservative tracers, the DSC model which was used for this study has been modified to simulate only steady-state conditions of a conservative tracer (Carroll and Pohll, 2007). Consequently, values are not necessary for cell volumes and source/sink rates (e.g., decay rates, reaction rates, adsorption/desorption coefficients). Model inputs include the number of cells, rates and concentrations for recharge, connections between cells, and cell head ranks A conceptual representation of a DSC model framework and components is provided in Figure 5. Conceptually, one can envision the cell's rank as a surrogate for the cell's groundwater head. Flow will only occur from a cell with higher groundwater levels (i.e., higher rank) to a cell with relatively lower groundwater levels (i.e., lower rank). Flow directions between connected cells may either be specified or left unspecified. If flow directions are left unspecified, ranks for these cells are varied during model optimization to determine flow direction.

The steady-state assumption requires that volume and mass discharging from a cell are equal to all inputs of volume and mass to that cell. The algorithm of an instantaneously mixed cell may be expressed as:

$$C_i = \frac{\overbrace{\sum_{j=1}^{N}\left(Q_{i,j}^{r} C_{i,j}^{r}\right)}^{\text{Mass from recharge}} + \overbrace{\sum_{k=1}^{D}\left(f_{k,i} Q_k^d C_k^d\right)}^{\text{Mass from GW inflow}}}{\underbrace{\sum_{j=1}^{N}\left(Q_{i,j}^{r}\right)}_{\text{Recharge rate}} + \underbrace{\sum_{k=1}^{D}\left(f_{k,i} Q_k^d\right)}_{\text{GW inflow rate}}} \tag{5}$$

where C_i is the steady-state modeled concentration for cell i, $Q_{i,j}^{r}$ is the recharge rate for the jth recharge to cell i, $C_{i,j}^{r}$ is the tracer concentration for the jth recharge to cell i, N is the number of recharge inputs to cell i, Q_k^d is the total discharge from cell k, $f_{k,i}$ is the fraction of flow Q_k^d discharging from cell k to cell i, C_k^d is the steady-state modeled concentration for cell k, and D is the number of cells discharging to cell i. Discharge can occur to another cell (as interbasin groundwater flow within the model domain) or out of the model domain (as ET or interbasin groundwater flow out of the model domain. Therefore,

$$\sum_{h=1}^{P} f_{i,h} + f_{i,out} = 1.0 \tag{6}$$

where P is the number of outflows to adjacent cells from cell i, $f_{i,h}$ is the fraction of flow and mass discharged from cell i and received by cell h, and $f_{i,out}$ is the fraction of flow and mass discharged from cell i out of the model domain.

3.4.2 DSC Model Optimization

Optimization (or calibration) of the DSC model is achieved by minimizing an objective function that defines the overall error between observed and predicted values

for each cell in the model. A typical objective function used for model optimization is the weighted root mean squared error (wRMSE), which is expressed generically as:

$$wRMSE = \sqrt{\frac{\sum_{i=1}^{N} w_i \left(P_i - O_i\right)^2}{N}} \tag{7}$$

where P_i, O_i, and w_i represent predicted value, observed value, and weight term, respectively, for cell i, and N is the total number of cells.

DSC model optimization has traditionally been performed by manually adjusting cell-to-cell and boundary fluxes until modeled tracer concentrations in each cell most closely match observed values. Automated optimization has recently been achieved by coupling a modified DSC model to the Shuffled Complex Evolution (SCE) optimization algorithm (Duan et al., 1992) to allow for rapid and automated model optimization (Carroll et al., 2006; Carroll and Pohll, 2007).

During model optimization, flow fractions ($f_{i,h}$ and $f_{i,out}$) and cell ranks are adjusted until the predicted cell concentrations and/or outflows best match observed cell concentrations and/or outflows. The parameters $f_{i,h}$ and $f_{i,out}$ effectively control the volume and mass moving between each cell and out of the model domain. If all flow directions are specified, then $f_{i,h}$ and $f_{i,out}$ are the only parameters adjusted during model optimization. If the direction of flow between a pair of cells is unknown or ambiguous, the cell ranks are adjusted during model optimization and at each iteration the fraction of

flow from the lower (ranked) cell to the higher (ranked) cell is automatically set to zero (Carroll et al. 2006).

3.5 Deuterium as a Groundwater Tracer

Deuterium (^2H or D) and protium (^1H) are the stable isotopes of hydrogen. The isotope ^1H is much more abundant than deuterium; on average the earth's water supply contains about one atom of D per 6,700 atoms of ^1H, or about 0.015 percent D (Drever, 1997). The ratio of deuterium to protium (^1H) is conventionally referenced to the Vienna Standard Mean Ocean Water (VSMOW) standard by the equation:

$$\delta D = \frac{\left(\frac{^2H}{^1H}\right)_{sample} - \left(\frac{^2H}{^1H}\right)_{VSMOW}}{\left(\frac{^2H}{^1H}\right)_{VSMOW}} \times 1000 \qquad (8)$$

where δD is the ratio, expressed as per mil (‰),of the difference between the D/^{1}H ratios of the sample and the reference to the D/^{1}H ratio of the reference. Analytical error for δD analyses is approximately 1 ‰ (Friedman et al., 2002).

Deuterium is a nearly ideal tracer for groundwater investigations because 1) it is part of the water molecule and is therefore generally not affected by reactions with geologic materials, and 2) it displays natural variability as a result of the processes of evaporation and precipitation of water (Sadler, 1990). Deuterium data are useful for the delineation of groundwater flow systems which include water from different source areas (Thomas et al., 1996). The isotopic signature or characteristic for recharge water, basin-fill aquifer groundwater, and deep carbonate-rock aquifer groundwater for various

groundwater flow systems within the Great Basin have been evaluated and used as a basis for mixing models to calculate interbasin flow (Feeney et al., 1987; Roth and Campana, 1989; Kirk and Campana, 1990; Sadler, 1990; Thomas et al., 2001; Earman and Hershey, 2005; Carroll et al., 2006).

Freshwater systems are typically depleted in deuterium compared to oceanic waters and consequently have negative δD values. The process by which water becomes enriched in heavier isotopes (isotopically heavier, more positive δD values) or depleted in heavy isotopes (isotopically lighter, more negative δD values) is referred to as fractionation. Isotopic fractionation of water molecules occurs through a variety of processes. When water evaporates, the resultant water vapor will be isotopically lighter than the liquid water; when water vapor condenses as precipitation, the resultant liquid water is isotopically heavier than the vapor (Drever, 1997). Variability in isotopic composition of precipitation has been attributed to multiple effects, as summarized by Hershey and Mizell (1995):

- <u>temperature effect</u> – fractionation during the formation of precipitation from clouds is controlled by the temperature at which changes in physical state occur
- <u>continental effect</u> – precipitation tends toward more negative δ values further away from the ocean
- <u>altitude effect</u> – precipitation becomes lighter (more negative δ values) at higher altitudes

- latitude effect – precipitation becomes lighter (more negative δ values) at higher latitudes
- amount effect – the greater the amount of precipitation, the more negative the δ values

In addition, storm-to-storm variation in δD occurs, but mixing during the recharge process causes smoothing toward the mean value (Gat, 1981; Darling and Bath, 1988). Because evaporation changes δD values, any study using deuterium as a conservative tracer should only examine a deep groundwater system that is minimally impacted by evaporative processes. The characteristic δD value for recharge is defined with groundwater springs in recharge source areas, as opposed to using precipitation δD values that are highly variable and could be significantly altered by pre-recharge evaporation. Groundwater springs in recharge areas represent surface expressions of precipitation which has recharged, and may be assumed to average out storm-to-storm, seasonal, yearly, and small geographic variations in the isotopic composition of precipitation (Ingraham and Taylor, 1991). Assuming the effects of past climate regimes on deuterium signatures are negligible and that alteration of the signature does not occur through processes such as evaporation, then δD is simply a function of geographic location and is therefore treated as a conservative tracer (Sadler, 1990).

The mass balance equation developed previously express mass flux as the product of a tracer's concentration (mass per volume) and a volumetric flow rate. A δD value is

not technically a concentration because it represents a difference between a water sample and VSMOW rather than an amount of D per volume or mass of water. However, δD can be treated as a concentration because it scales linearly with concentration and thus will not cause a difference in mass balance model results versus use of an actual D concentration.

4. METHODOLOGY

4.1 Approach

A groundwater accounting model was developed to evaluate basin and regional water budgets for the BARCAS study area and to estimate rates of interbasin groundwater flow within the study area and groundwater discharge to outside the study area. Model and water budget uncertainties were evaluated via deterministic-sensitivity and stochastic (Monte Carlo) uncertainty analyses.

The DSC model developed and applied for BARCAS is a single-layer model of regional and deep intermediate groundwater within consolidated carbonate rock and alluvium (Figure 3). For the context of the model, regional groundwater is defined as having long flowpaths spanning multiple hydrographic areas, discharge far from recharge, long travel times, and deep circulation. Deep-intermediate groundwater is considered to be groundwater that does not traverse multiple basins; however, this water does flow to sufficient depths to allow for heating and/or mixing with regional-type groundwater. Both regional groundwater and deep-intermediate groundwater are

important to the study because these are the groundwater types that may be representative of the regional aquifer.

Local groundwater systems, including shallow alluvial groundwater and perched aquifers within mountain blocks, were not included as cells in the DSC model. Local groundwater systems were not included as DSC model cells due to an insufficient amount of data to support the increased optimization parameters associated with a multi-layer model. However, groundwater samples collected from local systems were used to estimate characteristic recharge δD values.

The DSC model was developed through a series of tasks related to geochemistry, hydrology, modeling, and interpretation of results. The modeling approach included ten tasks:

1. Compile deuterium database
2. Classify deuterium data as recharge, regional/deep-intermediate groundwater, or neither
3. Identify model cells based on deuterium data and locations of intrabasin bedrock highs
4. Calculate recharge deuterium values and rates for model cells
5. Calculate observed deuterium values for model cells
6. Identify possible interbasin flow occurrences and directions (cell connectivity)
7. Run deterministic groundwater accounting model

8. Estimate probability distributions for recharge rates, recharge deuterium values, and groundwater ET discharge rates
9. Run Monte Carlo uncertainty analysis for groundwater accounting model
10. Present and discuss results

4.2 Assumptions

The following assumptions were made for the groundwater accounting model (modified from Sadler [1990]):

1. The system is at steady-state.
2. Deuterium behaves as a conservative tracer in the mass-balance mixing model. Fractionation of deuterium within the aquifer is assumed to not occur as a result of residence time or flow within the aquifer, water-rock interactions, or ET discharge.
3. The regional aquifer system may be represented as a series of cells, each of which contains a characteristic deuterium concentration for the fully mixed cell (sufficient data do not exist to subdivide into smaller cells).
4. The δD values used for calibration are representative of the δD content of regional/deep-intermediate groundwater in the study area.
5. The δD values for recharge to the regional/deep-intermediate aquifer is related to the δD values for springs, shallow wells, and some surface water within recharge areas and downgradient of recharge areas.

6. Recharge rates and δD values have remained constant for a sufficient period of time for steady-state conditions to be observed for the system. This assumption does not imply that short-term fluctuations in recharge rates or values do not occur; however, these fluctuations are assumed to be smoothed out (integrated) over time to yield the estimated average value.

7. Groundwater input to the study area does not occur as interbasin groundwater flow from outside the study area. This assumption implies that the only groundwater input to the system occurs as recharge from precipitation. Water budgets presented in previous reports identified "some" groundwater inflow to Little Smoky Valley from Stevens Basin and Antelope Valley (Rush and Everett, 1966) and unspecified amounts of groundwater inflow to Snake Valley from Pine Valley and Wah Wah Valley (Harrill et al., 1988). Groundwater inflow from outside the study area to Little Smoky Valley and Snake Valley was not modeled due to the non-quantitative nature of estimates for inflow reported in previous studies.

4.3 Deuterium Database

Deuterium data were used to assign characteristic recharge and mixed cell δD values and as a criterion for subdividing the larger basins of the study area into sub-basins. Deuterium data were managed in a database of stable isotope (deuterium, oxygen-18) sample results compiled for the study area and adjacent basins. Associated chemical parameters (e.g. temperature, specific conductance, chloride, sulfate, tritium,

etc.) were also included in the database for use in classifying sample locations. The database was queried from the USGS National Water Information System (NWIS) database (Reference). The NWIS database was updated during the BARCAS study to include relevant historic USGS samples, samples from previous DRI reports, unpublished theses, and samples collected for the BARCAS geochemistry task.

Plots of deuterium versus oxygen-18 were prepared to identify samples which are evaporated relative to global and local meteoric water lines. Sample locations with deuterium data were classified as 1) representative of recharge, 2) representative of regional/deep-intermediate type groundwater, or 3) neither representative of recharge or regional/deep-intermediate type groundwater. Sample classification was based on primarily on the location and water temperature; however, additional criteria were also used:

- previous studies which identified springs and wells as representative of regional groundwater (Harrill et al. 1988, Beddinger et al. 1985)
- revised regional potentiometric surface map for the BARCAS study area
- interpreted dissolved gas data (Hershey et al. 2007)
- surrounding geology
- conventional chemical parameters, such as sodium-potassium-sulfate-chloride plots described by Mifflin (1968)

Two-hundred thirty nine sample sites were identified as representative of recharge or potential recharge; these sites are listed in Appendix A and are shown on Figure 6.

Samples collected from springs, shallow groundwater wells, and some surface water sites were identified as representative of recharge or potential recharge based on one or more of the following criteria: cool water temperature, topographic setting, location relative to recharge areas, discharge characteristics (springs), surrounding geology, well depth, elevation relative to regional potentiometric surface, and variability in discharge rate or chemistry.

A total of 84 sites were identified as representative of regional / deep-intermediate groundwater; these sites are shown on Figure 7 and listed in Appendix B. Waters representative of regional or deep-intermediate groundwater were identified based on warm water temperatures, surrounding geology, depth of the regional potentiometric surface, deuterium composition relative to nearby recharge, previous reports identifying regional and large springs of the Basin and Range province (Bedinger et al., 1985; Harrill et al., 1988), and results from a geochemical evaluation of dissolved gases within groundwater samples collected for the BARCAS study (Hershey et al., 2007). Regional or deep-intermediate groundwater samples generally had temperatures greater than about 68 degreed Fahrenheit. In some cases, plots of conventional chemical parameters, such as sodium-potassium-sulfate-chloride plots described by Mifflin (1968) were used to provide additional support for sample classifications.

4.4 Model Inputs

The following subsections describe the specific assumptions and input parameters associated with the BARCAS DSC model, which serves as the "base case" for model evaluation. Revised assumptions and input parameters associated with the uncertainty analysis are provided in Section 4.6.

4.4.1 Model Cells

Model cells were identified based on hydrographic area boundaries and locations of intrabasin bedrock highs. Deuterium data for regional/deep-intermediate groundwater was compared with the locations intrabasin bedrock highs within the BARCAS study area (Welch and Bright, in review) to determine which basins support division into sub-basins. Intrabasin bedrock highs and DSC model cells are shown on Figure 8.

4.4.2 Cell Connectivity

The potential groundwater flowpaths between model cells shown on Figure 8 were identified based on the hydrographic area boundary classifications determined for the geology task and the regional potentiometric surface contours (Welch and Bright, in review). Boundary classifications for probable flow (green) or possible flow (yellow) were compared to the potentiometric surface in adjacent basins. If a gradient was present, then a potential interbasin flow was identified. If interbasin flow was possible based on the hydrographic boundary classification, but a gradient between basins was not apparent

based on the regional potentiometric surface, then a potential interbasin flow was identified with an undetermined direction. If a basin boundary was classified as flow not likely (red) or if a groundwater mound was present, no potential flow was identified. Potential interbasin groundwater flows were used to establish the cell network for the DSC model and are shown in Figure 8.

Interbasin groundwater flows out of the model domain are not shown on Figure 8 nor are these flows explicitly listed in the model's input or output. The DSC model predicts one rate for output from the model domain for each cell, and this rate of output from the model domain is not divided into components of interbasin groundwater flow and discharge as groundwater ET. Groundwater flow out of the model domain (or study area) may be estimated, however, by subtracting an estimated groundwater ET discharge rate from the total output from the model domain.

4.4.3 Head Rankings

Model cells were assigned head rankings from 1 (lowest head) to 20 (highest head) based on the regional potentiometric surface map generated under the BARCAS groundwater flow task (Welch and Bright, in review). Head rankings were assigned by calculating the average regional aquifer potentiometric elevation in each cell. Average elevations were determined by performing a simple interpolation of contour lines to generate a continuous potentiometric surface, then calculating the average value using ARCMap 9 geographic information system (GIS) software. Average heads ranged from

4,496 feet above mean sea level (amsl) for the northeast portion of Snake Valley to 6,747 feet amsl for the southern portion of Steptoe Valley. Average heads and head rankings are listed in Table 5 and shown on Figure 8.

4.4.4 Recharge Rates

Recharge rates for each cell were determined from the recharge estimates calculated for the BARCAS recharge task using the basin characterization model (BCM) methodology (Welch and Bright, in review). Summations of potential in-place recharge and potential runoff were calculated from the 886-foot grid BCM output using geographic information system (GIS) software. The assumed ratio of 15 percent of potential runoff becoming recharge was maintained for cell recharge estimates for consistency with the BARCAS recharge task. Calculations also assumed that topographic basin boundaries were representative of hydrographic area boundaries. Recharge rates in acre-feet/year for each cell are presented on Table 5.

4.4.5 Recharge δD Values

Recharge δD values were determined based on the identified recharge samples and the spatial distribution of recharge across the study area. Recharge δD data are not available for all areas where recharge is predicted to occur. To determine δD values in areas without data and to calculate deuterium values at unsampled locations, the recharge data set was interpolated using an inverse distance weighting (IDW) algorithm. The interpolated recharge δD prediction map, shown in Figure 6, was generated using GIS

and provides δD values for recharge at a 886-foot grid scale. The prediction map shows a pronounced trend in recharge δD values from isotopically heavier recharge δD in the south (warmer colors) to isotopically lighter recharge δD in the north (cooler colors) and suggests that at the scale of the study area, deuterium content is most influenced by latitude. The extent of the prediction map was limited to the east and west by the available recharge data. As such, the prediction map does not cover recharge areas in eastern Little Smoky Valley and the western portion of Snake Valley. These areas contribute relatively little recharge to the respective basins.

The final step in determining the δD value for recharge was to calculate a recharge-weighted average for each basin or sub-basin in the study area. Recharge-weighted average δD values were determined by multiplying the total potential recharge rate by the predicted recharge δD value for each 886-foot grid cell, summing these for the entire (sub)basin, then dividing by the total recharge rate for the entire (sub)basin. The resulting recharge-weighted averages are shown in Figure 6 and listed in Table 5. Recharge-weighted averages for Little Smoky Valley and select sub-basins of Snake Valley were estimated based on the extent of the interpolated recharge prediction map.

4.5 Calibration Parameters

4.5.1 Observed δD Values

Observed δD values were determined from the deuterium database. Regional / deep-intermediate groundwater sample locations are shown in Figure 7. Observed δD values for each cell were calculated as the average of all δD values for applicable sites within or in some cases near a model cell. No appropriate δD data were identified for Butte Valley, Jakes Valley, and the central portion of Snake Valley; therefore, observed δD values were not calculable for the cells corresponding to these basins. Observed δD values for DSC model cells are shown on Figure 7 and listed in Table 5.

4.5.2 Observation Weights

During model optimization, the errors between observed and predicted δD values for each cell were incorporated into an overall objective function using weighting criteria. The weighting criteria account for differing uncertainty in observed δD values and for most model cells were calculated as:

$$w_{c_i} = \frac{1}{\left(t_{0.05, n_i - 1} \frac{s_i}{\sqrt{n_i - 1}} \right)} \tag{9}$$

where w_{c_i} is the observed δD value weight for cell i, n is the number of regional / deep-intermediate-type groundwater samples associated with cell i, s_i is the standard deviation of observed values, and t is the Student t-statistic with $\alpha = 0.10$ and $df = n_i$-1. The

denominator for this weight function is analogous to one-half the 90-percent confidence interval about the observed mean, giving the δD weight units of $‰^{-1}$.

This weight function effectively takes into account both the number and the variability of data points used for calculating the observed concentration values (Carroll and Pohll, in press) and assumes that the variance in the observed concentration for a given cell is independent from observed variance in other cells' concentrations. This approach is consistent with the approach described by Hill (1998), who suggests that weights should be proportional to the inverse of the variance-covariance matrix. The inverse variance gives greater weight to more accurately observed values and lower weight to less accurately observed values. The inverse variance also effectively normalizes observed values such that one can use different parameters in the objective function.

Observed δD value weights for DSC model cells are presented in Table 5. Observed value δD weights were calculated as described above with the following exceptions:

- Butte Valley, Jakes Valley, and the central portion of Snake Valley had no observed δD values; therefore, the weights for these cells were set to zero.
- Calculation of standard deviation and confidence interval for observed δD values was not possible for Newark Valley and the northern portion of

Spring Valley because only one regional / deep-intermediate-type groundwater δD sample was identified for each of these cells (*n* = 1 sample). Observed δD value weights for these cells were assumed to be 0.1 $‰^{-1}$ to reflect relatively low confidence in the associated observed δD values.

- Calculation of the inverse confidence interval was not possible for the northeastern portion of Snake Valley due to a zero standard deviation for the observed δD values for this cell (*n* = 2 samples). The observed δD value weights for the northeastern portion of Snake Valley was assumed to be 0.5 $‰^{-1}$ to reflect an intermediate confidence in the associated observed δD value.
- The calculated inverse confidence interval for Long Valley (0.04 $‰^{-1}$) was about two orders of magnitude less than inverse confidence intervals calculated for other cells. The observed δD value weight for Long Valley was assumed to be 0.1 $‰^{-1}$ in order to reflect low confidence the observed δD value while keeping the error contribution from this cell to the overall objective function within the same order of magnitude as other cells in the model.

4.5.3 Groundwater ET Discharge Weights

For some model runs, optimization included a comparison of groundwater outflow from each cell to the groundwater ET rates calculated under the BARCAS Discharge Task (Welch and Bright, in review). In these cases, the BARCAS groundwater ET rates represent hypothetical minima for outflow rates from cells in the model. Standard deviations associated with the groundwater ET estimates for each basin and sub-basin were also calculated under the Discharge Task (Zhu, in press). Groundwater ET rates and their associated standard deviations are shown in Table 5.

For cell outflows, weights were calculated as the inverse of the standard deviation of the groundwater ET rate (s_{GWET}):

$$w_{Q_i} = \frac{1}{s_{GWET}} \tag{10}$$

where w_{Q_i} is the groundwater ET rate weight with units of (acre-feet/year)$^{-1}$.

4.5.4 Objective Functions

Weighted root mean squared error (wRMSE) or variations thereof were used as objective functions for model optimization. Early in the modeling process it became apparent that when optimized based only δD values, model-predicted rates for groundwater discharge from the model domain for multiple basins differed significantly from estimated groundwater evapotranspiration rates. To target δD values and discharge

rates, the model was run using three optimization scenarios: *c*, *o*, and *o**. Scenario *c* optimized the model based on target concentrations (δD values) only. Scenarios *o* and *o** both optimized the model based on target δD values and groundwater ET rates. Scenario *o* penalized the model if a basin's discharge out of the model domain was less than the groundwater ET rate, while scenario *o** incorporated more rigorous constraints on discharge rates for cells in the interior of the model domain. The weight terms for both concentration and outflow are squared when used in the objective function(s) to become the dimensionally correct inverse variance term suggested by Hill (1998).

Each optimization scenario had a specific objective function. The optimization scenarios and associated objective functions are described below.

Optimization Scenario C

Under scenario C, the model was optimized based on concentration only. This approach is consistent with traditional applications of the DSC model. The objective function for scenario *c* is expressed as:

$$wRMSE_c = \left(\frac{\sum_{i=1}^{N} w_{c_i}{}^2 \left(Co_i - Cp_i \right)^2}{N} \right)^{0.5} \tag{11}$$

where Co_i and Cp_i are the observed and predicted concentrations in cell i, respectively, N is the number of cells being modeled, and wc_i is the weight assigned to cell i for the observed concentration.

Optimization Scenario O

Model optimization scenario O included both concentration and outflow in the objective function. Scenario O penalized the model if a basin's discharge out of the model domain was less than the groundwater ET rate. The objective function for scenario o is modified as follows:

$$wRMSE_o = \left(\frac{\sum_{i=1}^{N} w_{c_i}{}^2 (Co_i - Cp_i)^2 + \sum_{i=1}^{N} \begin{Bmatrix} w_{Q_i}{}^2 (Q_{ET_i} - Q_{out_i})^2 ; \text{if } Q_{out} < Q_{ET} \\ 0 \quad ; \text{if } Q_{out} \geq Q_{ET} \end{Bmatrix}}{2N} \right)^{0.5} \quad \textbf{(12)}$$

where Q_{ET_i} and Q_{out_i} are the groundwater ET rate from the BARCASS discharge task and the cell outflow predicted by the DSC model, respectively, and w_{Q_i} is the weight assigned to the groundwater ET rate.

Optimization Scenario O*

Given the extent of the study area, the assumed DSC model cell connectivity, and/or the interpreted hydrogeologic boundaries, groundwater outflow out of the model domain is not possible for cells 4 (southern Spring Valley), 7 (northern White River

Valley), 9 (southern Steptoe Valley), 10 (Jakes Valley), 11 (central Steptoe Valley), 15 (central Spring Valley), and 16 (northern Spring Valley) (Figure 8). For example, northern White River Valley is surrounded by other DSC model cells to the north, east and south and by a geologic structure to the west through which groundwater flow is not likely. For these cells, groundwater outflow from the model should only consist of groundwater ET. In order to deter excessive predicted outflow rates for these cells, the objective function was modified for scenario O*.

Model optimization scenario O* included both concentration and outflow in the objective function. Scenario O* incorporated more rigorous constraints on discharge rates for interior cells by penalizing the model for any difference between discharge out of the model domain and target groundwater ET rates for the interior cells of the model domain. Under this scenario, the objective function is expressed as:

$$wRMSE_o = \left(\frac{\sum_{i=1}^{N} w_{c_i}{}^2 \left(Co_i - Cp_i\right)^2 + \sum_{i=1}^{N} \begin{Bmatrix} w_{Q_i}{}^2 \left(Q_{ET_i} - Q_{out_i}\right)^2 & \text{if } Q_{out} < Q_{ET} \\ 0 & \text{if } Q_{out} \geq Q_{ET} \\ w_{Q_i}{}^2 \left(Q_{ET_i} - Q_{out_i}\right)^2 & \text{if } Q_{out} \neq Q_{ET}, \text{int} \end{Bmatrix}}{2N} \right)^{0.5} \quad (13)$$

where different criteria apply to interior (int) model cells.

4.6 Uncertainty Analysis

Having developed the base DSC model for the BARCAS study area, in Sections 4.4 and 4.5, the next step was to evaluate model uncertainty. The uncertainty analyses may be generally classified as either deterministic-sensitivity or stochastic types. Deterministic-sensitivity type analyses were performed by varying either a single set of model inputs (e.g. average recharge δD values for cells) or the objective function and evaluating the effect on model output. This type of analysis generates one set of model output for each variation, and is therefore used to evaluate the sensitivity of deterministic model results. Stochastic type uncertainty analyses were performed by running Monte Carlo simulations with the model, where model parameters are assigned distributions of values (rather than single values) and the model is run repeatedly using randomly-selected values for model parameters. Output from stochastic type uncertainty analyses includes many sets of model output.

The following sections describe the deterministic-sensitivity and stochastic uncertainty analysis which were performed.

4.6.1 Deterministic-Sensitivity Uncertainty Analyses

Deterministic-sensitivity type analyses were performed by varying either a single set of model inputs or the objective function. The analyses incorporated different recharge δD value estimation methods and/or the selected objective function for model optimization. A total of seven deterministic-sensitivity analyses were performed by

combining four optimization approaches and two recharge δD value estimation methods. The salient characteristics for the seven deterministic-sensitivity analyses (numbered DS-1 through DS-7) are presented on Table 6. Analyses DS-1, DS-2, and DS-3 represent the base BARCAS DSC model, where recharge δD value estimation and model optimization were performed as described in Sections 4.4.4 and 4.5.4, respectively. Analyses DS-4, DS-5, and DS-6 maintain the base BARCAS optimization scenarios, but use an alternative method for estimating recharge δD values, described below. Analysis DS-7 uses recharge δD values from the base BARCAS model, but uses a new objective function for model optimization.

Recharge δD Value Estimation Methods

Two recharge δD estimation methods were used for the deterministic-sensitivity analyses. The first is the method used for the base BARCAS DSC model, described in Section 4.4.5, where representative recharge δD values for model cells were determined from a prediction map for recharge deuterium δD values developed using an inverse distance weighting (IDW) interpolation algorithm. The IDW algorithm generates a continuous prediction map over the horizontal and vertical extent of the data set; however, the BCM model predicts no recharge to occur at the valley floors of the study area basins. The distribution of BCM-predicted recharge is shown on Figure 6, where the IDW-interpolated recharge δD values have been masked in areas where zero recharge is predicted by the BCM model. The distribution of recharge, including areas with zero

predicted recharge, was factored into the calculated recharge δD values by using recharge-weighted averages for recharge δD values for model cells.

A second, simpler method for estimating recharge δD values was developed using a simple linear regression of recharge sample δD values against latitude. Figure 9 is a plot showing average δD values for recharge samples versus latitude. Regressing average δD values against latitude yields the relationship:

$$\delta D_R = -13.14 \times Lattitude + 400.44 \tag{14}$$

where δD_R is the predicted recharge δD value and *Latitude* is in decimal degrees, North American Datum 1983 (NAD1983). The coefficient of determination (r^2) for the regression is 0.78, indicating that variability in recharge δD value is explained reasonably well by latitude. Recharge δD values for model cells were calculated by applying the latitude regression equation to the latitude for each model cell's centroid. Model cell centroids were determined using GIS. Recharge δD values for model cells estimated by the IDW-interpolation and latitude regression methods are shown in Table 7.

Objective Functions

A total of four objective functions were used for the deterministic-sensitivity uncertainty analysis. The first three objective functions correspond the optimization scenarios *c*, *o*, and *o** for the base BARCAS DSC model, described in Section 4.5.4. Optimization scenarios *c*, *o*, and *o** incorporated target δD values and discharge rates to varying degrees using a weighted root mean squared error (wRMSE) type objective

function (see equations 11, 12, and 13). The fourth objective function is the sum of absolute errors for concentrations (SAE_C), which is expressed as:

$$SAE_C = \sum_{i=1}^{N_o} \left| Co_i - Cp_i \right| \tag{15}$$

where Co_i and Cp_i are the observed and predicted concentrations (δD values), respectively, for cell i and N_o is the number of cells with observed concentrations. The SAE_C function provides a non-weighted objective function which reduces the potential overweighting of large errors that may occur with squared error type functions such as root mean squared error (RMSE). As only concentration is used for model optimization, the SAE_C function is similar to the $wRMSE_C$ function used for optimization scenario *c* of the base BARCAS DSC model. Incorporating both target discharge rates and δD values into a non-weighted objective function is unattractive due to the different physical dimensions of discharge rates and δD values.

4.6.2 Monte Carlo Uncertainty Analyses

Stochastic uncertainty analyses were performed by running a series of Monte Carlo simulations. The Monte Carlo uncertainty analysis was performed by randomly sampling model parameters from distributions for a given realization, then running the model to achieve the best fit for that realization. The process is then repeated with new random values selected for model parameters. A total of 1,000 realizations were performed in this fashion.

The Monte Carlo simulations included a variety of distributions for cell recharge rates, recharge δD values, and target discharge rates. Seven Monte Carlo simulations were developed by combining three distributions for recharge rates and δD values, two distributions for target groundwater discharge rates, and three optimization approaches. To evaluate the uniqueness of model results, an eighth Monte Carlo simulation was performed by running 1,000 simulations of a model using constant values for model parameters. The salient characteristics of the eight Monte Carlo simulations, referred to as MC-1 through MC-8, are presented on Table 8. The following subsections describe the distributions for recharge rate, recharge δD values, and target groundwater discharge rates.

Recharge Rates

Monte Carlo simulations MC-1 through MC-7 included one of three distributions for recharge rates. Recharge rate distributions were identified 1) from BCM-predicted recharge rates and associated uncertainty described for the BARCAS study, 2) using the bootstrap brute force recharge model (BBRM) developed by Epstein (2004) to calculate recharge distributions, and 3) through an evaluation of ranges of recharge rates presented in the BARCAS study and previous studies. For simulation MC-8, recharge rates were kept constant using BARCAS BCM-predicted rates where 15 percent of runoff was assumed to become recharge.

As described in Section 4.4.4, recharge rates calculated for the BARCAS study by the BCM methodology assumed that total recharge equals potential in-place recharge plus 15 percent of potential runoff. The uncertainty associated with recharge predictions by the BCM method is greater for areas with a larger component of potential runoff (Flint and Welch, in review). A range of BCM-predicted recharge rates was evaluated by adjusting the proportion of potential runoff becoming recharge between 0 percent and 30 percent while keeping the amount of potential in-place recharge constant. Recharge calculations were performed using GIS and the coverages for potential in place recharge and potential runoff from the BCM. A uniform distribution of recharge rates was then generated using this range of BCM-predicted recharge rates for Monte Carlo simulations MC-1, MC-2, and MC-3. Ranges of BCM-predicted recharge rates for model cells are shown on Figure 10.

Distributions for recharge rates were also developed by applying the BBRM. The BBRM method relates recharge to precipitation using four precipitation intervals from the PRISM map and multiplying the annual amount of precipitation by a coefficient relating volume recharged to precipitation volume (Epstein 2004). BBRM coefficients were determined by a bootstrap selection for 1,000 realizations, with each realization using one million brute-force inverse optimization iterations. By using the coefficients from each of the 1,000 realization, a distribution of recharge rates was developed for each model cell. The PRISM map showing precipitation intervals for the study area is provided in Figure 11. Precipitation volumes associated with each precipitation interval for each model cell were calculated using GIS by multiplying the area of each

precipitation interval by the precipitation amount. Precipitation volumes were summed for the precipitation intervals used in the BBRM (0 to 10 inches, >10 to 20 inches, >20 to 30 inches, and >30 inches) and recharge volumes were then calculated by multiplying precipitation volumes for each interval by the appropriate coefficient. The precipitation volumes for each interval did not change between realizations; only the recharge coefficients. The BBRM method generated 1,000 recharge rates for each model cell which were input directly into the DSC model for use in Monte Carlo simulations MC-4 and MC-5. The upper and lower bounds of the 95% confidence interval for each basin's BBRM recharge are shown on Figure 10. The confidence interval was calculated by sorting the recharge rates for each cell then taking the 26th and 975th value from the sorted rates. The confidence intervals shown on Figure 10 reflect the total recharge to each basin; therefore, the recharge volumes for associated sub-basins were totaled for those basins which are divided into sub-basins (Snake Valley, Spring Valley, Steptoe Valley, and White River Valley).

The third method used for developing recharge rate distributions was based on the ranges of recharge rates provided in previous studies and from the BARCAS study. As described in Section 3.3.2, a variety of previous studies have included recharge estimates for hydrographic area in the BARCAS study area. The individual values from previous studies are presented on Table 1 and the ranges of estimates are shown on Figure 10. The distributions for recharge for Monte Carlo simulations MC-6 and MC-7 were identified based on the minimum and maximum estimates from previous studies, the BARCAS BCM-predicted rates, and the rates calculated using the BBRM, described above. These

minimum and maximum rates defined the lower and upper bounds for a uniform distribution of recharge rates. Because previous studies have not used the same basin subdivisions as were used for the DSC model cells, the net recharge for the entire basin (i.e. the sum of individual sub-basins) was compared to recharge estimates from previous studies for hydrographic areas which were subdivided for the DSC model (Figure 10). For White River Valley, the maximum recharge rate was reported by Thomas et al. (2001). In order to estimate maximum values for recharge rates associated with the White River Valley sub-basins, the maximum rates from the BBRM model were multiplied by a factor equal to the maximum BBRM recharge for White River Valley divided by the White River Valley recharge reported by Thomas et al. (2001). This approach facilitated estimates for maximum recharge rates which summed to the maximum value while keeping the same proportion of recharge associated with each sub-basin. A similar method was used for generating sub-basin minimum recharge rates for Snake Valley, Spring Valley, and Steptoe Valley, where the minimum reported recharge rates are by Flint et al. ([2004], Snake Valley) and by Watson et al. ([1976], Spring Valley and Steptoe Valley). Ranges for recharge rates calculated for the minimum and maximum of available estimates are shown on Figure 10.

Recharge δD Values

Three distributions for recharge δD values were developed for Monte Carlo simulations MC-1 to MC-7. Uniform distributions were assumed for recharge rates and

δD values based on insufficient data to support the selection of more specific distributions. Monte Carlo simulation MC-8 used constant recharge δD values.

The recharge δD distributions for simulations MC-1 to MC-5 were created by varying model cells' recharge δD values by a factor of ± 1.5 ‰. This factor was selected based on the typical analytical variability of deuterium analyses (± 1 ‰) and the variability of δD values for groups of samples from within zones of high recharge rates. For simulations MC-1 to MC-3, model cells' recharge values were calculated from the BCM-predicted recharge distribution and IDW-interpolated recharge δD prediction map, as described in Section 4.4.5. This method was consistent with the use of BCM recharge rates for these Monte Carlo simulations. As simulations MC-4 and MC-5 used distributions of model cell recharge rates created using BBRM, recharge δD values for model cells were calculated based on the spatial distribution of recharge from the BBRM and the IDW-interpolated recharge δD prediction map. This calculation was performed using the mean coefficients from all BBRM bootstrap realizations. Recharge distributions were then created by varying model cells' recharge δD values by ± 1.5 ‰.

The third recharge δD distribution was developed to represent the potential range of δD values which are calculable based on combinations of the ranges of recharge distributions calculated by BCM and BBRM methods and the recharge δD prediction maps interpolated using the IDW algorithm and latitude regression. Using GIS, spatial recharge distributions were developed representing BCM-predicted recharge with assumed potential runoff to recharge factors of 0 percent, 15 percent, and 30 percent.

Spatial recharge distributions were also developed for the recharge predicted by the BBRM using the average coefficient values and the sets of coefficients which resulted in the minimum and maximum recharge rates. Each of these six spatial recharge distributions was then combined with the IDW and latitude regression recharge δD prediction maps to yield twelve potential recharge δD values for each model cell (Table 9). An additional set of recharge δD values were developed by applying the latitude regression model (see equation 14) to the centroid of each model cell. Centroids for model cells were calculated using GIS. The regression model was also used to calculate the upper and lower limits of the 95 percent confidence interval on the mean recharge δD value for model cell centroids.

The twelve recharge δD values calculated by combining spatial recharge distributions with δD prediction maps and the three recharge δD values calculated using the latitude regression model (mean, lower 95 percent confidence limit, upper 95 percent confidence limit) provided a total of fifteen basis values for determining minimum and maximum recharge δD values for each model cell (Table 9). The minimum and maximum basis δD values were used to define recharge δD value distribution if the difference between minimum and maximum basis δD values was greater than or equal to 3 ‰. If the difference between minimum and maximum basis values was less than 3‰, the recharge δD value distribution was assumed to equal the average of the minimum and maximum basis values ± 1.5 ‰. Recharge δD distributions are provided on Table 10. For comparison purposes, Table 10 also includes recharge δD values calculated as the

simple average of all recharge samples within 6.2 miles of a model cell, as well as average recharge values presented in previous studies, where available.

Target Groundwater ET Discharge Rates and Weights

Target groundwater ET discharge rates were used for Monte Carlo simulations where the DSC model included target discharge rates in its objective function. As shown on Table 8, optimization scenario *o* was used for Monte Carlo simulations MC-2, MC-5, MC-7, and MC-8 and optimization scenario *o** was used for simulation MC-3. Target groundwater ET rates were kept constant in simulations MC-2 and MC-3; therefore, uncertainty associated groundwater ET rate estimates are not incorporated in these Monte Carlo uncertainty analysis. This may limit the predicted uncertainty bounds for interbasin flow estimates. Constant groundwater ET discharge rates were also used with simulation MC-8, consistent with the constant values used for other model parameters in this simulation. Distributions for target discharge rates for simulations MC-5 and MC-7 were identified based on results from an uncertainty analysis of estimated groundwater ET rates performed for BARCAS study (Zhu 2006) and the ranges of groundwater ET estimates available from previous and current studies, respectively.

Uncertainty analysis for groundwater ET discharge rates was completed for the BARCAS study by performing a 10,000-realization Monte Carlo simulation for discharge calculations using assumed distributions for each calculation parameter (ET unit rates, unit areas, and precipitation) for each (sub)basin in the study area (Zhu 2006). The

resulting distributions of groundwater ET discharge rates resemble normal-type distributions, i.e. the probability distribution functions are reasonably bell-shaped. The standard deviations from the distributions of groundwater discharge provided the basis for target discharge rate weighting criteria described in Section 4.5.3. For the DSC model uncertainty analysis, 1,000 groundwater ET discharge rates were selected from the 10,000 realizations performed for the BARCAS groundwater ET discharge uncertainty analysis. These 1,000 groundwater ET discharge rates were input directly into the DSC model for use in Monte Carlo simulation MC-5. The upper and lower bounds of the 95% confidence interval for groundwater ET discharge rates are shown in Figure 12. The confidence interval was calculated by sorting the groundwater ET discharge rates for each cell then taking the 26th and 975th value from the sorted rates.

A comparison between the sum of recharge rates for all model cells and the sum of total target groundwater ET discharge for all model cells was made for each Monte Carlo realization in simulation MC-5. If the total recharge for a realization was less than the total target groundwater ET discharge, then that realization was skipped. This step was necessary to be consistent with the assumption that groundwater input to the study area does not occur as interbasin groundwater flow from outside the study area, and to prevent the use of unrealistic model parameters when optimization included target groundwater ET discharge rates. Of the 1,000 sets of recharge and groundwater ET discharge rates identified for simulation MC-5, 260 sets had total recharge less than total target groundwater ET discharge and were skipped, resulting in 740 Monte Carlo realizations for simulation MC-5.

For Monte Carlo simulation MC-7, target groundwater ET distributions were developed as uniform distributions using the minimum and maximum groundwater ET rates presented in previous studies and from the BARCAS study. Groundwater ET discharge rates from previous studies are described in Section 3.3.2 and presented in Table 2. Figure 12 shows groundwater ET discharge rates from previous studies along with the 95% confidence interval for groundwater ET discharge rates calculated for the BARCAS groundwater ET discharge uncertainty analysis. For model cells representing entire basins, the range for target groundwater ET rates was defined by the minimum and maximum rates from previous studies and the BARCAS study as shown on Figure 12. For model cells which represent sub-basins of Snake Valley, Spring Valley, Steptoe Valley, and White River Valley a comparison was made between ranges of estimates of groundwater ET discharge rates was made on a net-basin basis. As the 95% confidence intervals for BARCAS study groundwater ET discharge rates encompassed the minimum and maximum estimates from previous studies, the 95% confidence intervals for BARCAS study groundwater ET discharge rates were used to define the upper and lower limits of the groundwater ET discharge rate distributions for Snake Valley, Spring Valley, and Steptoe Valley for Monte Carlo simulation MC-7. In White River Valley, the groundwater ET discharge rate presented in Water Resources Bulletin 33 (Eakin 1966) was less than the lower limit of the 95 percent confidence interval for the BARCAS study groundwater ET discharge estimate. In order to estimate minimum values for groundwater ET discharge for the White River Valley sub-basins, the lower limits from the 95% confidence intervals for BARCAS study groundwater ET discharge

rates for each sub-basin were multiplied by a factor equal to the lower limit for the BARCAS 95% confidence interval for net groundwater ET discharge for White River Valley divided by the White River Valley groundwater ET discharge reported by Eakin (1966). This approach is consistent with the development of the recharge distributions for simulations MC-6 and MC-7, described above.

As described above for simulation MC-5, a comparison between total recharge and total groundwater ET discharge was also necessary for simulation MC-7. Whereas for MC-5 a discrete set of 1,000 realizations were available for recharge and groundwater ET discharge rates, an infinite number of recharge and groundwater ET discharge rates for simulation MC-7 could be generated using the uniform distributions described above. For each realization of Monte Carlo simulation MC-7, model-generated recharge rates and groundwater discharge rates were summed for all cells and compared. If the total recharge was less than the total groundwater ET discharge, that set of values was discarded and a new set was generated. In this manner it was possible to run 1,000 realizations which met the requirement that total recharge was greater than total groundwater ET discharge.

For each realization of Monte Carlo simulations MC-5 and MC-7, groundwater ET discharge weights for each cell were calculated as the inverse of the product of the coefficient of variation of the BARCAS study groundwater ET rate for cell i ($CV_{GWET\,i}$) and the target groundwater ET discharge rate of cell i for realization n ($Q_{GWET_{i,n}}$):

$$w_{GWET_{i,n}} = \frac{1}{CV_{GWET\,i} \times Q_{GWET_{i,n}}} \tag{16}$$

where w_{Q_i} is the groundwater ET rate weight for cell *i* with units of (acre-feet/year)$^{-1}$. This approach adjusted the weighting terms according to the magnitudes of the groundwater ET discharge rates. Coefficients of variation for BARCAS study groundwater ET rates were calculated by dividing the standard deviation of the groundwater ET rate by the estimated BARCAS groundwater ET rate (Table 5).

5. MODEL RESULTS

This section is broken into three parts: results from deterministic modeling for the base BARCAS DSC model, results from the deterministic-sensitivity uncertainty analyses, and results from the stochastic (Monte Carlo) uncertainty analyses. For each model run, the DSC model generated as output the set of volumetric groundwater flow rates between model cells and out of the model domain that best satisfied the optimization criteria. Model output also included predicted δD values and objective function values.

5.1 BARCAS DSC Base Model

The results from the base BARCAS DSC model provide the first set of results as a base case against which subsequent model results can be compared. The DSC water budget accounting model was applied using recharge estimates and groundwater ET

discharge rates from the BARCAS study. The deterministic model results from one of these model runs provided the interbasin and intrabasin groundwater flow rates reported in the BARCAS SIR (Welch and Bright, in review). The BARCAS DSC model is documented in the DRI satellite report which was prepared for the BARCAS study (Lundmark et al., 2007). In addition to their relevance with respect to the BARCAS study, the results from the base BARCAS DSC model provide examples for evaluating the effects on model optimization approach, a topic examined in more detail in the deterministic-sensitivity analysis section of this report.

Three sets of results were generated for the base BARCAS DSC model; one set for each of the three optimization scenarios C, O, and O*. For each optimization scenario, the DSC model generated as output the set of fractional and volumetric groundwater flow rates between model cells and out of the model domain that best satisfied the calibration criteria. Predicted δD values, predicted outflow rates, and objective function (wRMSE) values are presented in Table 10. Summary water budgets for the 12 basins of the study area are presented in Table 11, where results for sub-basins are combined to yield net basin values. Figure 13 presents a summary of predicted interbasin groundwater flow rates for the 20 model cells and provides estimates for interbasin groundwater outflow from the study area, calculated by subtracting the estimated groundwater ET discharge from the model-predicted total outflow from the model domain. Modeling results for each of the three base BARCAS DSC model optimization scenarios are described below.

5.1.1 Optimization Scenario C: Concentration

The DSC model was initially run using only concentration criteria for model optimization. Absolute error in predicated deuterium values ranged from 0 ‰ for Lake Valley (cell 2), southern White River Valley (cell 5), Newark Valley (cell 12), and Tippet Valley (cell 18) to 7 ‰ for Long Valley (cell 19). The overall $wRMSE_c$ (concentration only) for this scenario was 0.85. If evaluated using the $wRMSE_o$ and $wRMSE_{o*}$ concentration + outflow objective functions, the overall wRMSE values for scenario C were 2.98 and 6.37, respectively.

Optimization using only concentration criteria successfully predicted locations and rates for interbasin groundwater flow; however, predicted rates of groundwater outflow (combination of groundwater flow out of the study area and discharge as groundwater ET) appeared significantly lower than the estimated groundwater ET rates for selected basins (Table 5). Under scenario *c* the DSC model predicted practically no outflow for Butte Valley (cell 13), Lake Valley (cell 2), and Spring Valley (cells 4, 15, and 16), indicating that groundwater outputs for these basins are entirely interbasin groundwater outflow and that no groundwater ET discharge occurs. Conversely, under scenario *c* the DSC model predicted outflow rates for central Steptoe Valley (cell 11) and northern White River Valley (cell 7) which are significantly greater than the groundwater ET discharge estimates for these sub-basins which have no outlet for interbasin

groundwater outflow to outside the study area given the assumed cell configuration and hydrogeologic boundaries of the sub-basins.

5.1.2 Optimization Scenario O: Concentration + Outflow

To deter model-predicted outflow rates which were significantly less than the groundwater ET discharge estimates, the objective function was modified to include both concentration and outflow criteria for scenario O. Under this scenario, an iteration was penalized if a cell's outflow rate was less than the estimated groundwater ET rate. Errors for predicted versus observed δD values were comparable to the *c* scenario, with absolute errors ranging from 0 ‰ for Lake Valley (cell 2), southern White River Valley (cell 5), Newark Valley (cell 12), and Tippett Valley(cell 18) to 6 ‰ for Long Valley (cell 19) and central Steptoe Valley (cell 11). The overall $wRMSE_c$ for predicted versus observed concentrations was 0.93. For concentration + outflow objective functions, overall values for scenario o were 0.66 ($wRMSE_o$) and 1.35 ($wRMSE_{o*}$).

Predicted outflow rates compared more favorably with the estimated groundwater ET rates, with total outflow rates being greater than or equal to total groundwater ET rates for all basins except Lake Valley (cell 2), Long Valley (cell 19), and Spring Valley (cells 4, 15, and 16). Elevated outflow rates were still observed for the central Steptoe Valley (cell 11) and northern White River Valley (cell 7); however, there was a significant reduction in the predicted outflow rate for northern White River Valley.

5.1.3 Optimization Scenario O*: Concentration + Modified Outflow

Given the extent of the study area, the assumed DSC model cell connectivity, and/or the interpreted hydrogeologic boundaries, interbasin groundwater outflow out of the model domain is not possible for Jakes Valley, northern White River Valley, central Steptoe Valley , southern Steptoe Valley, northern Spring Valley, central Spring Valley, and southern Spring Valley. For example, northern White River Valley is surrounded by other DSC model cells to the north, east, and south and by a geologic structure to the west through which groundwater flow is not likely. For these cells, predicted groundwater outflow from the model should represent only discharge as groundwater ET. To deter model-predicted outflow rates from significantly exceeding groundwater ET discharge estimates for interior cells, the objective function was modified for the O* scenario to penalize the model if interior cells' outflow rates were greater than or less than the estimated groundwater ET rates. Other cells were assessed using the same criteria as the scenario O.

Error for predicted versus observed deuterium values for the scenario O* were comparable to scenarios C and O, with absolute errors ranging from 0 ‰ to 6 ‰. Considering concentration only, the overall objective function ($wRMSE_c$) for scenario O* was 0.98. For concentration + outflow objective functions, overall values for scenario O* were 0.70 for both $wRMSE_o$ and $wRMSE_{o*}$. Model results shown in Table 3 and Figure 6 show that the additional optimization criteria were successful at reducing predicted

outflow rates from selected cells; however, the revised criteria had an unfavorable effect on the predicted net outflow from White River Valley where the net outflow rate was less than the predicted groundwater ET rate.

5.2 Deterministic-Sensitivity Uncertainty Analyses

Model simulations run for the deterministic-sensitivity analyses provide information on the effects of different optimization criteria, objective functions, and recharge δD value interpolation methods. Seven deterministic-sensitivity analysis simulations are presented here, as summarized on Table 6. The first three simulations (DS-1, DS-2, and DS-3) are identical to the base BARCAS DSC model runs with optimization scenarios C, O ,and O*, respectively. The remaining four simulations reflect different recharge δD interpolation method (simulations DS-4, DS-5, and DS-7) or a different objective function (DS-7).

Model results from the seven deterministic-sensitivity uncertainty analysis simulations are summarized on Table 12. The summary includes values directly output by the DSC model (cell-to-cell flow rates, outflow from the model domain, and predicted concentrations for each cell) and water budget values calculated from the model output and/or input values (net interbasin groundwater inflow, net interbasin groundwater outflow within the model domain, potential interbasin groundwater outflow out of the model domain). The following subsections describe the sensitivity of model results to

variations in recharge δD value interpolation method and the objective function used for model optimization.

5.2.1 Recharge δD Estimation Method

As described in Section 4.6.1, recharge δD values for model cells were estimated either by: 1) combining a prediction map generated by an IDW algorithm with the spatial recharge distribution to generate recharge-weighted average δD values for model cells interpolation, or 2) applying a latitude regression model to the latitude of each model cell's centroid. Recharge δD values from both estimation methods were used as model inputs for the deterministic-sensitivity uncertainty analysis.

The different estimation methods yielded different δD values (Table 7). The difference between recharge δD values (ΔδD) for model cells calculated using the different estimation methods were generally between +2‰ and -2‰; however for four cells the ΔδD was larger: Little Smoky Valley(cell 6, ΔδD = 8‰), Jakes Valley (cell10, ΔδD = 3‰), Newark Valley (cell 12, ΔδD = 3‰) and Spring Valley – north (cell 16, ΔδD = -3‰). The relatively large differences for Little Smoky Valley and Newark Valley are a result of sparse recharge deuterium sample locations within these basins and relatively lighter (more negative) average recharge δD values by the IDW method than model cells at similar latitudes. Similarly, there are relatively few recharge deuterium sample locations associated with northern Spring Valley and the average recharge δD value for

this model cell is relatively heavier (less negative) than recharge deuterium samples at similar latitude to the west. Jakes Valley has a relatively high density of recharge samples along its western boundary; however, the associated δD values are lighter (more negative) than recharge samples at similar latitude in the study area to the west. IDW-interpolated Recharge δD values calculated by the latitude regression method were typically heavier (less negative δD value) than the values calculated by the IDW method.

Model sensitivity to recharge δD estimation method is demonstrated by comparing model results from simulation pairs DS-1 and DS-4, DS-2 and DS-5, and DS-3 and DS-6. Each of these simulation sets has used the same objective function but different recharge δD interpolation methods (Table 6). The three objective functions used were wRMSEc (simulations DS-1 and DS-4), wRMSEo (simulations DS-2 and DS-5), and wRMSEo* (simulations DS-3 and DS-6).

A comparison of interbasin (cell to cell) groundwater flow rates for each pair of simulations indicates that the recharge estimation method has a variable effect on model predictions. Of the 27 interbasin groundwater flows included in the model, 9 were dramatically affected by recharge δD estimation method under one or more optimization scenario. The remaining 18 interbasin groundwater flow rates were relatively unaffected by recharge δD estimation method.

Interbasin flowrates to and from Newark Valley were strongly affected by recharge δD estimation method for each optimization scenario. A reversal in flow direction between Newark Valley (cell 12) and Little Smoky Valley (cell 6) occurs depending on recharge δD estimation method. Hundreds to thousands of acre-feet/year of flow are predicted from Little Smoky Valley to Newark Valley when recharge δD values from the IDW method are used as model inputs, while tens of thousands of acre-feet/year of flow are predicted from Newark Valley to Little Smoky Value when recharge δD values from the latitude regression method are used. Flow from Long Valley (cell 19) to Newark Valley also increased dramatically when recharge δD values from the latitude regression method were used, and under optimization scenario O* the increased flow from Long Valley to Newark Valley was compensated by increase flow from Butte Valley (cell 13). The changes to flow dynamics amongst Little Smoky Valley, Newark Valley, and Long Valley were a result of the following:

- Recharge δD values for Little Smoky Value changed from lighter than the observed concentration to heavier than the observed δD value, pulling isotopically lighter groundwater from Newark Valley into Little Smoky Valley.
- Increased (heavier) recharge δD value for Newark Valley relative to the observed δD value pulls isotopically lighter groundwater from Long Valley.

The revised recharge δD value interpolation method affected substantial increases of groundwater flowrates between central Spring Valley (cell 15) and Tippett Valley (cell 18) for all optimization scenarios and between Tippett Valley and northern Snake Valley (cell 14) under optimization scenario *c*. The increased flow from central Spring Valley to Tippett Valley was a response to the lighter (more negative) recharge δD value for Tippett Value from the latitude regression method.

Other interbasin flow rates were affected substantially for only two or one optimization scenarios. These include flows from Cave Valley (cell 3) to southern White River Valley (cell 5) under scenarios C and O, central Steptoe Valley (cell 11) to northern White River Valley (cell 7) under scenario O, and southern Steptoe Valley (cell 9) to southern Spring Valley (cell 4) under scenarios O and O*.

Recharge δD interpolation method affected the predicted rates for groundwater outflow from the model domain; however, the variations in groundwater outflow rates are influenced more strongly by optimization criteria. When optimization criteria did not include target groundwater ET discharge rates, model-predicted outflows from the model domain were simply the excess water remaining after cell-to-cell fluxes were optimized to achieve the best fit for observed δD values in model cells and from this perspective changes in groundwater outflow from the model domain are a side-effect of changes in cell-to-cell flowrates which were affected by different recharge δD assumptions.

The recharge δD values calculated by the different interpolation methods affected slight differences in model performance, as evident by the variations in calculated objection function values (Table 12). When optimized criteria included only concentration, the model performed slightly better with recharge δD values calculated by the IDW-interpolation method than when values calculated by latitude regression were used, as evident by the slightly lower wRMSEc value for simulation DS-1 (0.85) compared to simulation DS-4 (0.87). Based on the overall objective function values, IDW-interpolated recharge δD values also appear to have resulted in better model performance for optimization scenarios O and O*, as evident by lower wRMSEo values for simulation DS-2 (0.66) compared to DS-5 (0.72) and lower wRMSEo* values for simulation DS-3 (0.70) compared to DS-6 (0.74).

Another indicator of recharge δD estimation method performance is a comparison between estimated recharge δD values and observed δD values in model cells whose only input is recharge. Cells may have only recharge as input if they are either 1) not downstream of any model cell based on the DSC model cell connectivity, shown in Figure 8, or 2) do not receive interbasin flow from any other model cells after model optimization. Model cells which are not downstream of any other model cells are southern Steptoe Valley (cell 9), Butte Valley (cell 13), and northern Spring Valley (cell 16). Model cells which are predicted to receive either no flow or very little flow (less than 10 acre-feet/year) under all optimization scenarios include Cave Valley (cell 3), central Steptoe Valley (cell 11), and northern Steptoe Valley (cell 20). As the only input

to these cells is recharge, the observed δD value should match the recharge δD value. A comparison between recharge and observed δD values is not possible for Butte Valley because no representative data were identified for calculating and observed value. For the other cells, a comparison between recharge δD values calculated by the two estimation methods with observed δD values indicates that the recharge δD value estimated by IDW-interpolation more closely match observed δD value for southern Steptoe Valley, while recharge δD values estimated by latitude regression more closely match observed δD values for Cave Valley, northern Spring Valley, and northern Steptoe Valley.

5.2.2 Optimization Criteria and Objective Functions

The set of simulation results from the BARCAS DSC base model (simulations DS-1, DS-2, and DS-3) and the set of results from the analogous simulations DS-4, DS-5, and DS-6, where optimization criteria were the same but different recharge δD estimation methods were employed, provide a basis for comparing the effects of optimization criteria and objective function on model results for optimization scenarios C, O and O*. A detailed discussion on the effects of optimization criteria and the associated objective functions was presented with the results from the BARCAS base DSC model in Section 5.1, where model results from optimization scenarios C, O ,and O* were described. The general pattern in model results between optimization scenarios for simulations DS-4, DS-5, and DS-6 was similar to the pattern of results for simulations DS-1, DS-2, and DS-3.

The optimization scenarios C, O, and O* represent increasing constraint on predicted rates for outflow from the model domain. Under optimization scenario C, model results represent the best fit for predicted versus observed δD values for model cells. The results from optimization scenario C for some model cells may be unrealistic for two reasons: 1) predicted outflows for some model cells were either close to zero or much less than estimated groundwater ET discharge rates, or 2) model-predicted outflow rates were much higher than estimated groundwater ET discharge rates for model cells which are either located in the interior of the model domain or for which interbasin groundwater out of the model domain is not permitted based on the geology. The implementation of a target minimum groundwater ET discharge rate via the wRMSEo objective function (used for optimization scenario O) corrects for the first type of unrealistic predicted outflow rates and the invocation of an additional constraint on outflow rates for interior-type model cells corrects for the second type of unrealistic predicted outflow rates. A comparison of model results between the set DS-1, DS-2, and DS-3 and set DS-4, DS-5, and DS-6 illustrates that model behavior is very sensitive to optimization criteria.

The objective functions associated with optimization scenarios C, O, and O* are all variations of the weighted RMSE function (see equation 7). To further evaluate the sensitivity of the model to objective function selection, the SAE function was used for simulation DS-7. The SAE function is a non-weighted objective function which reduces

the potential overweighting of large errors that may occur with squared error type functions such as root mean squared error. Simulations DS-3 and DS-7 represent a set of model runs were all model inputs were identical, the optimization criteria (concentration only) was the same, and only the objective function used for model optimization was varied. As shown on Table 12, cell-to-cell flow rates varied by greater than 10,000 acre-feet/year for 9 out of 28 flowpaths between simulations DS-1 and DS-7. Predicted groundwater flow rates within Snake Valley were strongly effected, with variations in flow rate greater than 100,000 acre-feet/year for flows between southern (cell 1) and central (cell 8), central and northern (cell 14), and northern and northeastern (cell 17) sub-basins for the DS-1 and DS-7 simulations. Predicted rates of outflow from the model domain for simulations DS-1 and DS-7 varied by greater than 10,000 acre-feet/year for seven model cells, including cells associated with Butte Valley (cell 13), Snake Valley (cells 1, 8, and 17), Spring Valley (cell 15), Tippett Valley (cell 18), and White River Valley (cell 7).

A comparison of calculated objective functions between simulations DS-1 and DS-7 (Table 12) shows that when optimized based on concentration only, model results from simulation DS-1 had a better (lower) calculated wRMSEc, wRMSEo, and SAE value, while simulation DS-7 yielded a lower wRMSEo* value. This suggests that the combination of weighting and error-squaring associated with optimization objective function for simulation DS-1 (wRMSEc) was better able to match predicted δD values to observed δD values. The lower wRMSEo* value calculated for simulation DS-7 results

suggest that using the SAE objective function for model optimization yielded model results which were less inconsistent with conceptual groundwater flow and ET discharge assumptions.

The results from the deterministic-sensitivity analysis illustrate how model performance is strongly affected by optimization criteria and objective function selection. The inclusion of both concentration (δD values) and groundwater outflow rates as optimization criteria generates a multiple-objective optimization problem. For the simulations described above, the multiple-objective problem was translated into a single-objective problem in the simulations described above by utilizing objective functions which used weighting terms to combine concentration errors and outflow errors into a single value. A limitation to this approach is that it may not adequately represent the multiple-objective optimization problem for which the solution is characteristically non-unique (Yapo et al., 1998).

Another approach to multiple-objective optimization problems is through the evaluation of Pareto-optimal solutions, where the model is optimized to generate a set of model results which represent minima within the objective space of two or more objective functions. The Multiple-Objective COMplex Evolution (MOCOM) algorithm is an example of an automated global optimization algorithm for multiple-objective problems (Yapo et al., 1998). Appendix C presents a comparison of optimization approaches applied to an eight-cell DSC model comprising a subset of the BARCAS

study area basins. Optimization approaches compared include SCE and MOCOM algorithms, as well as a uniform random search approach.

5.3 Monte Carlo Uncertainty Analyses

The results for the Monte Carlo uncertainty analysis simulations MC-1 through MC-7 are presented in Table 13 and on Figure 14 as 95-percent confidence intervals for water budget components. Each of the 1,000 realizations from Monte Carlo simulations MC-1 through MC-4, MC-6, and MC-7 generated a set of interbasin groundwater flows and outflows for the model cells. For each cell, the 1,000 simulated interbasin inflows, interbasin outflows, and outflows from the model domain were sorted in ascending order. The 26th and 975th values from the sorted results were identified as the lower confidence limit (LCL) and upper confidence limit (UCL) for the 95-percent confidence interval, respectively. For simulation MC-5, 740 Monte Carlo realizations were performed and the LCL and UCL of the 95-percent confidence interval were identified from the 19th and 721st values from the sorted results. In addition to the flow rate information, Table 13 also provides the median results and a statistical summary of the objective function values which were output by the model during optimization for each realization.

The potential variability in water budget components for the 12 study area basins is shown on Figure 14. Basin water budgets are presented which include the following items:

- “Inputs” include recharge from precipitation and interbasin inflow.

- "Outputs" include outflow from the model domain, target groundwater ET discharge rates, and interbasin outflow. Note that groundwater ET rates are not subtracted from the total outflow from the model domain.
- "Intrabasin flow" is included for hydrographic areas which have been divided into sub-basins (Snake Valley, Spring Valley, Steptoe Valley, and White River Valley).

The magnitudes for water budget components show large range, with some basins not having any water budget component greater than 50,000 acre-feet/year, compared to Snake Valley, where multiple water budget components may exceed hundreds of thousands of acre-feet per year. Generally, basin water budgets could be classified into small, medium and large as follows:

- Basins with small water budgets (no component greater than 50,000 acre feet/year) include Cave Valley and Tippett Valley. These basins are characterized by relatively little recharge and interbasin groundwater inflow.
- Basins with medium water budgets (some components between 50,000 acre-feet/year and 100,000 acre-feet/year) include Butte Valley, Lake Valley, Little Smoky Valley, Long Valley, Newark Valley, and Spring Valley. These basins, comprising half of the study area basins, are characterized by greater potential recharge rates or interbasin groundwater inflow from other study area basins.

- Basins with large water budgets (some components exceeding 100,000 acre-feet/year) include Jakes Valley, Snake Valley, Steptoe Valley, and White River Valley. These basins all receive potentially large amounts of interbasin groundwater inflow from one or more other basins.

The two basins with the largest water budget components for simulations are Snake Valley and White River Valley. These basins are representative of integrators for multi-basin flow systems predicted by the model for the study area. White River Valley receives interbasin groundwater inflow from Cave Valley, Jakes Valley, and potentially Long Valley via Jakes Valley. Snake Valley receives inflow from Spring Valley, Lake Valley (via Spring Valley), Steptoe Valley (via Lake Valley and Spring Valley), and potentially Tippett Valley. These multi-basin flow systems constitute groundwater sources for the Colorado Regional Flow System and the Great Salt Lake Desert Regional Flow System (Figure 3).

The bars on Figure 14 illustrate that while there is substantial uncertainty associated with model cells' water budget components as a function of Monte Carlo simulation, some sets of model results for individual water budget components are always greater than zero while others are never greater than zero. Outflows from the model domain were always tens of thousands of acre-feet/year or greater for southern White River Valley (cells 5), northeast Snake Valley (cell 17), and northern Steptoe Valley (cell 20). Interbasin groundwater flow rates were always greater than 1,000 acre-feet/year between southern Spring Valley and southern Snake Valley (cells 4 to 1),

southern Steptoe to Lake Valley (cells 9 to 2), and Jakes Valley to northern White River Valley (cells 10 to 7). Intrabasin groundwater flows were always hundreds of acre-feet/year or greater within Snake Valley (cells 1 to 8 to 14 to 17), White River Valley (cells 7 to 5), and from northern to central Spring Valley (cells 16 to 15). Model-predicted flow rates were always less than 10 acre-feet/year for southern Steptoe Valley (cell 9) to Cave Valley and central Spring Valley (cells 3 and 15, respectively) and for central to northern Steptoe Valley (cell 11 to cell 20) and less than 600 acre-feet/year for Jakes Valley to Long Valley (cell 10 to cell 19).

Flow directions between model cells 6 (Little Smoky Valley) and 12 (Newark Valley) and between cells 10 (Jakes Valley) and 19 (Long Valley) were determined by the model during the optimization process. Flows between these cells are listed in both "Input" and "Output" categories on the water budget component figure (Figure 14). For the set of Monte Carlo simulations performed, the model predicted flow to primarily occur from Long Valley (cell 19) to Jakes Valley (cell 10), as the flow from Jakes Valley to Long Valley was usually zero or less than about 600 acre-feet/year. Flow direction between Newark Valley and Little Smoky Valley showed more variability, however the upper control limits for 95-percent confidence intervals for all Monte Carlo simulations are greater for flow from Newark valley to Little Smoky Valley than for Little Smoky Valley to Newark Valley.

5.3.1 Water Budget Component Frequency Distributions

The upper and lower limits of the 95-percent confidence intervals provided in Table 13 and on Figure 14 provide a general description for the ranges of distributions for model inputs and model-predicted values; however, these summary statistics do not provide any description for distributions' shapes. As a method for illustrating the distributions associated with water budget components, frequency distributions were developed for Spring Valley. A frequency distribution shows the frequency that a value falls within a specific bin of values and is a useful tool for approximating a probability distribution function. Spring Valley was selected as an example basin due to its range in recharge and discharge rates and its interaction with other model cells via inflow and outflow.

A water budget component frequency distribution for Spring Valley from Monte Carlo simulation MC-5 is shown on Figure 15. The frequency distribution includes the following components:

- total recharge to Spring Valley (sum of recharge rates for cells 4, 15, and 16)
- total groundwater ET discharge (GWET, sum for cells 4, 15, and 16)
- total outflow minus GWET (sum of outflows from model domain minus the sum of GWET rates for cells 4, 15, and 16)
- total interbasin inflow (sum of inflow rates from cells 2 [Lake Valley] and 9 [southern Steptoe Valley])

- total interbasin outflow (sum of outflow rates to cells 1 [southern Snake Valley], 14 [northern Snake Valley], and 18 [Tippett Valley])

The total for each of these components were calculated for each of the 1,000 realizations, then the frequency distributions for the summed components were determined.

The shapes for the frequency distributions appear bell-shaped for total GWET and total interbasin inflow, more uniform for total recharge and total interbasin outflow, and much narrower for total outflow minus GWET. The reasonably normal-shaped distribution for total GWET illustrates that when three uniform distributions of GWET were combined, the resulting total GWET distribution appears more normal than uniform. This effect is less pronounced for recharge. The frequency distribution also illustrates that there is more uncertainty (i.e., a wider distribution) associated with interbasin outflow rates than inflow rates. The relatively narrow distribution and predominantly negative rates for total outflow minus GWET suggest that for Monte Carlo simulation MC-5 the optimization objective function (wRMSEo) yielded minimum GWET discharge rates and that the model does not predict groundwater flow to outside the model domain from Spring Valley.

5.3.2 Stability of Statistics

The stability of statistics for model results was evaluated by plotting the mean and 95-percent confidence interval about the mean versus realization number for selected

model outputs. The 95-percent confidence interval for parameter x about the mean for realization n, $X(n)_{\alpha=0.05}$, is calculated as:

$$X(n)_{\alpha=0.05} \approx \bar{x}(n) \pm t_{\alpha/2,n-1} \frac{s(n)}{\sqrt{n}} \tag{17}$$

where n is the realization number, $\bar{x}(n)$ is the mean value of x for realizations 1 through n, $t_{\alpha/2,n-1}$ is the Student's t-statistic, and $s(n)$ is the standard deviation of x for realizations 1 through n.

Plots for the stability of statistics for water budget components for Spring Valley for Monte Carlo simulation MC-5 are provided in Figure 16 (interbasin inflow), Figure 17 (interbasin outflow), and Figure 18 (outflow from the model domain). Spring Valley was selected for this example because of its inclusion of all water budget components and to allow comparison with the water budget component frequency distributions described in the previous section. The stability plots begin at realization $n = 5$.

Statistics are consistently stable across the entire 1,000 realization simulation for inflow from cell 9 (southern Steptoe Valley) to cell 15 (central Spring Valley) and outflow from the model domain for cell 16 (northern Spring Valley). Small perturbations in statistics are apparent overt the first 100 realizations for inflow from cell 9 to cell 4 (southern Spring Valley), outflow from cell 15 to cell 18 (Tippett Valley), and outflow from the model domain for cell 15. Relatively large variability in statistics versus realization is apparent for inflow from cell 2 (Lake Valley) to cell 4, outflow from cell 4 to cell 1 (southern Snake Valley) and cell 15 to cell 14 (northern Snake Valley), and

outflow from cell 4. Statistics for outflow from cell 15 to cell 14 and outflow from to model domain from cell 4 appear to stabilize relatively quickly, on the order of a few hundred realizations. Statistics for inflow to cell 2 from cell 4 and outflow from cell 4 to cell 1 appear to gradually stabilize over the 1,000-realization simulation,; however, a slight upward trend in the statistics plots are still visible at realization n = 1,000. This suggests that a greater number of realizations may be necessary to more completely characterize these components of the water budget.

5.4 Uniqueness of Model Solutions

The Monte Carlo uncertainty analysis results presented and described in Section 5.3 were for simulations MC-1 through MC-7 which included distributions for model input parameters. Simulation MC-8 differed from the other Monte Carlo simulations by using the same model inputs for all 1,000 realizations. In this manner, this simulation evaluated how the starting population of simplex complexes for the SCE algorithm (determined by a random generator) affects model output. The variability of model output from this simulation provides an estimate for how non-uniqueness affects the model solutions.

Table 14 provides the median and upper and lower control limits for the 95-percent confidence interval for model output parameters for simulation MC-8, similar to the summary provided in Table 13 for simulations MC-1 through MC-7. A comparison between the upper and lower control limits of the 95-percent confidence interval provides

an indicator for the range of results which are attributable to model uncertainty. Confidence interval ranges are generally small for model-predicted flowrates between cells and outflow from the model domain; however, ranges are greater than 1,000 acre-feet/year for six interbasin or intrabasin (cell-to-cell) flowrates and for outflow rates for five model cells. Ranges in model-predicted flowrates were greater than 1,000 acre-feet/year for Lake Valley (cell 2) to southern Spring Valley (cell 4), Little Smoky Valley (cell 6) to Newark Valley (cell 12), northern White River Valley (cell 7) and Cave Valley (cell 3) to southern White River Valley (cell 5), and southern Steptoe Valley (cell 9) to Lake Valley (cell 2) and southern Spring Valley (cell 4). The largest range in cell-to-cell flow rates is associated with flow from northern to southern White River Valley (cell 7 to cell 5), where the range in flowrates was about 12,700 acre-feet/year. Ranges in flowrates out of the model domain are greater than 1,000 acre-feet/year for model cells 3 (Cave Valley), 5 (southern White River Valley), 6 (Little Smoky Valley), 7 (northern White River Valley), and 12 (Newark Valley), with the largest ranges associated with southern and northern White River Valley at about 17,800 acre-feet/year and about 12,700 acre-feet/year, respectively.

The sometimes elevated ranges associated with model-predicted results suggest that the model solution is non-unique with respect to several multi-basin groundwater flow paths. This effect appears to be most pronounced in association with White River Valley, where both cell-to-cell flowrates and outflow from the model domain exhibited relatively large (greater than 10,000 acre-feet/year) variability. The ranges for these

model-predicted flowrates are still well below the expected (median) flowrates associated with intrabasin flow within and outflow from the White River Valley basin.

6. DISCUSSION

The DSC model developed and applied to for this study produced a balanced water budget which includes groundwater recharge, groundwater ET discharge, and interbasin groundwater flow components. The study area water budget was evaluated through the mass-balance modeling of a conservative tracer (deuterium) through a network of interconnected cells representing basins. Flows between model cells and out of the model domain were evaluated by varying the optimization criteria of the model to allow for increasing constraint on discharge predictions. Of the three base BARCAS DSC modeling runs, results from optimization scenario O appear to be most realistic given the unrealistic discharge (ET) rates and interbasin flow rates for scenarios C and O*, respectively, as described in the results section.

Results from the base BARCAS scenario *o* DSC model suggest that multi-basin groundwater flow systems discharge from the southern portion of White River Valley and the northeast portion of Snake Valley, the sub-basins having lowest average potentiometric surfaces within the study area. The flow system comprising Long Valley, Jakes Valley, Cave Valley, and White River Valley and discharging from the southern portion of White River Valley is consistent with the White River Regional Flow System, which has been described previously (Eakin, 1966; Kirk and Campana, 1990; Thomas et

al., 2001). The system comprising the southern portion of Steptoe Valley, Lake Valley, Spring Valley, and Snake Valley includes components that have been described previously (e.g., flow from the southern portion of Spring Valley into Snake Valley as described by Hood and Rush [1965] and Harrill et al. [1988]) as well as new potential flowpaths, notably flow from the southern portion of Steptoe Valley into Lake Valley and Spring Valley and flow from Lake Valley into Spring Valley.

The southern portion of Steptoe Valley is an important area because it has the highest average potentiometric surface within the study area, receives greater than 35,000 acre-feet/year groundwater recharge, and has a relatively low estimated groundwater ET discharge rate of less than 4,000 acre-feet/year, resulting in about 31,000 acre-feet/year of excess groundwater input which must be accounted for as interbasin groundwater outflow. Based on the available δD data for Steptoe Valley, groundwater from the southern portion of Steptoe Valley (estimated recharge δD range -111 ‰ to -115.5 ‰) does not appear to travel as intrabasin flow to the central portion of Steptoe Valley where δD values for recharge (estimated δD = -116.2 ‰ to -118.3 ‰) and the observed δD value for the cell (δD = -123 ‰) are both isotopically lighter. Groundwater recharge occurring in the southern portion of Steptoe Valley may travel south and east as interbasin flow to Lake Valley and the southern portion of Spring Valley, where the observed δD values (-111 ‰ and -110 ‰, respectively) are isotopically lighter than the intrabasin recharge occurring to these (sub)basins (approximately -105 ‰ and -108 ‰, respectively).

Rates of groundwater outflow from the study area, calculated as the total outflow from the model domain minus the groundwater ET rate, are greater than 10,000 acre-feet/year for the interior sub-basins central Steptoe Valley and central Spring Valley for scenario *o* of the base BARCAS DSC model. These elevated outflow rates may indicate 1) groundwater recharge rates are overestimated, 2) groundwater ET rates underestimate actual discharge, 3) available stable isotope (deuterium) data do not fully characterize recharge or regional aquifer characteristics, or 4) groundwater discharge occurs in a manner that is not manifested in available deuterium data for adjacent basins (i.e., groundwater discharge occurs as deep underflow or is masked by contributions from local recharge).

Interbasin groundwater inflow and outflow rates calculated for the base BARCAS DSC model for optimization scenario O, along with rates from previous estimates are presented in Figure 19 (inflow) and Figure 20 (outflow). Results from the Monte Carlo uncertainty analysis for scenario O (simulation MC-2) are shown in Figures 19 and 20 as error bars on the inflow and outflow rates. Groundwater inflow rates calculated from the DSC model were generally higher than previous estimates, with inflow rates for Jakes Valley, Lake Valley, Snake Valley, and Spring Valley being much higher than previously reported. Groundwater outflow rates calculated from the DSC model are generally comparable to previous estimates with the exception of Lake Valley, Spring Valley, and Steptoe Valley, where the DSC model predicted much higher rates than previous studies.

These higher outflow rates are reasonable given that the BCM recharge predictions developed for the BARCAS study the greater than any previously reported values for Tippett Valley, Spring Valley, Snake Valley, and Steptoe Valley (Welch and Bright, in review).

The error bars on Figures 19 and 20 illustrate how relatively small changes in recharge rates or deuterium values can have substantial effects on net basin groundwater inflow and outflow rates. Historically, most water budgets have been presented with tabulated discrete entries for water budget components and with little or no discussion of uncertainties associated with the estimated rates. The modeling presented in this thesis has attempted to demonstrate the interaction of uncertainty associated with water components.

As the accounting model integrates data from multiple aspects of the BARCAS study, and each aspect contributes to the uncertainty for the groundwater flow within the basins, within the study area, and to adjacent areas, results from the accounting model have a substantial amount of associated uncertainty. For example, the accounting model framework was based on an interpreted geology of hydrographic area boundaries and the regional potentiometric surface which was inferred from relatively few control points. Model input δD values were calculated from a geochemical database which was sparse for several areas, and recharge and discharge estimates each have uncertainty associated with their calculation methods. The Monte Carlo uncertainty analyses presented in this

thesis have quantitatively evaluated how potential variability in recharge flux and groundwater ET rates affect interbasin flows within and out of the study area.

In addition to the Monte Carlo uncertainty analysis results, another indicator of model uncertainty is provided by inspection of the results for groundwater flow and discharge rates shown from the deterministic-sensitivity analyses. The variation between optimization scenarios and recharge δD estimation methods for groundwater flow rates and patterns within and out of the study show that some regional flow patterns for the study area predicted by the DSC model change as a result of constraints on groundwater discharge (ET) rates during model optimization.

The uncertainty analyses illustrated that there is considerable variability associated with flow rates and flow paths within the study area. Calculated outflow from the study area also varied; however several basins were predicted to discharge significant quantities of water from the study area regardless of optimization approach. Based on the deterministic-sensitivity and Monte Carlo uncertainty analyses White River Valley and Steptoe Valley discharge at least 10,000 acre-feet/year of groundwater from the study as interbasin outflow and Snake Valley discharges at least 50,000 acre-feet/year. These calculated outflows from the model domain represent the water that is excess after satisfying the estimated groundwater ET discharge rates. The wide variability in calculated groundwater outflow from the model domain for Spring Valley indicates that based on the deuterium data and assumed water budget component distributions used in

the model, it is uncertain whether groundwater outflow from the study area occurs from Spring Valley.

While the model does incorporate a driver for achieving minimum outflows under certain optimization scenarios, there do not exist explicit sinks for water (or tracer) outside of the study area boundary. For this reason, calculated discharges from the study result from drivers within the study area, rather than drivers (constraints) at the model boundaries. For example, Lake Valley is generally predicted to not have significant outflow from the study area because fluxes of water (and tracer) from this cell are pulled into southern Spring Valley and southern Snake Valley and there is no "competition" from outside the study area for Lake Valley's groundwater. This condition illustrates the model's potential limitation for predicting flow to outside the study area.

Butte Valley, the northern portion of Spring Valley, and the southern portion of Steptoe Valley are "upgradient" cells that do not have potential inflow from any other model cell. As upgradient cells, the only input to each cell is precipitation recharge, therefore the observed δD values should equal the recharge δD values. Observed δD values are about 4 per mil lighter (more negative) than recharge for the southern portion of Steptoe Valley and about 5 per mil lighter for the northern portion of Spring Valley. An observed deuterium value for Butte Valley was not calculable because no appropriate δD data were identified for this basin; however, the observed value for Long Valley, which is located adjacent and east of Butte Valley, is isotopically lighter than any recharge δD values for model cells. The differences between observed δD values for

these cells compared to recharge δD values suggest that 1) there are errors associated with the assumed δD values, 2) these cells receive groundwater input from adjacent model cells, or 3) a different model or set of assumptions is necessary to explain the observed and recharge δD values.

The variability of results between optimization scenarios for the deterministic and Monte Carlo simulations illustrate an over-arching issue of model optimization based on both observed concentrations (δD values) and target outflow rates. While a model that clearly defines correlation between concentration and outflow has not been developed, it is reasonable and likely that concentration and outflow influence each other. A complicated, non-linear relationship between concentration and outflow is a reason that an inverse problem-type parameter estimation method was chosen for model optimization. Uncertainties associated with model predictions may be reduced if a revised model structure is developed which reduces the influence of potential correlation between concentration and outflow.

7. CONCLUSIONS AND RECOMMENDATIONS

The groundwater accounting model developed for this study met the objective of evaluating the uncertainty associated with basin and regional groundwater budgets using available estimates for groundwater recharge and discharge. Additional research could improve the predictive capability of the model and the interpretation of model results,

especially with respect to the uncertainty analysis and for areas with sparse or no deuterium data for recharge or regional groundwater. The following are recommendations for future research:

- The DSC model structure could be modified to explicitly include a specified component for discharge from the model domain (e.g. a groundwater ET discharge rate) for each mixed cell. Currently, target groundwater ET discharge rates are used only in objective function calculations when outflow is included as optimization criteria. Modifying the model to include a specified discharge component for each mixed cell would allow for model optimization using a single objective (deuterium values) compared to the multiple objective optimization used in this study for scenarios which include target groundwater ET outflows. If modified, the model should allow for incorporation of variability in groundwater ET discharge rates via Monte Carlo analyses.
- The distributions for recharge and groundwater ET rates used in the Monte Carlo analyses could be refined to better reflect spatial and/or temporal variability in these water budget components. Revisited distributions for recharge and groundwater ET discharge may also provide an enhanced understanding of the uncertainty in the regional water budget as a result of an extended dry period or climate change.
- A more rigorous evaluation of uncertainty associated with recharge δD values could improve the uncertainty analysis and the resulting description

of model sensitivity to assumed recharge δD values. Model uncertainty related to observed δD values could also be evaluated by incorporating distributions for cell observed δD values into the Monte Carlo uncertainty analysis.

- Groundwater samples representative of regional aquifer could be collected for chemical and isotopic analysis from (sub) basins with no data (Jakes, Butte, Central Snake Valley) or limited data (Newark Valley, central Steptoe, southern Steptoe, northeast Snake Valley)
- Additional samples from recharge areas could be collected for chemical and isotopic analysis. Deuterium data are sparse for multiple recharge areas, notably the ranges in the northwest corner of the study area (Needles, Pancake, and Maverick Springs ranges and Butte Mountains), along the southern portion of the Schell Creek Range, and from eastern areas (Deep Creek and Confusion ranges).
- The model domain could be expanded to include hydrographic areas which are adjacent to the boundaries of the current study area. The expanded model domain could allow for evaluation of the direction and rates of interbasin groundwater outflow from the current study area.
- Deuterium value inputs or DSC model cell connectivity could be re-evaluated for the upgradient cells associated with the northern portion of Spring Valley and the southern portion of Steptoe Valley. For these cells, the difference between the observed deuterium values for these cells

compared the recharge deuterium values indicates that either there are errors associated with the assumed deuterium values or these cells receive groundwater input from adjacent model cells.

- Cell input and output fluxes could be checked using chloride data for samples collected from wells and springs. Assuming there are no mineral sinks for chloride in the flow system, chloride may acts as another conservative tracer and could be used to help validate mix ratios predicted by the deuterium-calibrated DSC model. Possible flowpaths identified for the DSC model could also be evaluated using a geochemical modeling program such as NETPATH (Plummer et al. 1991). Geochemical modeling using NETPATH was completed for a subset of interbasin and intra basin flowpaths as part of the BARCAS study and the results from this modeling may help to verify or refute potential groundwater flowpaths used for the current DSC model.

8. REFERENCES

Avon, L. and T.J. Durbin, 1994. Evaluation of the Maxey-Eakin Method for Estimating Recharge to Ground-Water Basins in Nevada. *Water Resources Bulletin* 30:99-111.

Bedinger, M.S., J.R. Harrill, W.H. Langer, J.M. Thomas, and D.A. Mulvihill. 1985. Maps showing ground-water levels, springs, and depth to ground water, Basin and Range Province, Nevada: U.S. Geological Survey Water-Resources Investigations Report 83-4119-B.

Brothers, K., T.S. Buqo, and J.V. Tracy. 1993. Hydrology and Steady State Ground-water Model of Snake Valley, East-Central Nevada, and West-Central Utah. LVWD Report No. 9.

Brothers, K., T.S. Buqo, J.V. Tracy, M. Stock, C. Bentley, A. Zdon. and J. Kepper. 1993. Hydrology and Steady State Ground-water Model of Cave Valley, Lincoln and White Pine Counties, Nevada. LVWD Report No. 11.

Brothers, K., A.J. Bernholtz, T.S. Buqo, and J.V. Tracy. 1994. Hydrology and Steady State Ground-water Model of Spring Valley, Lincoln and White Pine Counties, Nevada. LVWD Report No. 13.

Calhoun, S.C. 2000. Regional groundwater flow at the Nevada Test Site using stable isotopes and trace element chemistry, M.S. thesis: University of Nevada Reno.

Campana, M.E. 1975. Finite-state models of transport phenomena in hydrologic systems, University of Arizona, Tuscon. PhD Dissertation.

Campana, M.E., W.R. Sadler, N.L. Ingraham and R.L. Jacobson. 1997. A deuterium-calibrated compartment model of transient flow in a regional aquifer system. *Tracer Hydrology 97*. A. Kranjc: 389-496.

Carroll, R.W.H., Pohll, G.M., Earman, S., and R.L. Hershey. Global optimization of a deuterium calibrated, discrete-state compartment model (DSCM): Application to the eastern Nevada Test Site. in review. Journal of Hydrology.

Carroll, R.W.H. and G.M. Pohll. In press. A User's Manual for the Discrete-state Compartment Model-Shuffled Complex Evolution (DSCM-SCE). Division of Hydrologic Sciences, Desert Research Institute.

Daly, C., R.P. Nelson and D.L. Phillips. 1994. A Statistical-topographical Model for Mapping Climatological Precipitation over Mountainous Terrain. *Journal of Applied Meteorology* 33: 140-158.

Darling, W.G. and A.H. Bath. 1988. A stable isotope study of recharge processes in the English Chalk. *Journal of Hydrology* 101: 31-46.

Dettinger, Michael, 1989, Reconnaissance Estimates of Natural Recharge to Desert Basins in Nevada, U.S.A., by Using Chloride-balance Calculations. *Journal of Hydrology*, 106 (1989) 55-78.

Dingman, S.L. 2002. *Physical Hydrology*. Prentice-Hall, Inc. Upper Saddle River, New Jersey. 2nd ed.

Drever, J.I. 1997. *The Geochemistry of Natural Waters: Surface and Groundwater Environments* - 3rd ed. Upper Saddle River, New Jersey, Prentice-Hall, Inc.

Duan, Q., S. Sorooshian, and V. Gupta. 1992. Effective and efficient global optimization for conceptual rainfall-runoff models. *Water Resources Research* 28(4): 1015-1031.

Eakin, T.E. 1960. Ground-water Appraisal of Newark Valley, White Pine County, Nevada. Nevada Department of Conservation and Natural Resources Ground Water Reconnaissance Series Report No. 1

Eakin, T.E. 1961. Ground-water Appraisal of Long Valley, White Pine and Elko Counties, Nevada. Nevada Department of Conservation and Natural Resources Ground Water Reconnaissance Series Report No. 3

Eakin, T.E. 1962. Ground-water Appraisal of Cave Valley in Lincoln and White Pine Counties, Nevada. Nevada Department of Conservation and Natural Resources Ground Water Reconnaissance Series Report No. 13

Eakin, T.E. 1966. A regional interbasin ground-water system in the White River area, southeastern Nevada. *Water Resources Research* (2): 251-271.

Eakin, T.E., J.L. Hughes and D.O. Moore, 1967. Water Resources Appraisal of Steptoe Valley, White Pine and Elko Counties, Nevada. Nevada Department of Conservation and Natural Resources Ground Water Reconnaissance Series Report No. 42.

Earman, S. and R. Hershey. In review. Groundwater recharge estimates for basins in south-central Nevada (eastern Nevada Test site and vicinity) developed using a deuterium-calibrated discrete-state compartment model, Division of Hydrologic Sciences, Desert Research Institute.

Epstein, B.J. 2004. Development and Uncertainty Analysis of Empirical Recharge Prediction Models for Nevada's Desert Basins. Hydrologic Sciences Program, University of Nevada, Reno, Master's Thesis.

Feeney, T.A., M.E. Campana, and R.L. Jacobson. 1987. A Deuterium-Calibrated Groundwater Flow Model of the Western Nevada Test Site and Vicinity, Desert Research Institute Water Resources Center Publication 45057.

Flint, A.L., L.E. Flint, J.A. Hevesi, and J.B. Blainey. 2004. Fundamental Concepts of Recharge in the Desert Southwest: A Regional Modeling Perspective. in: *Groundwater recharge in a desert environment: the southwest United States.* AGU Water Science and Application 9.

Friedman, I., J.M. Harris, G.I. Smith, and C.A. Johnson. 2002. Stable isotope composition of waters in the Great Basin, United States. 1. Air-mass trajectories. *Journal of Geophysical Research*, Vol. 107, No. D19, 14 p.

Gat, J.R. 1981. Groundwater, in Stable Isotope Hydrology, Deuterium and Oxygen-18 in the Water Cycle. Ed. J.R. Gat and R. Gonfiantini. Technical Report Series No. 210, pp. 223-240. IAEA, Vienna.

Glancy, P.A., 1968. Water Resources Appraisal of Butte Valley, Elko and White Pine Counties, Nevada. Nevada Department of Conservation and Natural Resources Ground Water Reconnaissance Series Report No. 49.

Hardman, G. 1936. Precipitation Map of Nevada *in* Nevada Agricultural Experiment Station.

Harrill, J.R. 1971. Water-resources Appraisal of the Pilot Creek Valley Area, Elko and White Pine Counties, Nevada. Nevada Department of Conservation and Natural Resources Ground Water Reconnaissance Series Report No. 56

Harrill, J.R., Gates, J.S., and Thomas, J.M. 1988. Major ground-water flow systems in the Great Basin region of Nevada, Utah, and adjacent states: U.S. Geological Survey Hydrologic Investigations Atlas HA-694-C.

Harrill, J.R., and Prudic, D.E., 1998. Aquifer systems in the Great Basin Region of Nevada, Utah, and adjacent states - Summary report: U.S. Geological Survey Professional Paper 1409-A.

Hershey, R.L., and S.A. Mizell. 1995, Water Chemistry of Spring Discharge from the Carbonate-rock Province of Nevada and California: Desert Research Institute, Water Resources Center, Publication No. 41140, 42 p., 6 appendix.

Hershey, R.L, L. Justet, V.M. Heilweil, P.M. Gardner, B.F. Lyles, S. Earman, J.M. Thomas, and K.W. Lundmark. In press. A Water Chemistry and Water Quality Assessment of Groundwater in the BARCAS Study Area. Division of Hydrologic Sciences, Desert Research Institute.

Hill, M.C. 1998. Methods and guidelines for effective model calibration: U.S. Geological Survey Water-Resources Investigations Report 98-4005: 90 p.

Hood, J.W., and F.E. Rush, 1965. Water-resources Appraisal of the Snake Valley Area, Nevada and Utah. Nevada Department of Conservation and Natural Resources Ground Water Reconnaissance Series Report No. 34

Ingraham, N.L., and B.E. Taylor. 1991. Ligth Stable Isotope Systematics of Large-Scale Hydrologic Regimes in California and Nevada. Water Resources Research, 27(1): 77-90.

Karst, G.B., M.E. Campana, and R.L. Jacobson. 1988. A mixing-cell model of the hydrothermal flow system, northern Dixie Valley, Nevada. *Transactions, Geothermal Resources Council* 12: 167-174.

Katzer, T., and D.J. Donovan. 2003. Surface Water Resources and Basin Water Budget for Spring Valley, White Pine and Lincoln Counties, Nevada. Las Vegas Valley Water District.

Kirk, S.T., and M.E. Campana, 1990. A Deuterium-calibrated Groundwater Flow Model of a Regional Carbonate-alluvial System. *Journal of Hydrology*, (119) 357-388.

Laczniak, R.J., J.L. Smith, P.E. Elliott, G.A. DeMeo, M.A. Chatigny and G.J Roemer. 2001. Ground-Water Discharge Determined from Estimates of Evapotranspiration, Death Valley Regional Flow System, Nevada and California. U.S. Geological Survey Water-Resources Investigation Report 01-4195.

Maxey, G.B. and T.E. Eakin. 1949. Ground-water in White River Valley, White Pine, Nye, and Lincoln Counties, Nevada. Nevada State Engineer Water Resources Bulletin 8, 59 p.

Mifflin, M.D. 1968. Delineation of ground-water flow systems in Nevada. University of Nevada, Reno, unpublished Doctoral Thesis, 213 p.

Mifflin, M.D. and Hess, J.W. 1979. Regional carbonate flow systems in Nevada. Journal of Hydrology, v.43, p. 217-237.

Natural Resources Conservation Service (NRCS). Climate Narrative for Eastern White Pine County Soil Survey Are, Nevada. Prepared by the NRCS Natioanl Water and Climate Center, Portland, Oregon.

Nichols, W.D. 2000. Regional Ground-water Evapotranspiration and Ground-water Budgets, Great Basin, Nevada, Chapter C. Regional Ground-water Budgets and Ground-water Flow, Eastern Nevada. U.S. Geological Survey Professional Paper 1628, 82 p.

Plummer, L.N., D.L. Prestemon, and D.C. Thorstenson. 1991. An interactive code (NETPATH) for modeling net geochemical reactions along a flow path. U.S. Geological Survey Water-Resources Investigation Report 91-4078.

Prudic, D.E., Harrill, J.R., and Burbey, T.J., 1995, Conceptual evaluation of regional ground-water flow in the carbonate-rock province of the Great Basin, Nevada, Utah, and adjacent states: U.S. Geological Survey Professional Paper 1409-D.

Roth, J.G. and M.E. Campana. 1989. A Mixing-cell Model of the Railroad Valley Regional Groundwater Flow System, Central Nevada, Desert Research Institute Water Resources Center Publication 41123.

Rush, F.E. and T.E. Eakin, 1963. Groundwater Appraisal of Lake Valley in Lincoln and White Pine Counties, Nevada. Nevada Department of Conservation and Natural Resources Ground Water Reconnaissance Series Report No. 24.

Rush, F.E. and S.A. Kazmi, 1965. Water Resources Appraisal of Spring Valley, White Pine and Lincoln Counties, Nevada. Nevada Department of Conservation and Natural Resources Ground Water Reconnaissance Series Report No. 33.

Rush, F.E. and D.E. Everett, 1966. Water Resources Appraisal of Little Fish Lake, Hot Creek, and Little Smoky Valleys, Nevada. Nevada Department of Conservation and Natural Resources Ground Water Reconnaissance Series Report No. 38.

Sadler, W.R. 1990. A Deuterium-Calibrated, Discrete-State Compartment Model of Regional Groundwater Flow, Nevada Test Site and Vicinity. Hydrologic Sciences Program. Reno, University of Nevada Reno, Master' thesis.

Scott, B.R., T.J. Smales, F.E. Rush, and A.S. Van Denburgh. 1971. Nevada's water resources: Nevada Division of Water Resources, Water for Nevada Report 3, 87 p.

Southern Nevada Water Authority. 2006. Southern Nevada Water Authority Clark, Lincoln, and White Pine Counties Groundwater Development Project Draft Conceptual Plan of Development. Prepared for U.S. Bureau of Land Management.

Thomas, J.M., Welch, A.H., and Dettinger, M.D., 1996, Geochemistry and isotope hydrology of representative aquifers in the Great Basin Region of Nevada, Utah, and adjacent states: U.S. Geological Survey Professional Paper 1409-C.

Thomas, J.M., S.C. Calhoun, and W.B. Apambire. 2001. A Deuterium Mass-balance Interpretation of Groundwater Sources and Flows in Southeastern Nevada. Division of Hydrologic Sciences, Desert Research Institute, Publication No. 41169.

Tóth, J.A. 1963. A Theoretical Analysis of Groundwater Flow in Small Drainage Basins. Journal of Geophysical Research, Vol. 68, No. 16

U.S. Geological Survey. 2005. Basin and Range Carbonate Aquifer System Study: U.S. Geological Survey Fact Sheet 2005-3035.

U.S. Geological Survey. 2006. National Water Information System (NWISWeb) data available on the World Wide Web, accessed September 12, 2006, at URL http://waterdata.usgs.gov/nv/nwis/nwis.

Watson, P., P. Sinclair and R. Waggoner. 1976. Quantitative Evaluation of a Method for Estimating Recharge to the Desert Basins of Nevada. *Journal of Hydrology*, 31 (1976) 335-357.

Welch, A.H., and D.J. Bright, ed. In review. Water Resources of the Basin and Range Carbonate Aquifer System in White Pine County, Nevada, and adjacent areas in Nevada and Utah. U.S. Geological Survey Report to Congress.

Zhu, J. In press. BARCAS Project Uncertainty Analysis of Annual Estimates of Ground-Water Discharge.

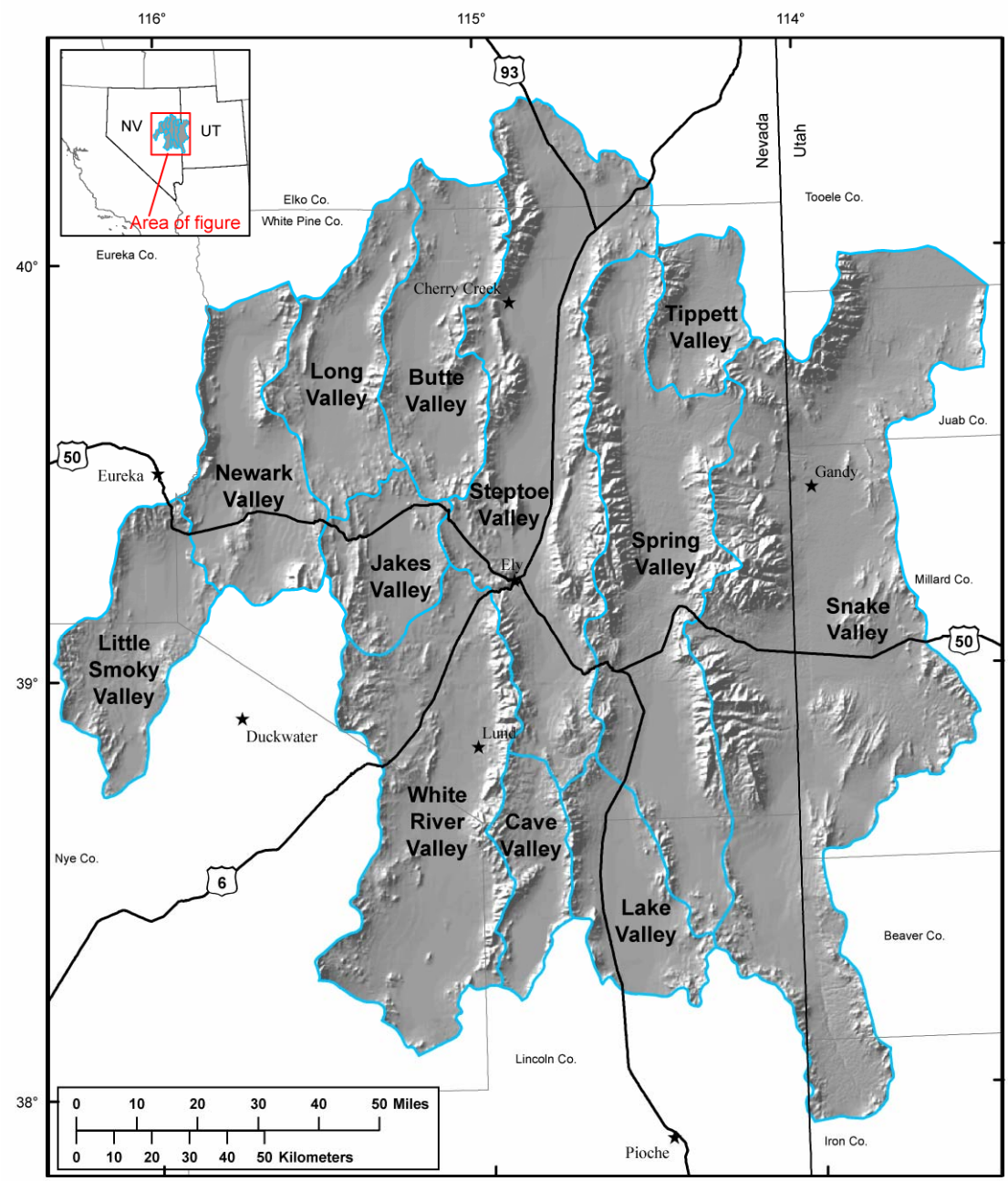

Figure 1. Study Area

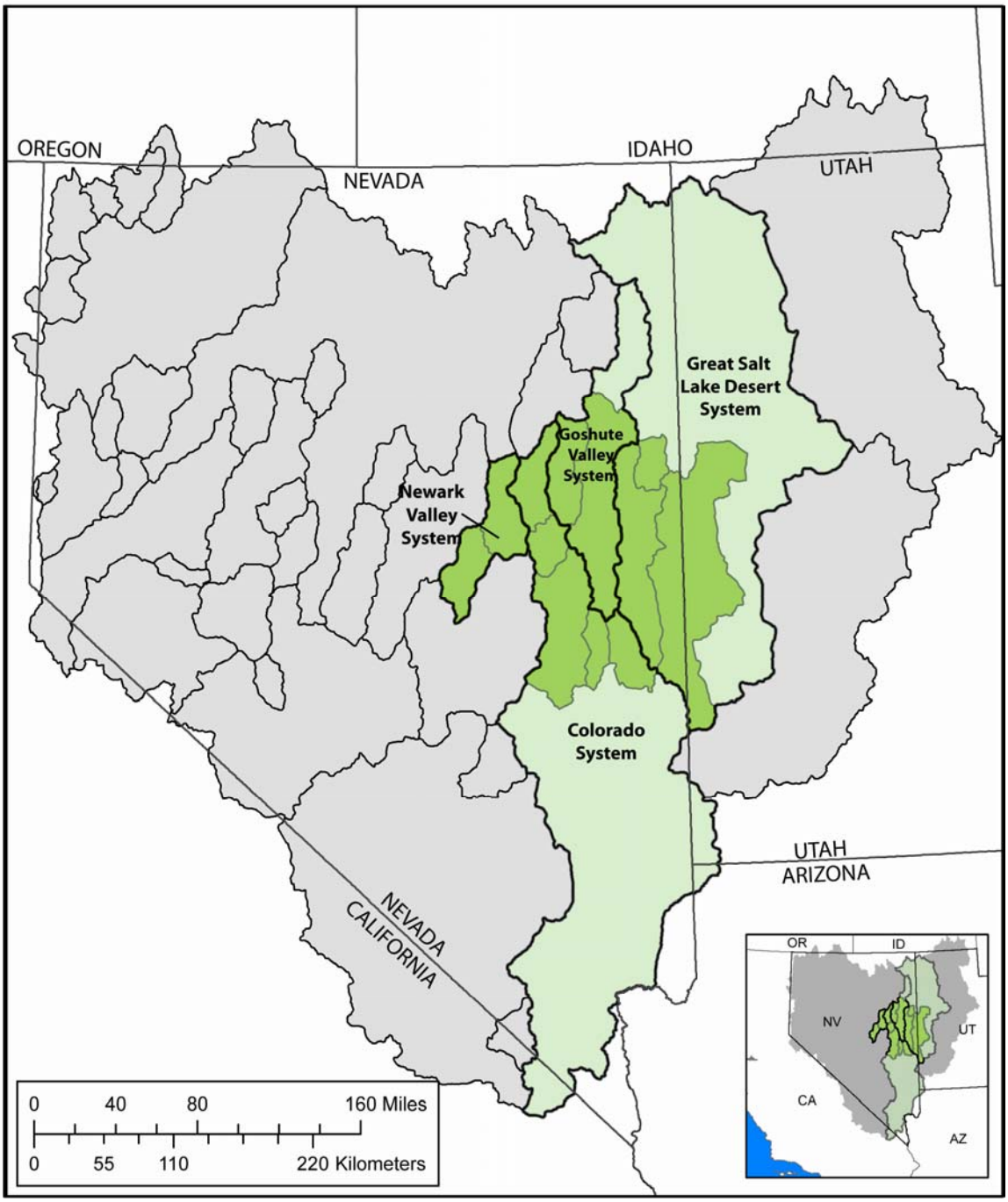

Figure 2. **Regional Groundwater Flow Systems Identified in the Great Basin Regional Aquifer System Analysis (RASA) Report.** Great Basin physiographic province is shown in gray with boundaries of regional flow systems shown as black lines. The regional flow systems associated with the BARCAS study area are shown in green, with the BARCAS study area highlighted dark green.

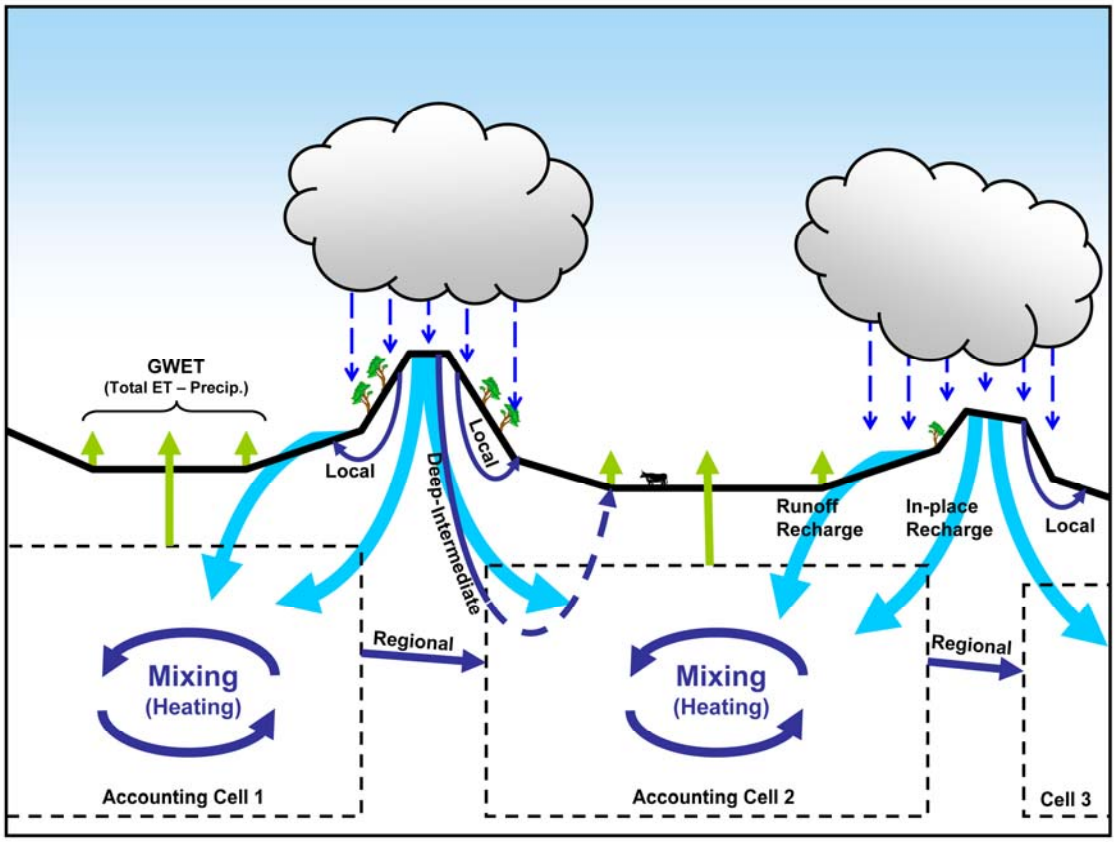

Figure 3. **Conceptual Model Showing Local, Deep-Intermediate, and Regional Groundwater Flow Systems and Water Budget Components for Accounting Model Cells**

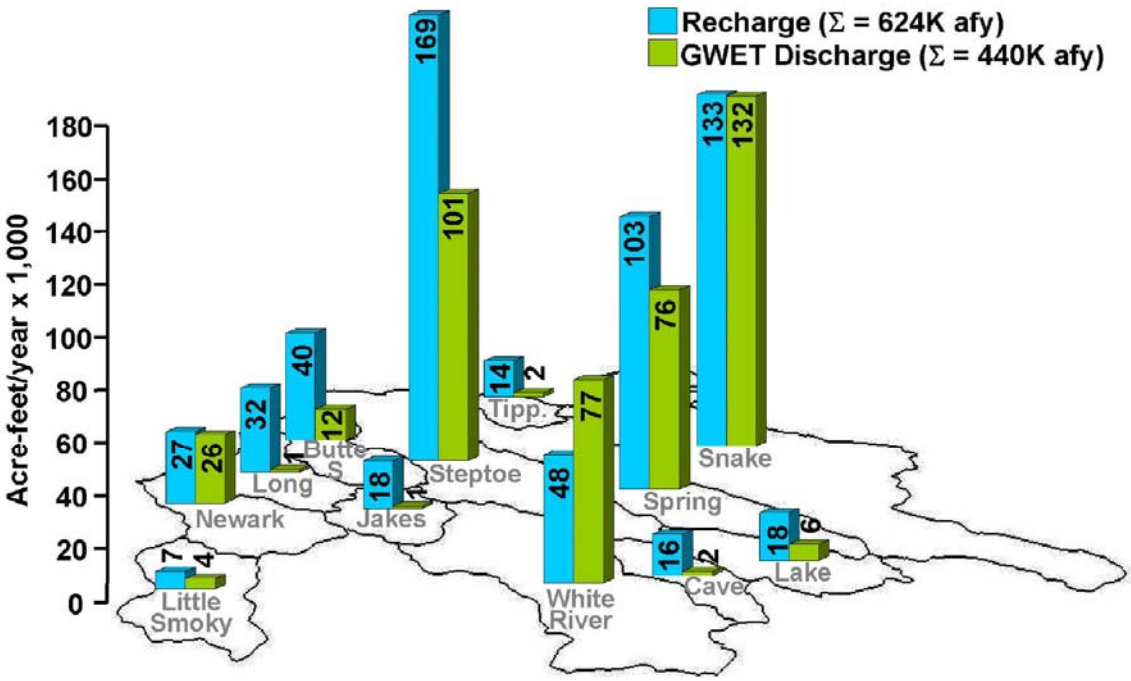

Figure 4. BARCAS Recharge and Groundwater Evapotranspiration (ET) Discharge Estimates for the Study Area

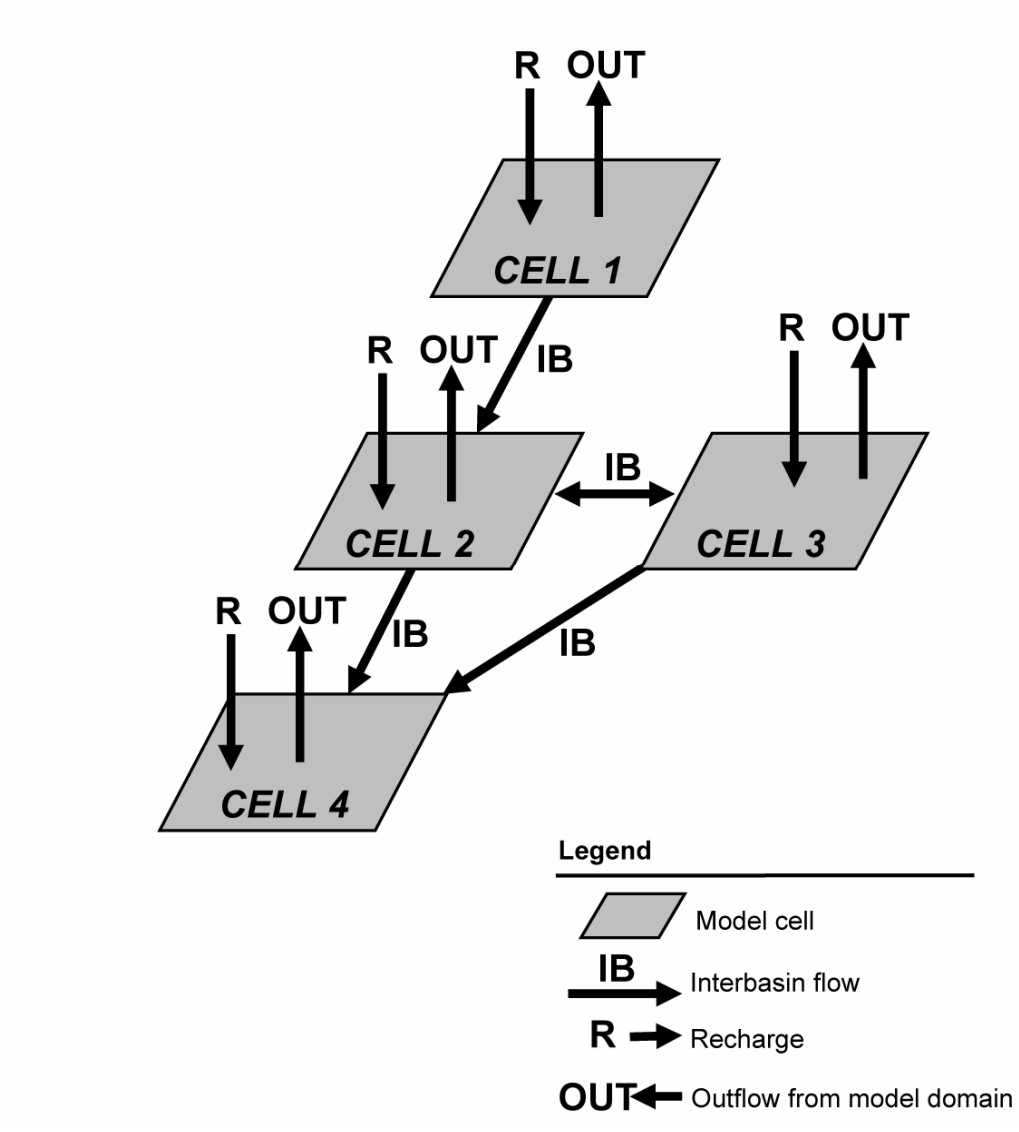

Figure 5. Discrete-State Compartment (DSC) Model Components

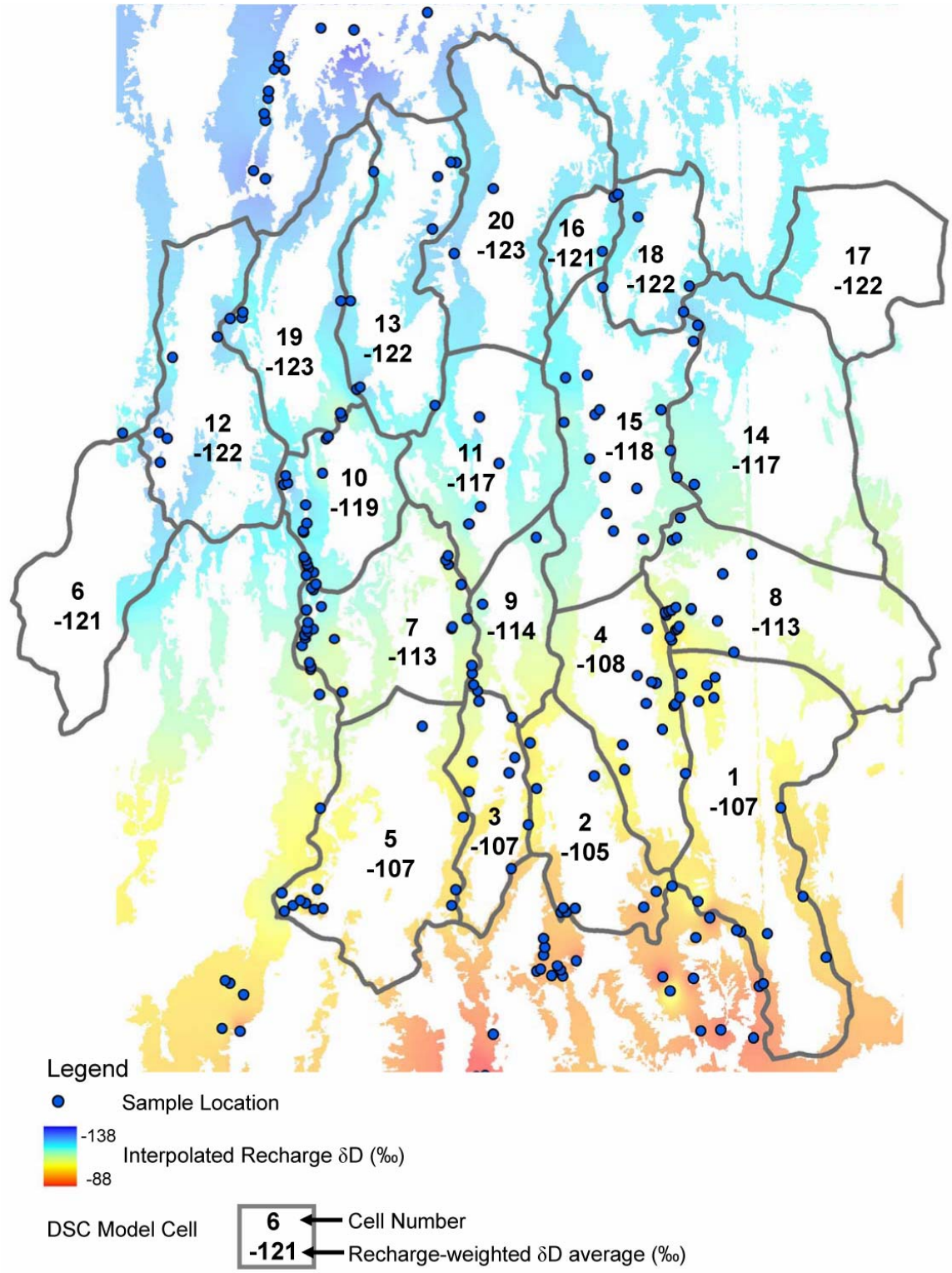

Figure 6. Recharge Deuterium Sample Locations, Inverse Distance Weighted (IDW) Interpolated Recharge Deuterium Values, and Recharge-Weighted Average Recharge Deuterium Values

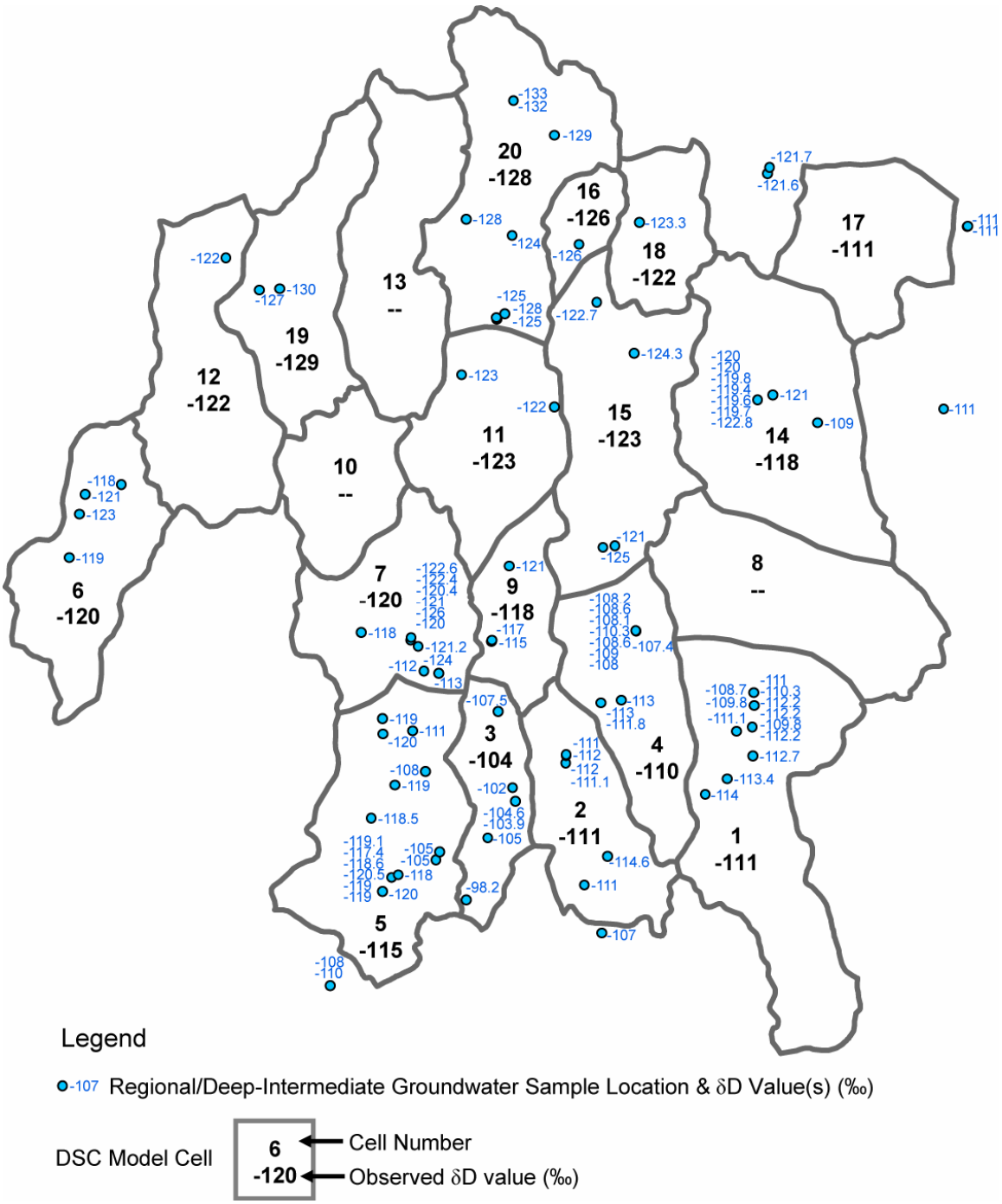

Figure 7. Regional / Deep-Intermediate Groundwater Deuterium Sample Locations and DSC Model Calibration (Observed) Deuterium Values

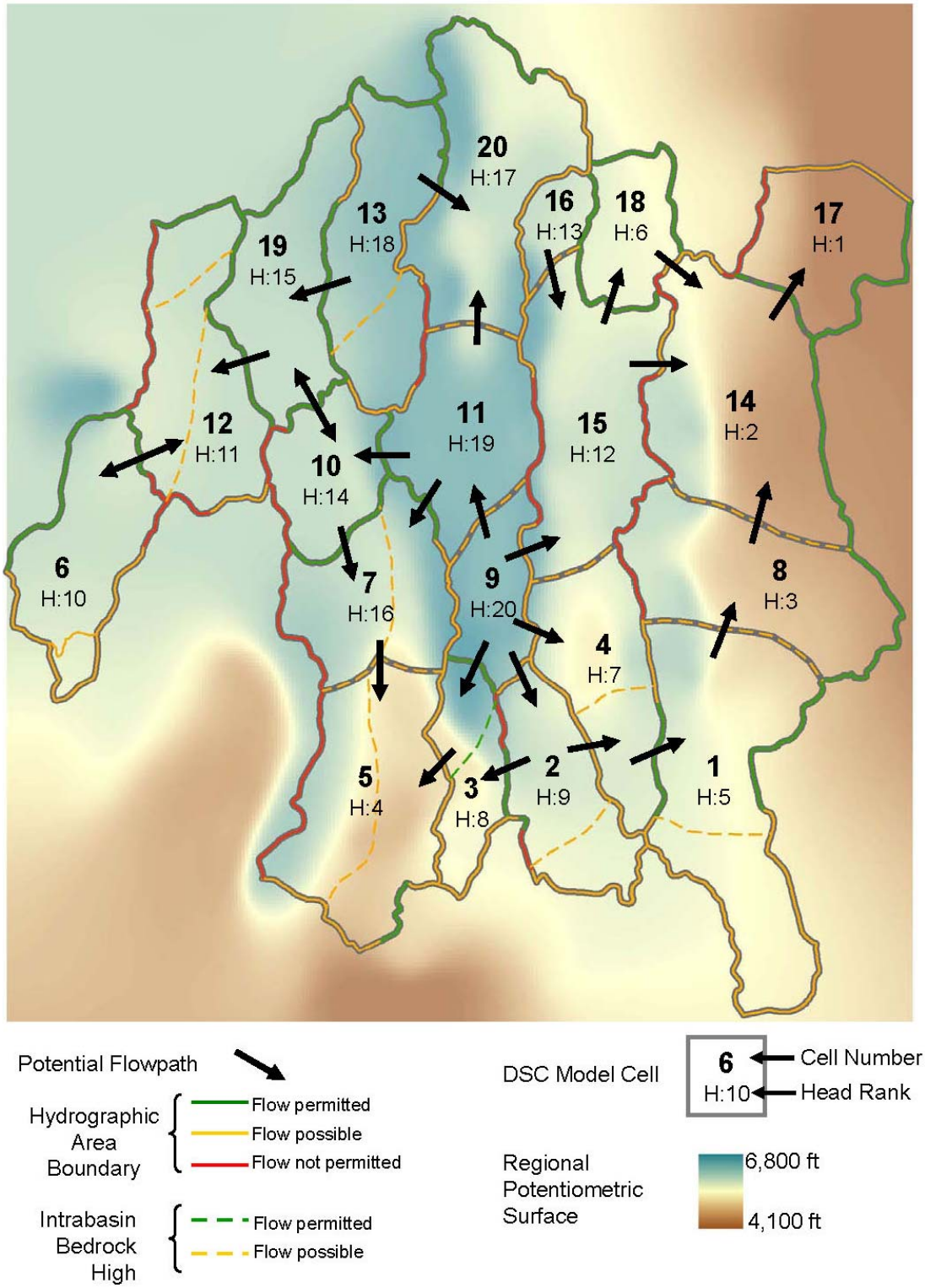

Figure 8. DSC Model Cell Connectivity and Head Ranks

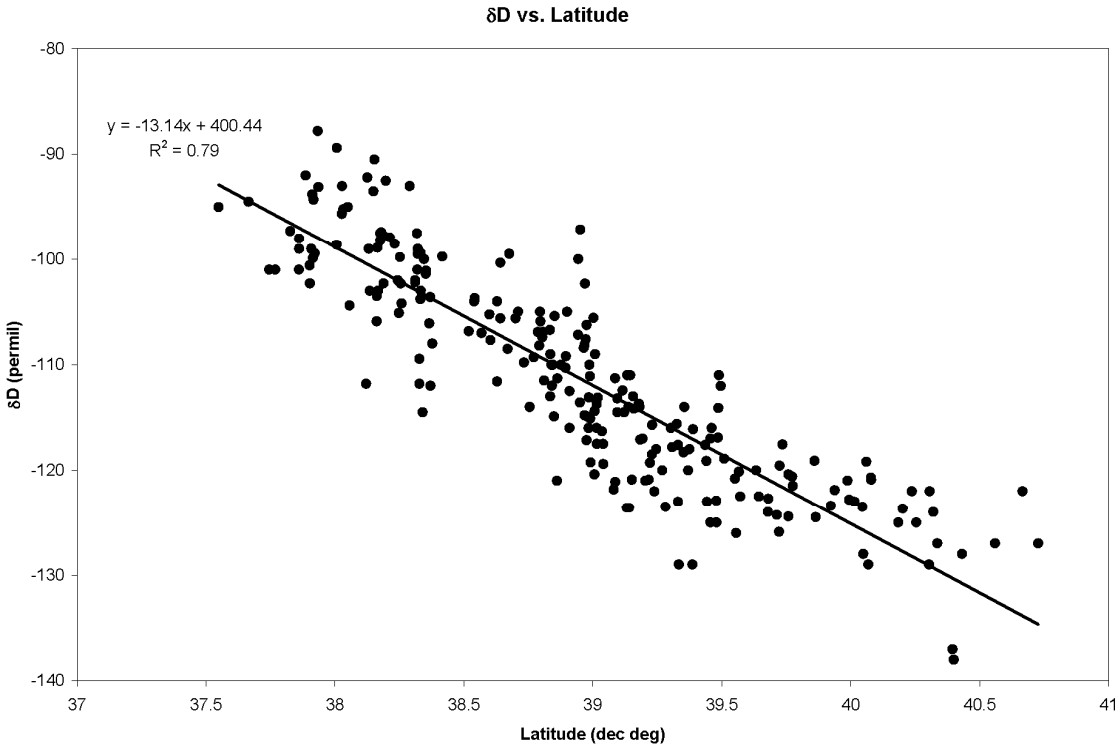

Figure 9. Plot Showing Recharge δD Values versus Latitude

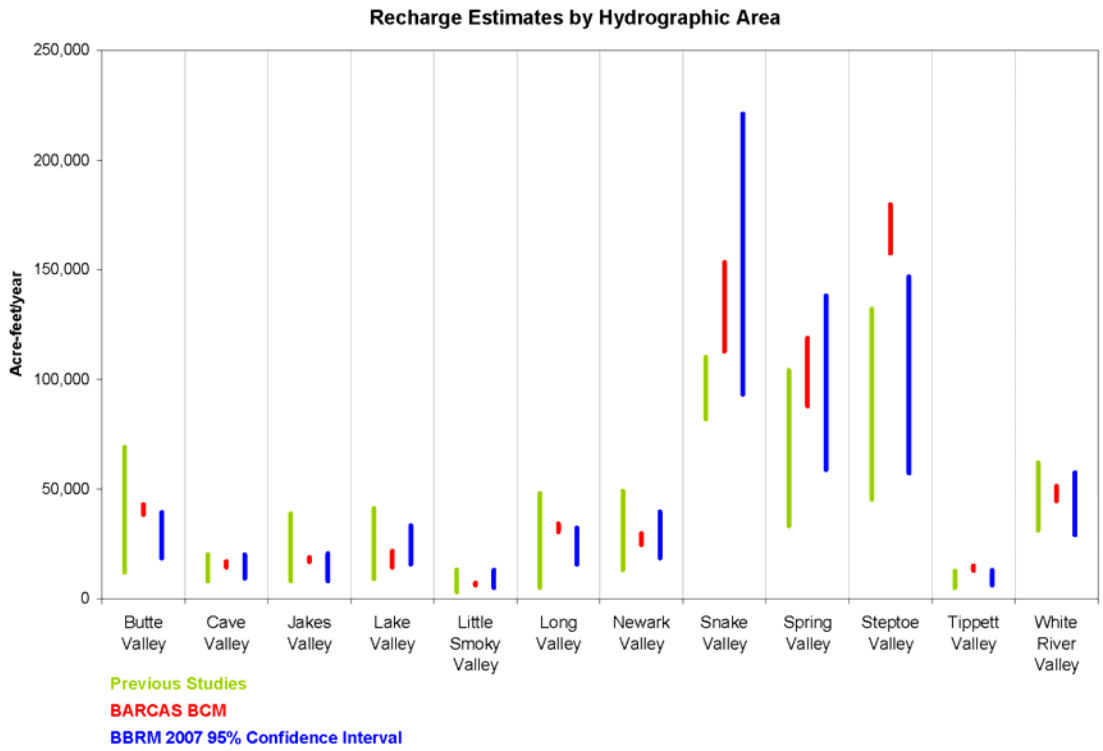

Figure 10. Ranges of Recharge Estimates Used for Developing Recharge Distributions for Monte Carlo Uncertainty Analysis Simulations

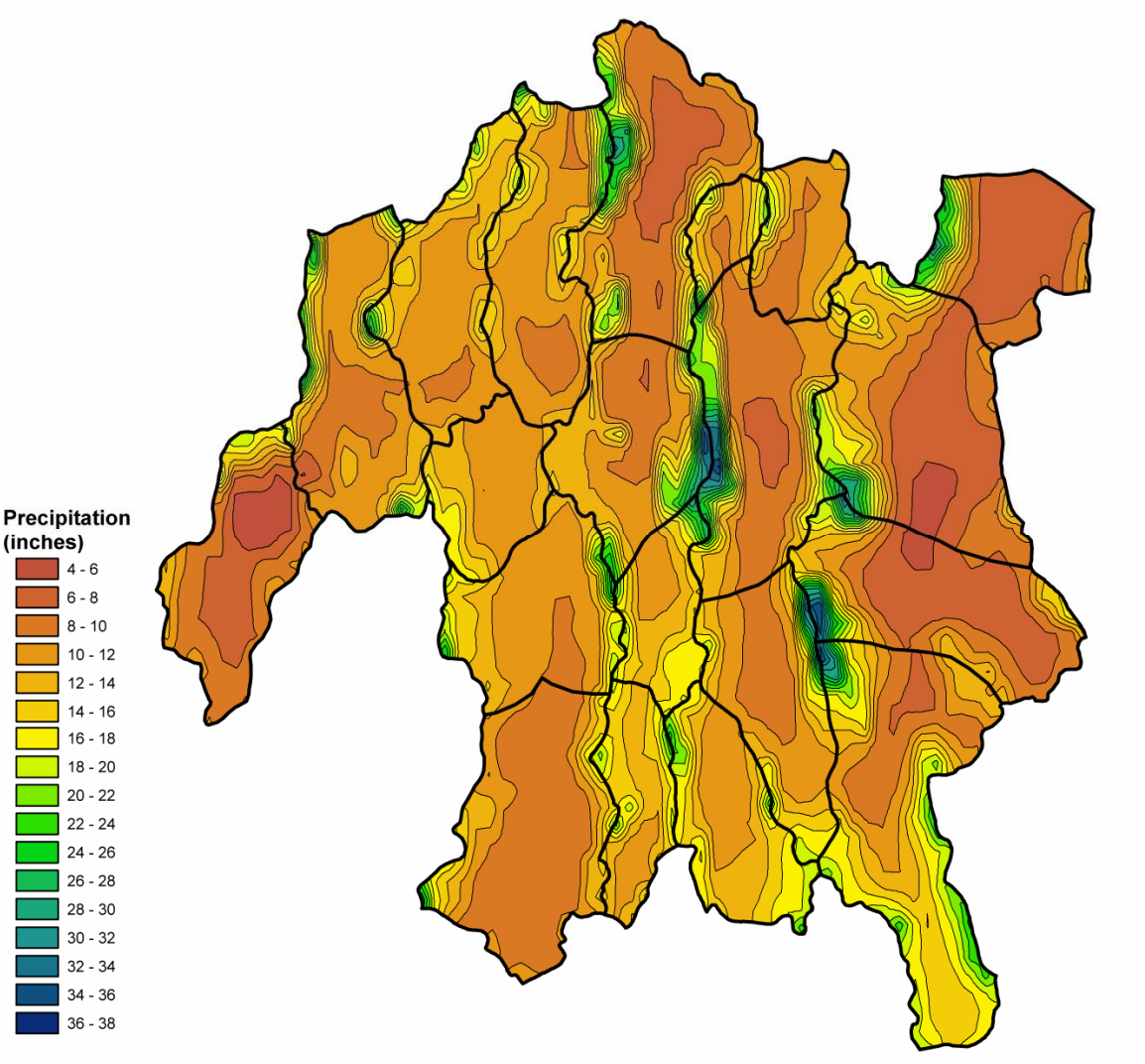

Figure 11. PRISM Map Showing Precipitation Intervals Used for Bootstrap Brute-Force Recharge Method (BBRM) Recharge Calculations

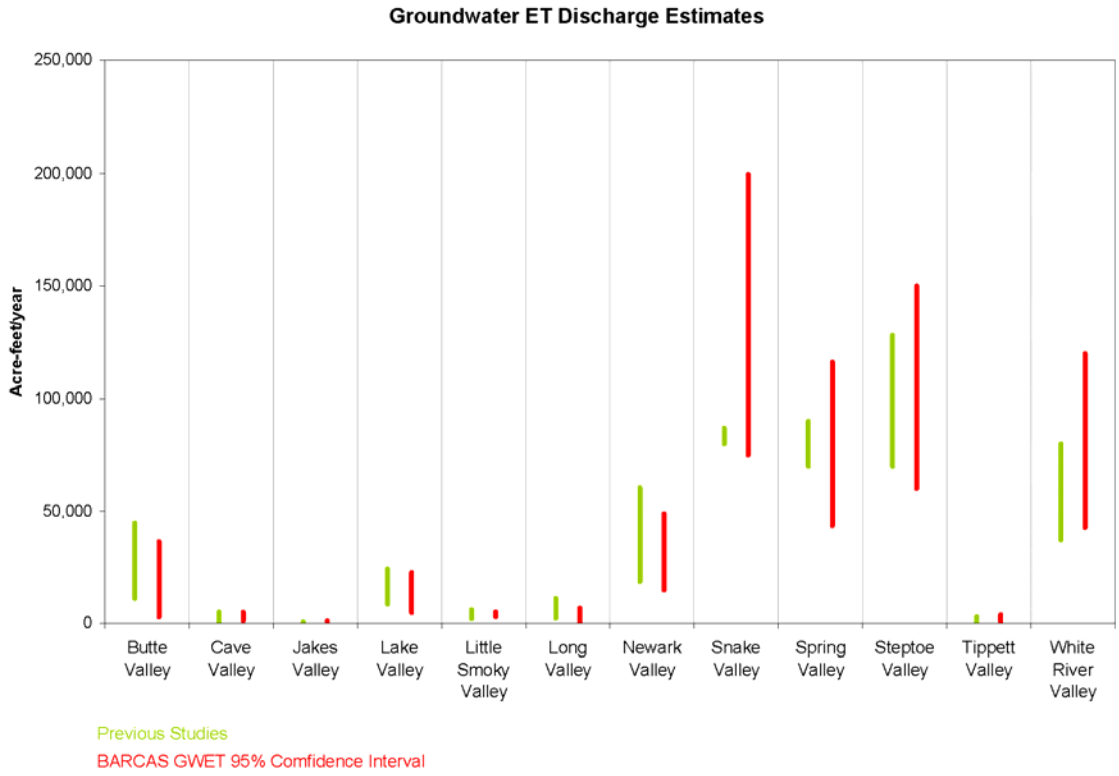

Figure 12. **Ranges of Groundwater Evapotranspiration (GWET) Estimates Used for Developing GWET Distributions for Monte Carlo Uncertainty Analysis Simulations**

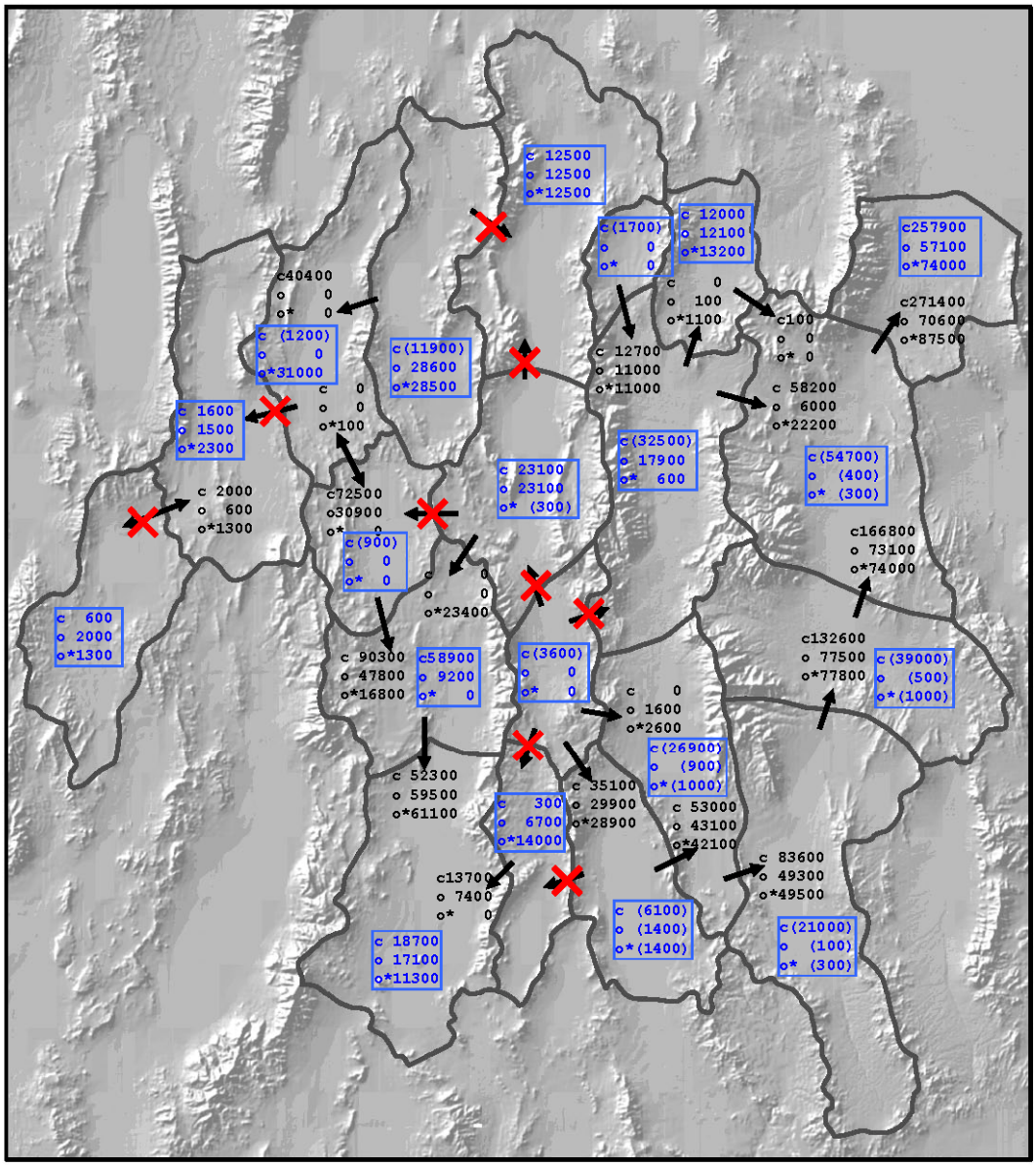

Legend

<100 acre-feet/year flow predicted by model for all scenarios

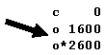

Interbasin groundwater flow rounded to the nearest 100 acre-feet/year. Values are shown for optimization scenarios *c*, *o*, and *o**.

Groundwater outflow from the study area (acre-feet/year) calculated by subtracting groundwater ET discharge from the DSC model-predicted outflow from the model domain. Negative values (in parentheses) show model results which predicted less total outflow than the estimated groundwater ET discharge rate. Values are shown for optimization scenarios *c*, *o*, and *o**.

Figure 13. Summary of Base BARCAS DSC Model Interbasin Groundwater Flow Rates

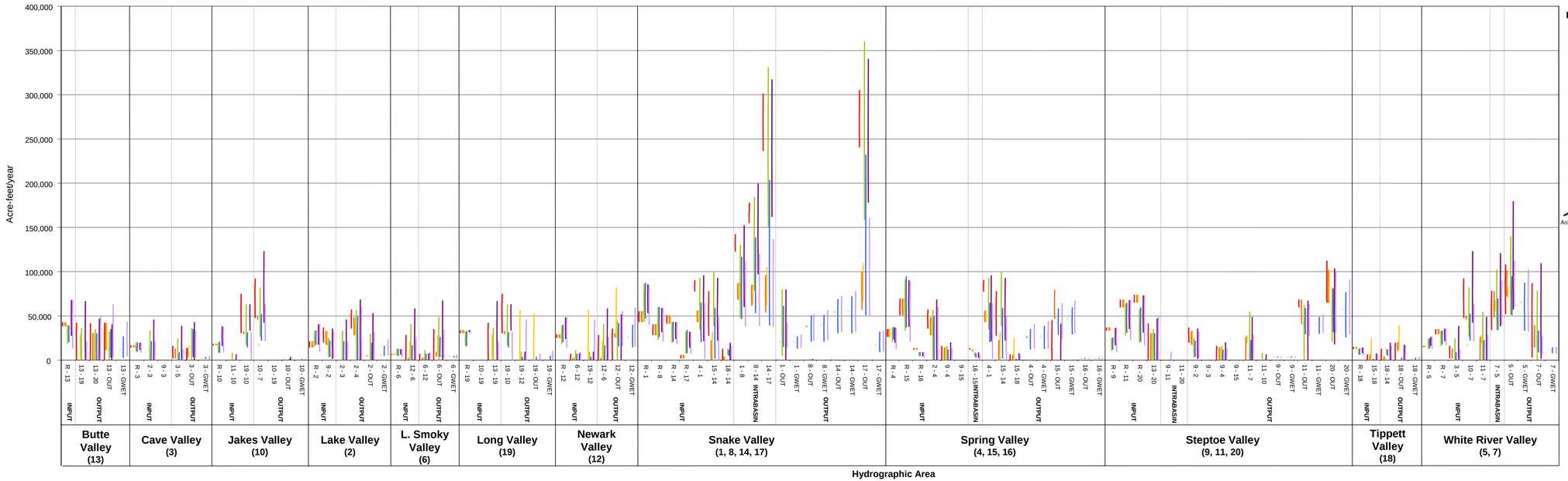

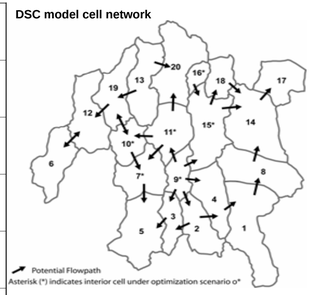

Monte Carlo Simulations

Simulation	Optimization Scenario	Target GWET Rates
MC-1	c	--
MC-2	o	Constant
MC-3	o*	Constant
MC-4	c	--
MC-5	o	Distribution
MC-6	c	--
MC-7	o	Distribution

Notes:
Bars show 95% confidence intervals
R = recharge
GWET = groundwater ET discharge
OUT = ouflow from model domain

Figure 14. Water Budget Summary for Monte Carlo Simulations MC-1 through MC-7

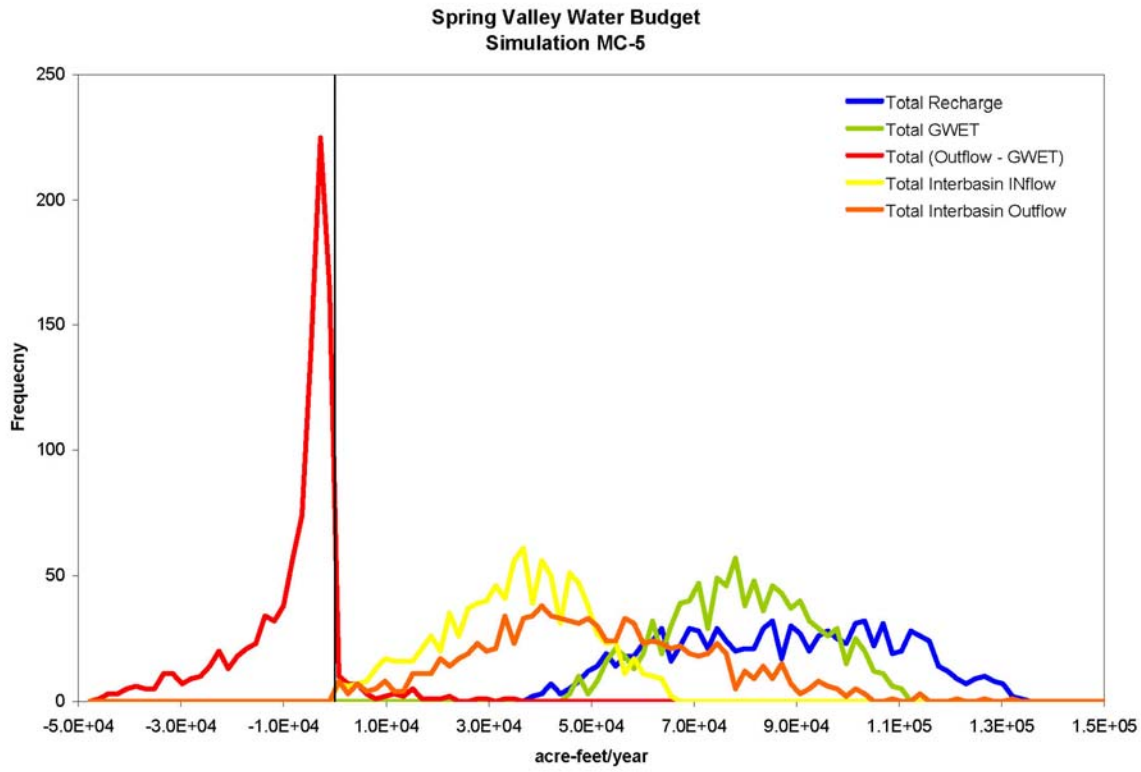

Figure 15. Water Budget Component Distributions for Spring Valley, Monte Carlo Simulation MC-5

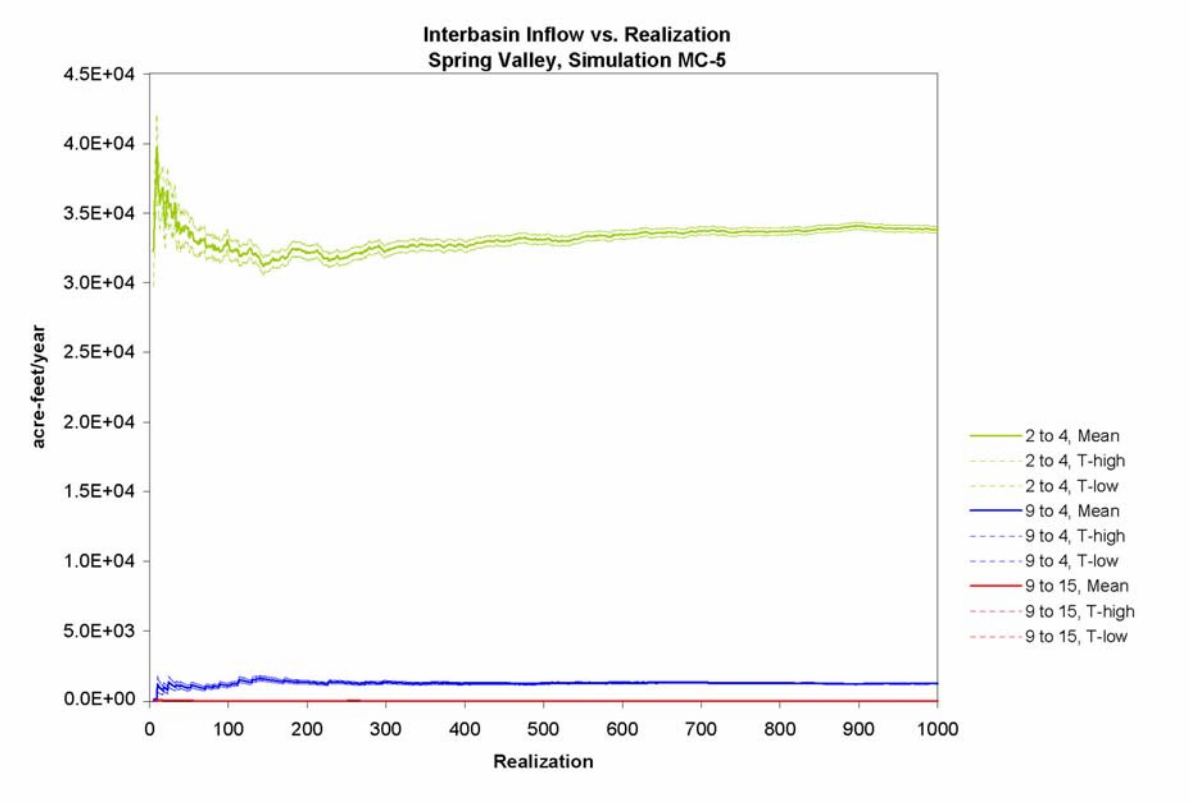

Figure 16. Stability of Statistics for Interbasin Inflow to Spring Valley, Monte Carlo Simulation MC-5

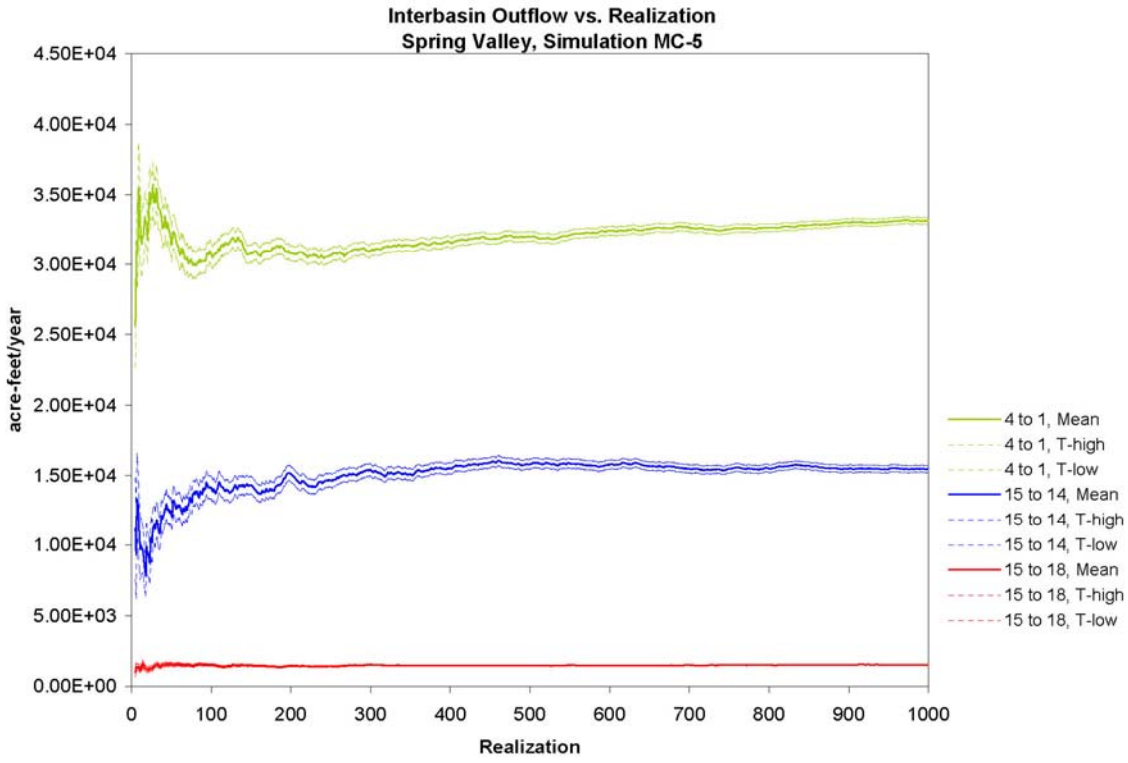

Figure 17. Stability of Statistics for Interbasin Outflow from Spring Valley, Monte Carlo Simulation MC-5

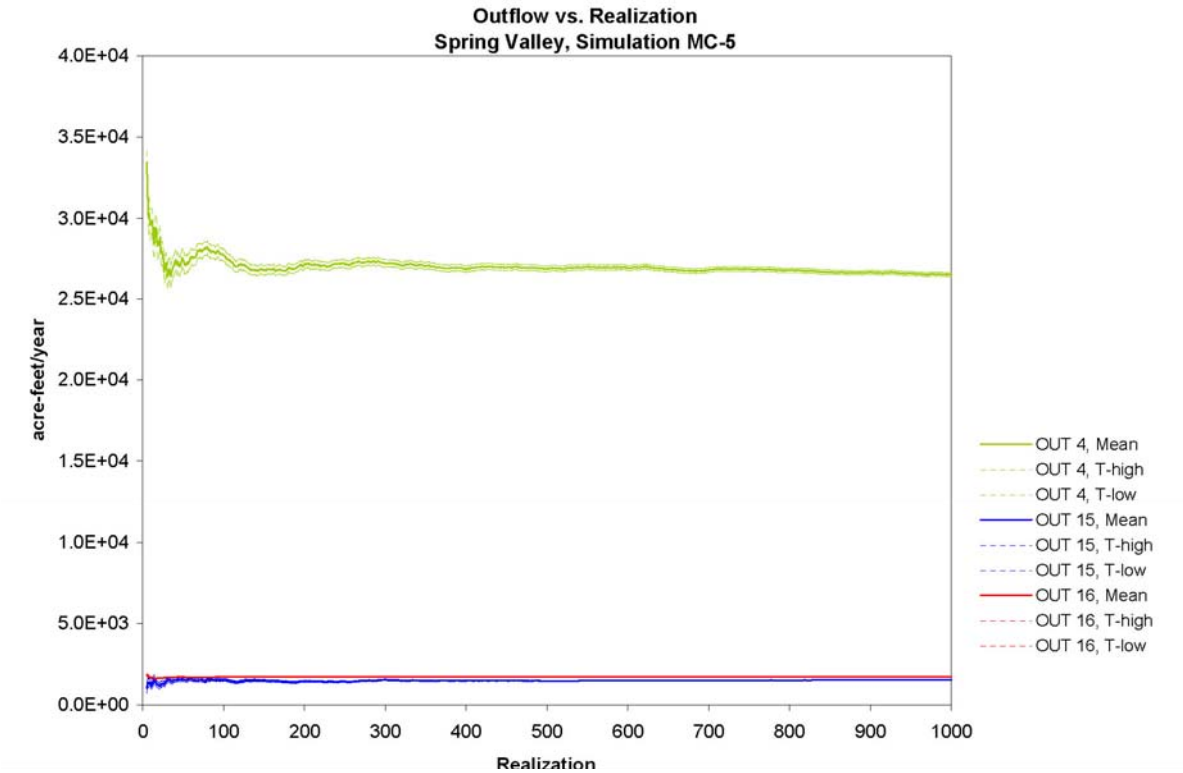

Figure 18. Stability of Statistics for Outflow from the Model Domain from Spring Valley, Monte Carlo Simulation MC-5

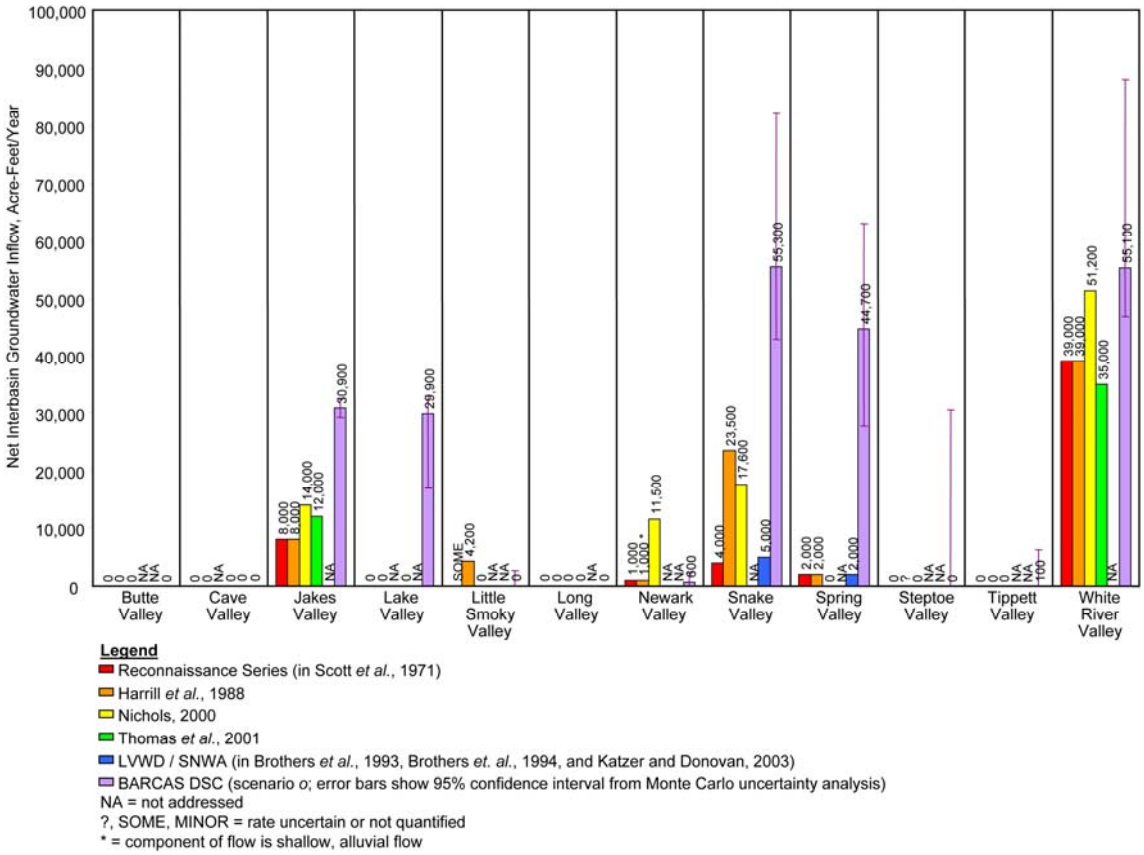

Figure 19. Summary of Interbasin Groundwater Inflow Rates from Previous Studies and Monte Carlo Simulation MC-2

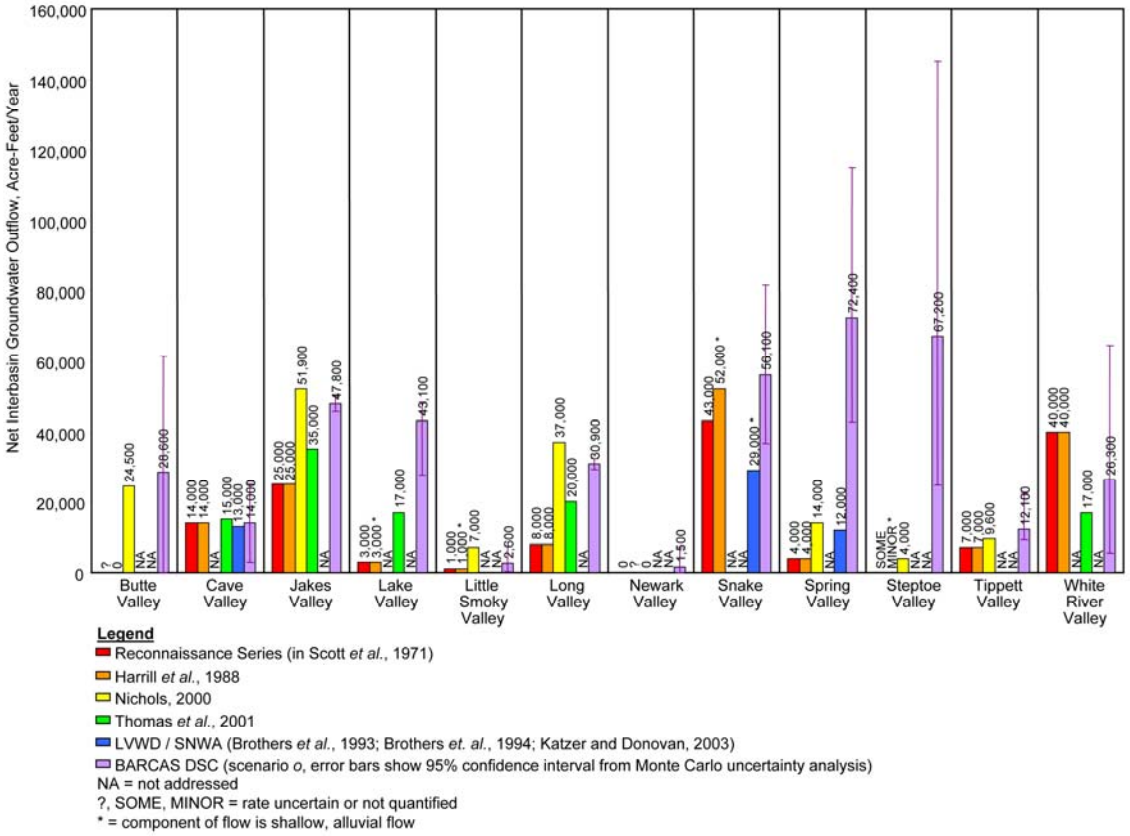

Figure 20. Summary of Interbasin Groundwater Outflow Rates from Previous Studies and Monte Carlo Simulation MC-2

Table 1. Previous Estimates for Groundwater Recharge

	Reconnaisance Series		Watson *et al.* 1976		Dettinger 1989		Kirk and Campana 1988	
Hydrographic Area (a)	Report Reference		Minimum	Maximum	Chloride Balance	Water Budget	Minimum	Maximum
Butte Valley	R49	< 15,000	11,925	15,632	12,165	12,165		
Cave Valley	R13	< 14,000					10,993	10,993
Jakes Valley	B33	17,000					17,998	23,009
Lake Valley	R24	13,000	8,671	11,000				
Little Smoky Valley	R38	4,200	3,058 (b)	7,820 (b)				
Long Valley	R3	10,000					5,011	5,011
Newark Valley	R1	17,500						
Snake Valley	R34	103,000						
Spring Valley	R33	< 75,000	32,708	74,000	61,636	73,801		
Steptoe Valley	R42	< 85,000	45,247	74,907				
Tippett Valley	R56	6,900						
White River Valley	B33	38,000					35,000	35,000

Table 1. Previous Estimates for Groundwater Recharge (continued)

Hydrographic Area (a)	Brothers *et al.* 1993-1994	Katzer and Donovan 2003	Nichols 2000	Thomas *et al.* 2001	Epstein 2004		Flint *et al.* 2004	
					Minimum	Maximum	Mean Annual	Time Series
Butte Valley			69,000		20,758	55,029	22,240	18,284
Cave Valley	13,000			20,000	13,592	45,913	10,264	9,380
Jakes Valley			38,500	24,000	11,834	30,405	10,974	8,310
Lake Valley				41,000	10,875	62,123	14,718	12,353
Little Smoky Valley			13,000 (c)		8,303	24,680	8,428	6,612
Long Valley			48,000	31,000	20,851	52,736	16,289	13,536
Newark Valley			49,000		20,715	52,279	18,428	15,390
Snake Valley	110,000						92,728	81,955
Spring Valley	110,000	124,000 (d)	104,000		53,335	139,194	66,987	56,179
Steptoe Valley			132,000		84,885	171,952	111,419	94,391
Tippett Valley			12,500		5,752	18,418	9,717	7,659
White River Valley				62,000	35,507	89,570	34,925	30,759

Notes:
Values given as acre-feet/year
(a) Hydrographic areas for Little Smoky Valley includes northern and central subareas and Butte Valley includes southern subarea
(b) Northern subarea only
(c) Includes Little Smoky Valley Northern, Central, and Southern subareas
(d) Includes groundwater recharge and surface water infiltration
Reconnissance Series
R33. Rush, F.E. and S.A. Kazmi, 1965; R34. Hood and Rush, 1965; R38. Rush, F.E. and D.E. Everett, 1966;
R42. Eakin, T.E., J.L. Hughes and D.O. Moore, 1967; R49. Glancy, P.A., 1968; R56. Harrill, 1971; B33. Eakin, 1966

Table 2. Previous Estimates for Groundwater Discharge as Evapotranspiration

Hydrographic Area (a)	Reconnaisance Series Report Reference		Brothers *et al.* 1993-1994	Katzer and Donovan 2003	Nichols 2000	Thomas *et al.* 2001
Butte Valley	R49	11,000			44,500	
Cave Valley	R13	200	0			5,000
Jakes Valley	B33	0			600	600
Lake Valley	R24	8,500				24,000
Little Smoky Valley	R38	1,900			6,000 (b)	
Long Valley	R3	2,200			11,000	11,000
Newark Valley	R1	18,500			60,500	
Snake Valley	R34	80,000	87,000			
Spring Valley	R33	70,000	108,000 (c)	111,000	90,000	
Steptoe Valley	R42	70,000			128,000	
Tippett Valley	R56	0			2,900	
White River Valley	B33	37,000				80,000

Notes:
Values given as acre-feet/year
(a) Hydrographic areas for Little Smoky Valley includes northern and central subareas and Butte Valley includes southern subarea
(b) Includes Little Smoky Valley Northern, Central, and Southern subareas
(c) Combination of springflow (drains) and ET
Reconnissance Series Report References: R1. Eakin 1960; R3. Eakin 1961; R13. Eakin 1962; R24. Rush, F.E. and T.E. Eakin 1963; R33. Rush, F.E. and S.A. Kazmi, 1965; R34. Hood and Rush, 1965; R38. Rush, F.E. and D.E. Everett, 1966; R42. Eakin, T.E., J.L. Hughes and D.O. Moore, 1967; R49. Glancy, P.A., 1968; R56. Harrill, 1971; B33. Eakin, 1966

Table 3. Previous Estimates for Interbasin Groundwater Flow

Hydrographic Area, HA (a)	Reconnaissance Series; Harrill et al. 1988				Nichols 2001			
	Interbasin Inflow	From HA	Interbasin Outflow	To HA	Interbasin Inflow	From HA	Interbasin Outflow	To HA
Butte Valley			?	Steptoe Valley	0		22,500	Clover Valley
							2,000	Ruby Valley
Cave Valley			14,000	White River Valley				
Jakes Valley	8,000	Long Valley	25,000	White River Valley	14,000	Long Valley	51,200	White River Valley
			?	Railroad Valley			700	Railroad Valley
Lake Valley			3,000 (a)	Patterson Valley				
Little Smoky Valley	4,000	Antelope Valley, Stevens Basin	1,000 (a)	Newark Valley	0		1,500	Newark Valley
							5,500	Railroad Valley
Long Valley			?	Newark Valley	0		10,000	Newark Valley
			8,000	Jakes Valley			14,000	Jakes Valley
							13,000	Railroad Valley
Newark Valley	1,000 (a)	Little Smoky Valley	?	Railroad Valley	100,000	Long Valley		
	?	Long Valley			1,500	Little Smoky Valley		
Snake Valley	4,000	Spring Valley	22,000 - 42,000	Tule Valley	14,000	Spring Valley		
	< 11,000	Pine Valley	?	Fish Springs Flat	3,600	Tippett Valley		
	< 8,500	Wah Wah Valley	10,000 (a)	Great Salt Lake Desert				
Spring Valley	2,000	Tippett Valley	4,000	Snake Valley	0		14,000	Snake Valley
Steptoe Valley	?	Butte Valley	Minor (a)	Goshute Valley	0		4,000	Goshute Valley
Tippett Valley			3,000	Antelope Valley	0		6,000	Great Salt Lake Desert
			2,000	Deep Creek Valley, Great Salt Lake Desert			3,600	Snake Valley
			2,000	Spring Valley				
White River Valley	14,000	Cave Valley	40,000	Pahroc Valley	51,200	Jakes Valley		
	25,000	Jakes Valley						

Table 3. Previous Estimates for Interbasin Groundwater Flow (continued)

Hydrographic Area, HA (a)	Thomas et al. 2001				Brothers et al. 1993 - 1994 (*), Katzer et al. 2003 (**)			
	Interbasin Inflow	From HA	Interbasin Outflow	To HA	Interbasin Inflow	From HA	Interbasin Outflow	To HA
Butte Valley								
Cave Valley	0		15,000	Pahroc Valley	0 *		13,000 *	White River Valley
Jakes Valley	12,000	Long Valley	35,000	White River Valley				
Lake Valley	0		17,000	Patterson Valley				
Little Smoky Valley								
Long Valley	0		12,000 8,000 ?	Jakes Valley				
Newark Valley								
Snake Valley					4,000 * 1,000 *	Spring Valley Pine Valley, Wah Wah Valley	14,000 * 15,000 *	Great Salt (a) Lake Desert Tule Valley
Spring Valley					2,000 * **	Tippett Valley	4,000 * 10,000 ** 2,000 **	Snake Valley Steptoe Valley
Steptoe Valley								
Tippett Valley							2,000 * **	Spring Valley
White River Valley	35,000	Long Valley	17,000	Pahroc Valley	13,000 *	Cave Valley		

Notes:
Values given as acre-feet/year
(a) Hydrographic areas for Little Smoky Valley includes northern and central subareas and Butte Valley includes southern subarea
(b) Flow through alluvial material

Table 4. Summary of Groundwater Recharge and Evapotranspiration (ET) Discharge Rate Estimates from the BARCAS Study

Hydrographic Area	Recharge	ET Discharge
Butte Valley	40,400	11,900
Cave Valley	15,600	1,600
Jakes Valley	17,700	900
Lake Valley	17,900	6,100
Little Smoky Valley	6,600	4,000
Long Valley	32,100	1,200
Newark Valley	27,000	26,100
Snake Valley	133,000	132,300
Spring Valley	103,300	75,600
Steptoe Valley	168,700	101,500
Tippett Valley	13,800	1,700
White River Valley	47,800	76,700
BARCAS Area Total	*623,900*	*439,600*

Notes:
Source = BARCAS SIR (Welch and Bright, in review)
Rates are acre-feet/year (afy), rounded to the nearest 100 afy.

Table 5. DSC Model Cell Input Parameters and Calibration Criteria

		Head Rank		Recharge		Groundwater ET		
Cell	Name	Average Head (ft)	Rank	Rate (afy)	Deuterium value, δD (‰)	Rate (afy)	Standard deviation, s_{GWET} (afy)	Inverse standard deviation, $1/s_{GWET}$ (afy^{-1})
1	Snake Valley - South	5,596	5	49,082	-107	21,049	4,133	2.4E-04
2	Lake Valley	5,838	9	17,896	-105	6,135	4,438	2.3E-04
3	Cave Valley	5,884	8	15,551	-107	1,551	812	1.2E-03
4	Spring Valley - South	5,780	7	30,579	-108	26,889	4,133	2.4E-04
5	White River Valley - South	5,473	4	15,684	-107	65,463	15,357	6.5E-05
6	Little Smoky Valley	5,935	10	6,562	-121	3,955	545	1.8E-03
7	White River Valley - North	6,114	16	32,129	-113	11,238	1,614	6.2E-04
8	Snake Valley - Central	5,240	3	34,174	-113	39,038	9,404	1.1E-04
9	Steptoe Valley - South	6,543	20	35,140	-114	3,569	371	2.7E-03
10	Jakes Valley	6,055	14	17,691	-119	858	91	1.1E-02
11	Steptoe Valley - Central	6,470	19	64,087	-117	40,983	5,612	1.8E-04
12	Newark Valley	5,962	11	26,986	-122	26,059	5,810	1.7E-04
13	Butte Valley	6,396	18	40,428	-122	11,877	8,682	1.2E-04
14	Snake Valley - North	5,129	2	45,893	-117	54,836	12,432	8.0E-05
15	Spring Valley - Central	5,981	12	59,976	-118	46,991	10,196	9.8E-05
16	Spring Valley - North	6,007	13	12,752	-121	1,733	236	4.2E-03
17	Snake Valley - Northeast	4,480	1	3,851	-122	17,361	6,382	1.6E-04
18	Tippet Valley	5,680	6	13,750	-122	1,742	852	1.2E-03
19	Long Valley	6,091	15	32,130	-123	1,234	1,747	5.7E-04
20	Steptoe Valley - North	6,120	17	69,448	-123	56,945	16,343	6.1E-05

Table 5. DSC Model Cell Input Parameters and Calibration Criteria (continued)

		Observed (calibration) values				
Cell	Name	Deuterium value, δD (‰)	Standard deviation (‰)	Confidence interval, *ci* (‰)	Inverse confidence interval, 1/*ci* ($‰^{-1}$)	Weight ($‰^{-1}$)
1	Snake Valley - South	-111	1.60	1.06	0.94	0.94
2	Lake Valley	-111	2.26	2.25	0.44	0.44
3	Cave Valley	-104	3.16	3.63	0.28	0.28
4	Spring Valley - South	-110	2.06	1.45	0.69	0.69
5	White River Valley - South	-115	5.63	2.88	0.35	0.35
6	Little Smoky Valley	-120	2.22	4.07	0.25	0.25
7	White River Valley - North	-120	4.29	3.02	0.33	0.33
8	Snake Valley - Central	na	--	--	--	0
9	Steptoe Valley - South	-118	3.06	9.29	0.11	0.11
10	Jakes Valley	na	--	--	--	0
11	Steptoe Valley - Central	-123	0.71	8.98	0.11	0.11
12	Newark Valley	-122	nc	--	--	0.1
13	Butte Valley	na	--	--	--	0
14	Snake Valley - North	-118	4.47	3.37	0.30	0.30
15	Spring Valley - Central	-123	1.78	3.27	0.31	0.31
16	Spring Valley - North	-126	nc	--	--	0.1
17	Snake Valley - Northeast	-111	0.00	0.00	nc	0.5
18	Tippet Valley	-122	0.95	2.90	0.34	0.34
19	Long Valley	-129	2.12	26.95	0.04	0.1
20	Steptoe Valley - North	-128	3.30	2.94	0.34	0.34

Notes:
afy = acre-feet/year
‰ = per mil
nc = standard deviation not calculable (less than two δD values for model cell)
na = not available (no δD data identified for model cell)

Table 6. Principle Characteristics of Deterministic-Sensitivity Uncertainty Analyses

Name	Recharge δD Interpolation Method	Otpimization Criteria	Objective Function	Base BARCAS DSC Model
DS-1	IDW	concentration	wRMSEc	Yes, opt. scenario *c*
DS-2	IDW	concentration + outflow	wRMSEo	Yes, opt. scenario *o*
DS-3	IDW	concentration + outflow	wRMSEo*	Yes, opt. scenario *o**
DS-4	Latitude Regression	concentration	wRMSEc	No
DS-5	Latitude Regression	concentration + outflow	wRMSEo	No
DS-6	Latitude Regression	concentration + outflow	wRMSEo*	No
DS-7	IDW	concentration	SAE	No

Notes:
IDW = inverse distance weighting
wRMSE = weigthed root mean squared error
SAE = sum of absolute errors

Table 7. Summary of DSC Model Cell Recharge δD Values Calculated Using Inverse Distance Weighting (IDW) and Latitude Regression Estimation Methods

	DSC Model Cell	Recharge δD Estimation Method		ΔδD (‰)
		IDW, δD (‰)	Latitude Regression, δD (‰)	
1	Snake Valley - South	-107	-106	1
2	Lake Valley	-105	-105	0
3	Cave Valley	-107	-106	1
4	Spring Valley - South	-108	-110	-2
5	White River Valley - South	-107	-105	2
6	Little Smoky Valley	-121	-113	8
7	White River Valley - North	-113	-112	1
8	Snake Valley - Central	-113	-112	1
9	Steptoe Valley - South	-114	-112	2
10	Jakes Valley	-119	-116	3
11	Steptoe Valley - Central	-117	-117	0
12	Newark Valley	-122	-119	3
13	Butte Valley	-122	-123	-1
14	Snake Valley - North	-117	-118	-1
15	Spring Valley - Central	-118	-117	1
16	Spring Valley - North	-121	-124	-3
17	Snake Valley - Northeast	-122	-122	0
18	Tippet Valley	-122	-123	-1
19	Long Valley	-123	-121	2
20	Steptoe Valley - North	-123	-125	-2

Notes:
‰ = per mil
δD values are rounded to the nearest ‰
IDW = inverse distance weighting
ΔδD = change (Δ) in recharge δD value, calculated by subtracting the Latitude Regression value from the IDW value

Table 8. Principle Characteristics of Monte Carlo Uncertainty Analysis Simulations

				Recharge Rate		Recharge δD Values		Groundwater ET Discharge Rate		
Name	**Optimization Criteria**	**Objective Function**	**Number Realizations**	**Distribution**	**Estimation Method and Range**	**Distribution**	**Estimation Method and Range**	**Distribution**	**Estimation Method**	**Discharge Weight**
MC-1	concentration	wRMSEc	1,000	Uniform	BCM Min: IPR Max: IPR + 30% Runoff	Uniform	IDW+BCM +/- 1.5 ‰	na	na	na
MC-2	concentration + outflow	wRMSEo	1,000	Uniform	BCM Min: IPR Max: IPR + 30% Runoff	Uniform	IDW+BCM +/- 1.5 ‰	Constant	BARCAS study	Constant, 1/sd
MC-3	concentration + outflow	wRMSEo*	1,000	Uniform	BCM Min: IPR Max: IPR + 30% Runoff	Uniform	IDW+BCM +/- 1.5 ‰	Constant	BARCAS study	Constant, 1/sd
MC-4	concentration	wRMSEc	1,000	Quasi-normal	BBRM	Uniform	IDW+BBRM +/- 1.5 ‰	na	na	na
MC-5	concentration + outflow	wRMSEo	740	Quasi-normal	BBRM	Uniform	IDW+BBRM +/- 1.5 ‰	Quasi-normal	BARCAS Monte Carlo Uncertainty Analysis	Variable, 1/(CV*ET)
MC-6	concentration	wRMSEc	1,000	Uniform	Minimum to Maximum of Avaliable Estimates	Uniform	Minimum to Maximum of Avaliable Estimates	na	na	na
MC-7	concentration + outflow	wRMSEo	1,000	Uniform	Minimum to Maximum of Avaliable Estimates	Uniform	Minimum to Maximum of Avaliable Estimates	Uniform	Minimum to Maximum of Avaliable Estimates	Variable, 1/(CV*ET)
MC-8	concentration + outflow	wRMSEo	1,000	Constant	BCM IPR + 15% Runoff	Constant	IDW+BCM	Constant	BARCAS study	Constant, 1/sd

Notes:
IDW = inverse distance weighting
wRMSE = weigthed root mean squared error
na = not applicable, outflow not used as optimization criteria
BCM = Basin Characterization Model
BBRM = Bootstrap Brute-force Recharge Model
IPR = Potential in-place recharge
BARCAS study = Basin and Range Carbonate Aquifer study
sd = standard deviation

Table 9. Summary of Recharge δD Values Estimated for DSC Model Cells

			DSC Model Cell						
			1	2	3	4	5	6	7
	Recharge δD Estimation Method								
Recharge δD Estimation Methods Used for Basis of Selected δD Recharge Range	IDW + BCM-predicted Spatial Recharge Distribution	0% Runoff	-106.6	-104.5	-106.5	-108.4	-106.7	-121.4	-113.0
		15% Runoff	-106.6	-104.6	-107.4	-107.8	-106.7	-121.1	-113.0
		30% Runoff	-105.5	-103.8	-106.5	-108.0	-106.6	-121.3	-113.2
	IDW + BBRM-predicted Spatial Recharge Distribution	Minimum	-105.5	-103.7	-104.9	-107.9	-107.6	-121.9	-113.7
		Average	-104.4	-103.6	-104.8	-107.4	-106.6	-121.7	-113.5
		Maximum	-103.4	-103.6	-104.3	-107.1	-106.2	-121.2	-113.1
	Latitude Regression + BCM-predicted Spatial Recharge Distribution	0% Runoff	-108.3	-104.0	-105.6	-110.1	-105.6	-111.9	-112.5
		15% Runoff	-107.6	-104.4	-105.8	-110.1	-105.7	-112.0	-112.3
		30% Runoff	-107.1	-104.6	-106.0	-110.1	-105.7	-112.1	-112.2
	Latitude Regression + BCM-predicted Spatial Recharge Distribution	Minimum	-107.2	-106.0	-106.9	-110.8	-105.5	-115.1	-112.3
		Average	-105.9	-105.7	-106.6	-109.9	-105.3	-114.1	-112.1
		Maximum	-104.9	-105.6	-106.5	-109.1	-104.7	-113.6	-112.0
	Latitude Regression x Model Cell Centroid Latitude	Predicted	-105.5	-105.2	-106.1	-109.7	-105.0	-113.5	-111.9
		95% CI Lower Limit	-106.2	-105.9	-106.8	-110.3	-105.7	-114.1	-112.5
		95% CI Upper Limit	-104.8	-104.5	-105.4	-109.1	-104.3	-112.9	-111.3
	Selected Recharge δD Range	Lower Bound	-108.5	*-106.25*	*-107.25*	-111	-107.5	-122	*-114*
		Upper Bound	-103.5	*-103.25*	*-104.25*	-107	-104.5	-112	*-111*
Recharge δD Values Presented for Comparison	Recharge δD Values from Previous Sutdies	Thomas *et al.* 2001	--	--	-107	--	-107	--	-114
		Kirk & Campana 1990	--	--	-102 to -97	--	-110.5 to -104	--	-113
	Recharge δD Samples within 6.2 miles of Model Cell	n	40	26	18	36	21	4	42
		Average	-105.0	-102.1	-106.7	-108.2	-107.5	-123.5	-114.9
		Standard Deviation	5.9	5.1	4.6	5.2	5.0	5.0	4.4

Table 9. Summary of Recharge δD Values Estimated for DSC Model Cells (continued)

			DSC Model Cell						
			8	9	10	11	12	13	14
	Recharge δD Estimation Method								
Recharge δD Estimation Methods Used for Basis of Selected δD Recharge Range	IDW + BCM-predicted Spatial Recharge Distribution	0% Runoff	-113.3	-113.6	-118.9	-117.3	-122.4	-122.2	-117.4
		15% Runoff	-113.1	-113.6	-118.9	-116.5	-121.9	-122.0	-117.2
		30% Runoff	-112.1	-113.6	-118.9	-117.4	-122.4	-122.1	-117.5
	IDW + BBRM-predicted Spatial Recharge Distribution	Minimum	-111.1	-115.6	-118.9	-118.2	-122.4	-122.2	-118.4
		Average	-109.7	-113.9	-118.9	-117.7	-122.3	-122.0	-117.5
		Maximum	-108.5	-113.0	-118.9	-117.3	-122.2	-121.8	-116.8
	Latitude Regression + BCM-predicted Spatial Recharge Distribution	0% Runoff	-111.0	-112.1	-115.1	-118.3	-120.5	-124.4	-119.0
		15% Runoff	-111.5	-112.1	-115.1	-118.3	-120.2	-124.4	-118.8
		30% Runoff	-111.8	-112.2	-115.1	-118.3	-120.0	-124.4	-118.7
	Latitude Regression + BCM-predicted Spatial Recharge Distribution	Minimum	-112.9	-113.8	-115.8	-117.0	-120.1	-125.3	-118.8
		Average	-112.6	-112.6	-115.8	-116.7	-119.6	-124.0	-117.9
		Maximum	-112.3	-112.0	-115.8	-116.4	-119.2	-123.3	-117.0
	Latitude Regression x Model Cell Centroid Latitude	Predicted	-112.1	-111.7	-115.7	-116.9	-119.4	-122.7	-117.8
		95% CI Lower Limit	-112.7	-112.3	-116.3	-117.6	-120.2	-123.7	-118.6
		95% CI Upper Limit	-111.5	-111.1	-115.0	-116.2	-118.6	-121.7	-117.1
	Selected Recharge δD Range	Lower Bound	-113.5	-115.5	-119	*-118.75*	-122.5	-125.5	*-119.5*
		Upper Bound	-108.5	-111	-115	*-115.75*	-118.5	-121.5	*-116.5*
Recharge δD Values Presented for Comparison	Recharge δD Values from Previous Sutdies	Thomas *et al.* 2001	--	--	-120	--	--	--	--
		Kirk & Campana 1990	--	--	-124	--	--	--	--
	Recharge δD Samples within 6.2 miles of Model Cell	n	31	15	26	18	16	14	11
		Average	-110.6	-111.1	-119.3	-117.1	-122.3	-120.8	-118.5
		Standard Deviation	5.1	4.7	4.4	4.4	3.7	3.9	3.4

Table 9. Summary of Recharge δD Values Estimated for DSC Model Cells (continued)

			DSC Model Cell					
			15	16	17	18	19	20
	Recharge δD Estimation Method							
Recharge δD Estimation Methods Used for Basis of Selected δD Recharge Range	IDW + BCM-predicted Spatial Recharge Distribution	0% Runoff	-117.4	-120.9	-120.3	-121.4	-122.4	-122.4
		15% Runoff	-118.3	-121.4	-122.1	-122.1	-122.7	-122.6
		30% Runoff	-117.5	-120.9	-120.4	-121.4	-122.4	-122.3
	IDW + BBRM-predicted Spatial Recharge Distribution	Minimum	-117.9	-120.9	-120.4	-121.5	-122.3	-122.4
		Average	-117.8	-120.9	-120.2	-121.4	-121.8	-122.3
		Maximum	-117.7	-120.9	-119.8	-121.4	-121.5	-122.3
	Latitude Regression + BCM-predicted Spatial Recharge Distribution	0% Runoff	-116.0	-124.4	-122.0	-123.0	-122.7	-124.8
		15% Runoff	-116.0	-124.3	-120.2	-122.9	-122.6	-124.8
		30% Runoff	-116.0	-124.3	-119.8	-122.8	-122.4	-124.7
	Latitude Regression + BCM-predicted Spatial Recharge Distribution	Minimum	-117.5	-123.8	-123.5	-123.9	-122.4	-125.6
		Average	-117.2	-123.6	-123.4	-123.7	-122.3	-125.2
		Maximum	-117.0	-123.2	-123.2	-123.6	-122.2	-124.7
	Latitude Regression x Model Cell Centroid Latitude	Predicted	-116.9	-123.7	-122.4	-123.3	-121.0	-124.9
		95% CI Lower Limit	-117.7	-124.7	-123.3	-124.3	-121.9	-126.0
		95% CI Upper Limit	-116.2	-122.7	-121.4	-122.3	-120.1	-123.8
	Selected Recharge δD Range	Lower Bound	*-118.5*	-124.5	-123.5	-124.5	-123	-126
		Upper Bound	*-115.5*	-121	-120	-121.5	-120	-122.5
Recharge δD Values Presented for Comparison	Recharge δD Values from Previous Sutdies	Thomas *et al.* 2001	--	--	--	--	-122	--
		Kirk & Campana 1990	--	--	--	--	-126	--
	Recharge δD Samples within 6.2 miles of Model Cell	n	25	5	0	9	17	10
		Average	-118.3	-121.3	--	-121.8	-120.3	-122.2
		Standard Deviation	3.3	1.4	--	1.5	4.7	1.4

Notes:
Italicized vlues indicate upper and lower bounds calculated as the average of minimum and maximum basis values +/- 1.5‰.
Underlined values were used for deterministic-sensitivity analysis simulations; see Tables 6 and 7.

Table 10. Model-Predicted δD Values and Outflow Rates and Calculated Objective Function Values for the Base BARCAS DSC Model

	Observed and predicted deuterium values					Groundwater ET and predicted outflow rates					Objective function values, wRMSE (unitless)		
	Observed (calibration) deuterium values		Predicted deuterium values, δD (‰)			Groundwater ET		Predicted outflow rate (acre-ft/year)					
Cell	dD (‰)	Weight ($‰^{-1}$)	c	o	o*	Rate (afy)	Weight (afy^{-1})	c	o	o*	c	o	o*
1	-111	0.94	-109	-108	-108	21,049	0.0002	54	20,912	20,757			
2	-111	0.44	-111	-111	-111	6,135	0.0002	0	4,759	4,713			
3	-104	0.28	-107	-107	-107	1,551	0.001	1,893	8,201	15,552			
4	-110	0.69	-110	-110	-110	26,889	0.0002	1	25,959	25,863			
5	-115	0.35	-115	-115	-114	65,463	0.00007	84,140	82,601	76,781			
6	-120	0.25	-121	-121	-121	3,955	0.002	4,588	5,979	5,222			
7	-120	0.33	-119	-118	-116	11,238	0.0006	70,123	20,421	11,234			
8	na	0	-110	-110	-110	39,038	0.0001	83	38,558	38,010			
9	-118	0.11	-114	-114	-114	3,569	0.003	0	3,552	3,552			
10	na	0	-122	-122	-119	858	0.01	1	860	857			
11	-123	0.11	-117	-117	-117	40,983	0.0002	64,061	64,083	40,658			
12	-122	0.1	-122	-122	-122	26,059	0.0002	27,642	27,593	28,317			
13	na	0	-122	-122	-122	11,877	0.0001	0	40,427	40,411			
14	-118	0.30	-113	-113	-113	54,836	0.00008	120	54,443	54,556			
15	-123	0.31	-119	-118	-118	46,991	0.00010	14,500	64,940	47,633			
16	-126	0.1	-121	-121	-121	1,733	0.004	2	1,732	1,733			
17	-111	0.5	-113	-113	-114	17,361	0.0002	275,271	74,444	91,370			
18	-122	0.34	-122	-122	-122	1,742	0.001	13,715	13,803	14,907			
19	-129	0.1	-122	-123	-123	1,234	0.0006	1	1,200	32,250			
20	-128	0.34	-123	-123	-123	56,945	0.00006	69,449	69,460	69,464			
All											0.85	0.93	0.98
All											4.13	0.08	0.08
All											8.97	1.66	0.09
All											2.98	0.66	0.70
All											6.37	1.35	0.70

Notes:
ET - evapotranspiration
wRMSE - weighted root mean squared error
DSC model optimization:
c - concentration only
o - concentration + outflow
o* - concentration + modified outflow

Table 11. Basin Water Budget Summary for the Base BARCAS DSC Model

	Inputs				Outputs									
					Interbasin Groundwater Outflow (within study area)			Outflow (discharge out of study area)			Outflow Components			
	Total	Interbasin Groundwater Inflow									Groundwater	Outflow - Groundwater ET		
Basin	Recharge	C	O	O*	C	O	O*	C	O	O*	ET	C	O	O*
Butte Valley	40,428	--	--	--	40,428	1	17	0	40,427	40,411	11,877	(11,876)	28,550	28,534
Cave Valley	15,551	0	0	0	13,658	7,350	0	1,893	8,201	15,552	1,551	342	6,650	14,001
Jakes Valley	17,691	72,544	30,930	0	90,257	47,761	16,833	1	860	857	858	(857)	2	(1)
Lake Valley	17,896	35,140	29,940	28,939	53,036	43,085	42,116	0	4,759	4,713	6,135	(6,135)	(1,376)	(1,422)
Little Smoky Valley	6,562	0	0	0	72,544	30,930	0	4,588	5,979	5,222	3,955	633	2,024	1,267
Long Valley	32,130	40,427	0	80	1,974	583	1,340	1	1,200	32,250	1,234	(1,233)	(35)	31,016
Newark Valley	26,986	1,990	584	1,340	0	0	0	27,642	27,593	28,317	26,059	1,582	1,534	2,258
Snake Valley	133,000	141,895	55,312	71,736	--	--	--	275,529	188,357	204,693	132,284	143,245	56,073	72,409
Spring Valley	103,306	53,036	44,733	44,766	141,841	55,381	72,850	14,502	92,631	75,229	75,614	(61,111)	17,017	(385)
Steptoe Valley	168,675	0	1	1	35,165	31,592	55,019	133,510	137,095	113,674	101,498	32,012	35,597	12,176
Tippet Valley	13,750	46	69	1,115	100	0	1	13,715	13,803	14,907	1,742	11,973	12,061	13,165
White River Valley	47,813	103,924	55,115	40,199	--	--	--	154,263	103,022	88,015	76,702	77,561	26,320	11,313

Notes:
All values are acre-feet/year
(Values in parentheses) indicate negative values
DSC model optimization:
C - concentration only
O - concentration + outflow
O* - concentration + modified outflow

Table 12. Summary of Deterministic-Sensitivity Uncertainty Analysis Simulation Results

		Simulation:	DS-1	DS-2	DS-3	DS-4	DS-5	DS-6	DS-7
		Recharge δD							
		Interpolation Method:	IDW	IDW	IDW	Lat. Regr.	Lat. Regr.	Lat. Regr.	IDW
		Objective Function:	wRMSEc	wRMSEo	wRMSEo*	wRMSEc	wRMSEo	wRMSEo*	SAE
Cell to Cell Rates (afy)									
	From Cell	To Cell							
	1	8	132,610	77,488	77,860	132,650	77,961	78,210	1,485
	2	3	0	0	0	0	0	0	0
	2	4	53,035	41,783	42,599	53,035	44,657	44,740	53,009
	3	5	15,122	8,423	1	8,561	1	1	15,433
	4	1	83,614	49,312	49,546	83,607	49,763	49,903	83,581
	6	12	588	1,246	118	0	0	0	2
	7	5	55,193	61,448	61,141	72,679	82,006	61,716	77,434
	8	14	166,750	73,190	74,015	166,640	73,698	74,338	9,572
	9	2	35,139	28,701	29,382	35,140	31,585	31,585	35,140
	9	3	0	0	0	0	0	0	0
	9	4	0	2,885	2,204	0	0	2	0
	9	11	0	0	0	0	0	0	0
	9	15	0	0	0	0	0	0	0
	10	7	90,260	47,766	16,790	80,029	37,850	16,833	49,818
	10	19	0	0	42	0	0	0	0
	11	7	1	3	23,447	7	23,299	23,979	11
	11	10	11	0	0	5	0	0	0
	11	20	0	1	0	0	0	1	1
	12	6	0	0	0	37,154	11,457	45,691	0
	13	19	40,427	0	0	40,427	0	28,726	0
	13	20	0	4	1	0	4	3	9
	14	17	270,660	70,296	87,699	277,850	72,478	84,963	146,270
	15	14	58,333	5,679	22,278	61,172	7,350	19,263	72,707
	15	18	33	8	1,049	3,730	3,511	4,282	0
	16	15	12,752	11,021	11,019	12,752	11,021	11,022	12,751
	18	14	31	4	0	4,715	7	4	13,624
	19	10	72,518	30,929	0	62,044	21,050	0	32,129
	19	12	0	1	1,167	10,506	9,920	59,627	1
Outflow Rates (afy)									
Cell	Target GWET Rate	Target GWET Weight							
1	21,049	0.0002	86	20,889	20,783	37	20,884	20,785	131,160
2	6,135	0.0002	0	4,810	4,669	1	4,819	4,739	27
3	1,551	0.0012	429	7,129	15,552	6,991	15,551	15,551	119
4	26,889	0.0002	1	25,965	25,836	0	25,467	25,406	7
5	65,463	0.0001	87,017	85,673	76,825	96,312	97,686	77,398	108,480
6	3,955	0.0018	5,974	5,316	6,444	43,758	18,023	52,590	6,560
7	11,238	0.0006	67,193	18,463	11,231	39,488	11,240	11,216	4,550
8	39,038	0.0001	35	38,465	38,056	17	38,433	38,023	27,544
9	3,569	0.0027	0	3,554	3,553	0	3,554	3,552	0
10	858	0.0110	4	858	858	1	857	858	1
11	40,983	0.0002	64,075	64,084	40,640	64,075	40,788	40,107	64,074
12	26,059	0.0002	29,763	28,247	29,979	61	25,487	40,483	26,990
13	11,877	0.0001	1	40,424	40,427	0	40,424	11,698	40,419
14	54,836	0.0001	47	54,431	54,555	25	54,563	54,501	188
15	46,991	0.0001	14,359	65,306	47,669	7,825	60,135	47,452	16
16	1,733	0.0042	0	1,731	1,733	0	1,731	1,730	1
17	17,361	0.0002	274,500	74,074	91,582	281,700	76,378	88,779	149,970
18	1,742	0.0012	13,749	13,773	14,799	12,658	17,245	18,118	128
19	1,234	0.0006	18	1,200	31,006	7	1,160	1,251	0
20	56,945	0.0001	69,450	69,458	69,457	69,449	69,455	69,453	69,479

Table 12. Summary of Deterministic-Sensitivity Uncertainty Analysis Simulation Results (continued)

		Simulation:	DS-1	DS-2	DS-3	DS-4	DS-5	DS-6	DS-7
		Recharge δD Interpolation Method:	IDW	IDW	IDW	Lat. Regr.	Lat. Regr.	Lat. Regr.	IDW
		Objective Function:	wRMSEc	wRMSEo	wRMSEo*	wRMSEc	wRMSEo	wRMSEo*	SAE
Predicted δD Values									
Cell	Observed δD Value (‰)	Observation Weight (‰$^{-1}$)							
1	-111	0.94	-108.8	-108.3	-108.3	-108.4	-107.9	-107.9	-108.8
2	-111	0.44	-111.0	-110.5	-110.6	-109.6	-109.5	-109.5	-111.0
3	-104	0.28	-107.0	-107.0	-107.0	-106.0	-106.0	-106.0	-107.0
4	-110	0.69	-109.9	-109.6	-109.6	-109.8	-109.7	-109.7	-109.9
5	-115	0.35	-115.1	-115.0	-113.9	-115.0	-114.2	-112.6	-115.0
6	-120	0.25	-121.0	-121.0	-121.0	-118.8	-117.2	-120.0	-121.0
7	-120	0.33	-119.5	-118.1	-115.7	-118.3	-116.0	-114.6	-118.2
8	na	na	-109.7	-109.8	-109.8	-109.1	-109.1	-109.1	-112.7
9	-118	0.11	-114.0	-114.0	-114.0	-112.0	-112.0	-112.0	-114.0
10	na	na	-121.8	-121.5	-119.0	-120.8	-118.7	-116.0	-121.6
11	-123	0.11	-117.0	-117.0	-117.0	-117.0	-117.0	-117.0	-117.0
12	-122	0.10	-121.9	-122.0	-122.1	-119.9	-119.5	-121.0	-122.0
13	na	na	-122.0	-122.0	-122.0	-123.0	-123.0	-123.0	-122.0
14	-118	0.30	-112.8	-112.8	-113.5	-112.8	-112.9	-113.3	-117.8
15	-123	0.31	-118.5	-118.5	-118.5	-118.2	-118.1	-118.1	-118.5
16	-126	0.10	-121.0	-121.0	-121.0	-124.0	-124.0	-124.0	-121.0
17	-111	0.50	-112.9	-113.3	-113.8	-112.9	-113.3	-113.7	-117.9
18	-122	0.34	-122.0	-122.0	-121.8	-122.0	-122.0	-121.8	-122.0
19	-129	0.10	-122.4	-123.0	-123.0	-122.1	-121.0	-121.9	-123.0
20	-128	0.34	-123.0	-123.0	-123.0	-125.0	-125.0	-125.0	-123.0
Objective Function Values									
wRMSEc (unitless)			0.85	0.93	0.98	0.87	1.02	1.05	1.08
wRMSEo (unitless)			2.98	0.66	0.70	3.11	0.72	0.74	3.02
wRMSEo* (unitless)			6.13	1.24	0.70	4.17	0.75	0.74	3.11
SAE (‰)			45.22	47.45	51.08	47.08	54.49	52.32	45.71
Model Outflow - GWET (afy)									
		Cell							
		1	-20,963	-160	-266	-21,012	-165	-264	110,111
		2	-6,135	-1,325	-1,466	-6,134	-1,316	-1,396	-6,108
		3	-1,122	5,578	14,001	5,440	14,000	14,000	-1,432
		4	-26,888	-924	-1,053	-26,889	-1,422	-1,483	-26,882
		5	21,554	20,210	11,362	30,849	32,223	11,935	43,017
		6	2,019	1,361	2,489	39,803	14,068	48,635	2,605
		7	55,955	7,225	-7	28,250	2	-22	-6,688
		8	-39,003	-573	-982	-39,021	-605	-1,015	-11,494
		9	-3,569	-16	-16	-3,569	-15	-17	-3,569
		10	-854	0	0	-857	-1	0	-857
		11	23,092	23,101	-343	23,092	-195	-876	23,091
		12	3,704	2,188	3,920	-25,998	-572	14,424	931
		13	-11,876	28,547	28,550	-11,877	28,547	-179	28,542
		14	-54,789	-405	-281	-54,811	-273	-335	-54,648
		15	-32,632	18,315	678	-39,166	13,144	461	-46,975
		16	-1,733	-2	0	-1,733	-2	-3	-1,732
		17	257,139	56,713	74,221	264,339	59,017	71,418	132,609
		18	12,007	12,031	13,057	10,916	15,503	16,376	-1,614
		19	-1,216	-34	29,772	-1,227	-74	17	-1,234
		20	12,505	12,513	12,512	12,504	12,510	12,508	12,534

Table 12. Summary of Deterministic-Sensitivity Uncertainty Analysis Simulation Results (continued)

Simulation:	DS-1	DS-2	DS-3	DS-4	DS-5	DS-6	DS-7
Recharge δD							
Interpolation Method:	IDW	IDW	IDW	Lat. Regr.	Lat. Regr.	Lat. Regr.	IDW
Objective Function:	wRMSEc	wRMSEo	wRMSEo*	wRMSEc	wRMSEo	wRMSEo*	SAE
Net Interbasin Inflow (afy)							
Butte Valley	0	0	0	0	0	0	0
Cave Valley	0	0	0	0	0	0	0
Jakes Valley	72,529	30,929	0	62,049	21,050	0	32,129
Lake Valley	35,139	28,701	29,382	35,140	31,585	31,585	35,140
Little Smoky Valley	0	0	0	37,154	11,457	45,691	0
Long Valley	40,427	0	42	40,427	0	28,726	0
Newark Valley	588	1,248	1,285	10,506	9,920	59,627	2
Snake Valley	141,978	54,996	71,824	149,494	57,120	69,170	169,912
Spring Valley	53,035	44,668	44,804	53,035	44,657	44,743	53,009
Steptoe Valley	0	4	1	0	4	3	9
Tippett Valley	33	8	1,049	3,730	3,511	4,282	0
White River Valley	105,383	56,192	40,238	88,596	61,150	40,813	65,262
Net Interbasin Outflow (in Study Area, afy)							
Butte Valley	40,427	4	1	40,427	4	28,729	9
Cave Valley	15,122	8,423	1	8,561	1	1	15,433
Jakes Valley	90,260	47,766	16,832	80,029	37,850	16,833	49,818
Lake Valley	53,035	41,783	42,599	53,035	44,657	44,740	53,009
Little Smoky Valley	588	1,246	118	0	0	0	2
Long Valley	72,518	30,930	1,167	72,550	30,970	59,627	32,130
Newark Valley	0	0	0	37,154	11,457	45,691	0
Snake Valley	0	0	0	0	0	0	0
Spring Valley	141,980	54,999	72,873	148,509	60,624	73,448	156,288
Steptoe Valley	35,151	31,589	55,034	35,151	54,885	55,567	35,152
Tippett Valley	31	4	0	4,715	7	4	13,624
White River Valley	0	0	0	0	0	0	0
Outflow from Study Area - BARCAS GWET (afy)							
Butte Valley	-11876	28547	28550	-11877	28547	-179	28542
Cave Valley	-1122	5578	14001	5440	14000	14000	-1432
Jakes Valley	-854	0	0	-857	-1	0	-857
Lake Valley	-6135	-1325	-1466	-6134	-1316	-1396	-6108
Little Smoky Valley	2019	1361	2489	39803	14068	48635	2605
Long Valley	-1216	-34	29772	-1227	-74	17	-1234
Newark Valley	3704	2188	3920	-25998	-572	14424	931
Snake Valley	142384	55575	72692	149496	57974	69804	176578
Spring Valley	-61253	17389	-375	-67787	11720	-1025	-75589
Steptoe Valley	32028	35599	12153	32027	12300	11615	32056
Tippett Valley	12007	12031	13057	10916	15503	16376	-1614
White River Valley	77509	27435	11355	59099	32225	11913	36329

Notes:
All simulationsBCM-predicted recharge rates assuming 15 percent potential runoff becoming recharge.
Underlined valuesindicate outflow rates for 'interior' model cells for optimization scenario O*.
afy = acre-feet/year
wRMSE = weighted root mean square error
SAE = sum of absolute errors
IDW = inverse distance weighting
Lat. Regr. = latitude regression

Table 13. Summary of Monte Carlo Uncertainty Analysis Results for Simulations MC-1 through MC-7

		MC-1			MC-2		
		Median	95% LCI	95% UCI	Median	95% LCI	95% UCI
Recharge (afy)							
Recharge	To cell						
R	1	49,085	42,880	55,250	48,980	42,730	55,400
R	2	18,035	14,570	21,300	17,870	14,460	21,310
R	3	15,575	14,380	16,710	15,560	14,420	16,720
R	4	30,515	26,170	34,930	30,225	26,260	34,920
R	5	15,710	15,100	16,270	15,660	15,100	16,270
R	6	6,548	6,126	7,001	6,572	6,123	6,998
R	7	32,005	29,410	34,840	32,100	29,440	34,840
R	8	33,990	28,120	40,250	34,560	28,180	40,300
R	9	35,220	33,530	36,780	35,230	33,490	36,750
R	10	17,660	16,780	18,600	17,680	16,790	18,600
R	11	64,200	59,730	68,500	64,150	59,680	68,560
R	12	26,885	24,710	29,290	27,000	24,720	29,250
R	13	40,400	38,310	42,610	40,480	38,300	42,570
R	14	45,880	41,210	50,570	45,860	41,250	50,570
R	15	59,830	50,480	69,400	60,290	50,590	69,440
R	16	12,770	11,860	13,640	12,740	11,860	13,620
R	17	3,848	1,532	6,124	3,765	1,512	6,123
R	18	13,780	12,790	14,700	13,750	12,800	14,710
R	19	32,080	30,490	33,730	32,050	30,510	33,760
R	20	69,480	64,840	74,030	69,275	64,840	74,080
Cell to Cell Fluxes (afy)							
From cell	To cell						
1	8	132,500	122,800	142,500	77,405	67,630	86,940
2	3	0	0	1	0	0	1
2	4	52,375	35,640	57,370	41,580	27,850	48,100
3	5	13,540	1,533	16,100	7,370	1,595	12,940
4	1	83,740	77,320	90,280	49,340	42,800	55,760
6	12	797	0	6,885	890	0	2,625
7	5	56,190	34,120	78,650	58,640	48,230	77,850
8	14	166,300	154,600	178,100	73,245	61,510	85,120
9	2	34,595	19,630	36,770	28,800	17,220	32,900
9	3	0	0	0	0	0	0
9	4	0	0	16,250	2,647	0	14,540
9	11	0	0	1	0	0	1
9	15	0	0	0	0	0	0
10	7	82,330	47,890	92,540	47,750	45,560	49,880
10	19	0	0	0	0	0	0
11	7	8	0	124	7	0	25,980
11	10	2	0	142	0	0	0
11	20	0	0	1	0	0	1
12	6	0	0	28,700	0	0	2,673
13	19	32,825	0	42,410	0	0	0
13	20	1	0	41,690	3	0	30,640
14	17	269,850	236,400	301,300	70,770	53,500	95,760
15	14	57,000	27,650	78,090	5,406	1	22,500
15	18	73	0	6,281	243	0	6,614
16	15	12,770	11,860	13,640	11,000	10,130	11,890
18	14	225	6	13,350	5	0	3,930
19	10	64,360	30,550	74,960	30,850	29,290	32,570
19	12	1	0	35	1	0	9

Table 13. Summary of Monte Carlo Uncertainty Analysis Results for Simulations MC-1 through MC-7 (contd.)

		MC-1			MC-2		
		Median	95% LCI	95% UCI	Median	95% LCI	95% UCI
Outflow from Model Domain (afy)							
From cell	To						
1	OUT	38	2	326	20,880	20,620	21,020
2	OUT	1	0	4	4,858	3,931	5,484
3	OUT	1,976	81	13,830	8,122	2,637	13,960
4	OUT	1	0	13	25,950	25,130	26,550
5	OUT	85,057	51,864	108,170	81,289	72,108	101,350
6	OUT	5,659	5	35,260	5,637	3,979	9,184
7	OUT	55,760	3,054	86,640	23,100	14,030	39,180
8	OUT	42	2	310	38,440	37,550	38,870
9	OUT	0	0	0	3,553	3,543	3,561
10	OUT	6	0	99	860	857	872
11	OUT	64,080	59,650	68,460	63,175	40,930	68,530
12	OUT	29,010	9	35,700	27,670	25,860	30,490
13	OUT	10	0	42,300	39,880	11,240	42,520
14	OUT	60	2	329	54,470	53,990	54,790
15	OUT	13,540	14	45,170	62,660	46,880	78,950
16	OUT	1	0	9	1,732	1,730	1,741
17	OUT	273,695	240,220	305,370	74,749	56,860	100,230
18	OUT	13,825	274	19,630	14,405	10,390	20,400
19	OUT	2	0	54	1,200	1,176	1,223
20	OUT	70,547	64,932	112,380	70,722	64,855	102,020
Target Groundwater ET Discharge Rate (afy)							
From cell	To						
1	GWET	--	--	--	21,049	21,049	21,049
2	GWET	--	--	--	6,135	6,135	6,135
3	GWET	--	--	--	1,551	1,551	1,551
4	GWET	--	--	--	26,889	26,889	26,889
5	GWET	--	--	--	65,463	65,463	65,463
6	GWET	--	--	--	3,955	3,955	3,955
7	GWET	--	--	--	11,238	11,238	11,238
8	GWET	--	--	--	39,038	39,038	39,038
9	GWET	--	--	--	3,569	3,569	3,569
10	GWET	--	--	--	858	858	858
11	GWET	--	--	--	40,983	40,983	40,983
12	GWET	--	--	--	26,059	26,059	26,059
13	GWET	--	--	--	11,877	11,877	11,877
14	GWET	--	--	--	54,836	54,836	54,836
15	GWET	--	--	--	46,991	46,991	46,991
16	GWET	--	--	--	1,733	1,733	1,733
17	GWET	--	--	--	17,361	17,361	17,361
18	GWET	--	--	--	1,742	1,742	1,742
19	GWET	--	--	--	1,234	1,234	1,234
20	GWET	--	--	--	56,945	56,945	56,945

Table 13. Summary of Monte Carlo Uncertainty Analysis Results for Simulations MC-1 through MC-7 (contd.)

	MC-1			MC-2		
	Median	95% LCI	95% UCI	Median	95% LCI	95% UCI
Predicted dD Values (‰)						
Cell						
1	-108.8	-109.7	-107.9	-108.8	-109.7	-107.9
2	-111.0	-111.5	-109.7	-111.0	-111.5	-109.7
3	-107.0	-108.4	-105.6	-107.0	-108.4	-105.6
4	-109.9	-110.9	-108.9	-109.9	-110.9	-108.9
5	-115.0	-115.1	-114.9	-115.0	-115.1	-114.9
6	-120.9	-122.3	-119.8	-120.9	-122.3	-119.8
7	-119.0	-119.9	-118.0	-119.0	-119.9	-118.0
8	-109.7	-110.5	-108.8	-109.7	-110.5	-108.8
9	-114.0	-115.4	-112.6	-114.0	-115.4	-112.6
10	-121.8	-122.8	-120.7	-121.8	-122.8	-120.7
11	-117.0	-118.4	-115.6	-117.0	-118.4	-115.6
12	-122.0	-123.0	-120.6	-122.0	-123.0	-120.6
13	-122.0	-123.4	-120.6	-122.0	-123.4	-120.6
14	-112.8	-112.8	-112.8	-112.8	-112.8	-112.8
15	-118.5	-119.8	-117.3	-118.5	-119.8	-117.3
16	-121.0	-122.4	-119.6	-121.0	-122.4	-119.6
17	-112.9	-113.0	-112.9	-112.9	-113.0	-112.9
18	-122.0	-122.0	-120.6	-122.0	-122.0	-120.6
19	-122.8	-124.4	-121.4	-122.8	-124.4	-121.4
20	-123.0	-124.4	-121.7	-123.0	-124.4	-121.7
Objective Function Values (unitless)						
wRMSEc	0.87	0.75	1.01	--	--	--
wRMSEo	--	--	--	0.67	0.58	0.78
wRMSEo*	--	--	--	--	--	--

Table 13. Summary of Monte Carlo Uncertainty Analysis Results for Simulations MC-1 through MC-7 (contd.)

		MC-3			MC-4		
		Median	95% LCI	95% UCI	Median	95% LCI	95% UCI
Recharge (afy)							
Recharge	To cell						
R	1	49,295	42,690	55,390	62,975	43,491	86,210
R	2	17,875	14,440	21,310	23,411	15,686	33,099
R	3	15,550	14,420	16,690	13,733	9,287	19,778
R	4	30,750	26,210	34,900	29,047	20,897	37,163
R	5	15,690	15,100	16,270	17,970	12,670	24,401
R	6	6,554	6,121	6,997	8,317	4,918	12,895
R	7	32,190	29,500	34,820	23,995	16,228	33,022
R	8	34,495	28,120	40,210	43,605	22,776	59,485
R	9	35,070	33,510	36,790	17,416	10,637	25,140
R	10	17,715	16,770	18,620	13,584	8,122	20,446
R	11	64,055	59,730	68,470	45,021	27,172	63,849
R	12	27,080	24,690	29,300	28,229	18,480	39,238
R	13	40,370	38,270	42,540	28,245	18,383	39,118
R	14	45,900	41,150	50,670	29,509	19,614	43,028
R	15	60,180	50,610	69,420	59,881	33,581	91,743
R	16	12,795	11,870	13,640	6,653	4,398	9,108
R	17	3,866	1,562	6,164	16,298	7,408	32,505
R	18	13,770	12,810	14,700	9,176	6,168	12,826
R	19	32,180	30,480	33,740	22,611	15,562	32,038
R	20	69,655	64,910	74,020	33,890	19,491	57,785
Cell to Cell Fluxes (afy)							
From cell	To cell						
1	8	78,030	68,980	87,210	81,030	47,350	130,300
2	3	0	0	1	0	0	33,120
2	4	41,800	28,170	48,490	38,575	0	56,520
3	5	5	0	110	9,442	192	24,590
4	1	49,550	43,040	55,780	66,780	34,600	93,060
6	12	1,071	0	2,750	0	0	11,350
7	5	61,130	55,430	67,780	59,160	34,160	102,500
8	14	74,035	62,970	85,500	123,650	78,610	184,300
9	2	29,290	17,360	33,010	16,390	3,072	24,880
9	3	0	0	1	0	0	0
9	4	2,274	0	14,640	0	0	16,000
9	11	0	0	1	0	0	0
9	15	0	0	5	0	0	0
10	7	16,820	15,870	17,780	50,565	26,140	81,960
10	19	0	0	573	0	0	0
11	7	23,395	19,140	27,690	33	1	55,030
11	10	0	0	0	16	0	8,272
11	20	0	0	5	0	0	4
12	6	0	0	21,170	17,850	0	40,430
13	19	4	0	29,450	16,650	0	36,460
13	20	4	0	30,620	13	0	34,920
14	17	85,305	62,190	105,100	230,200	149,900	331,200
15	14	19,430	91	31,970	66,510	38,600	99,670
15	18	1,582	0	25,100	1	0	1,172
16	15	11,060	10,140	11,910	6,648	4,395	9,108
18	14	4	0	3,522	9,245	6,156	13,100
19	10	0	0	0	36,495	16,800	63,310
19	12	10,064	0	56,530	2	0	9,242

Table 13. Summary of Monte Carlo Uncertainty Analysis Results for Simulations MC-1 through MC-7 (contd.)

		MC-3			MC-4		
		Median	95% LCI	95% UCI	Median	95% LCI	95% UCI
Outflow from Model Domain (afy)							
From cell	To						
1	OUT	20,790	20,530	20,990	45,835	4,547	79,690
2	OUT	4,755	3,881	5,416	1	0	29,930
3	OUT	15,520	14,360	16,680	5,437	118	36,470
4	OUT	25,870	25,090	26,470	1	0	18
5	OUT	76,786	70,919	83,555	86,496	51,364	140,160
6	OUT	5,450	3,987	27,870	21,865	27	48,550
7	OUT	11,230	11,210	11,250	21,435	429	78,470
8	OUT	38,160	37,250	38,820	177	6	1,345
9	OUT	3,553	3,543	3,562	0	0	0
10	OUT	858	857	859	11	0	130
11	OUT	40,650	40,280	40,970	40,280	0	62,430
12	OUT	34,760	25,880	81,790	4,726	5	44,510
13	OUT	39,030	11,210	42,450	7	0	32,450
14	OUT	54,550	54,200	54,780	40	2	224
15	OUT	47,500	46,890	48,150	7	0	74
16	OUT	1,732	1,730	1,735	2	0	15
17	OUT	89,399	66,431	109,460	245,990	158,510	360,360
18	OUT	15,150	11,840	39,090	15	1	101
19	OUT	23,205	1,309	52,890	4	0	90
20	OUT	70,970	65,017	102,360	42,514	20,634	81,852
Target Groundwater ET Discharge Rate (afy)							
From cell	To						
1	GWET	21,049	21,049	21,049	--	--	--
2	GWET	6,135	6,135	6,135	--	--	--
3	GWET	1,551	1,551	1,551	--	--	--
4	GWET	26,889	26,889	26,889	--	--	--
5	GWET	65,463	65,463	65,463	--	--	--
6	GWET	3,955	3,955	3,955	--	--	--
7	GWET	11,238	11,238	11,238	--	--	--
8	GWET	39,038	39,038	39,038	--	--	--
9	GWET	3,569	3,569	3,569	--	--	--
10	GWET	858	858	858	--	--	--
11	GWET	40,983	40,983	40,983	--	--	--
12	GWET	26,059	26,059	26,059	--	--	--
13	GWET	11,877	11,877	11,877	--	--	--
14	GWET	54,836	54,836	54,836	--	--	--
15	GWET	46,991	46,991	46,991	--	--	--
16	GWET	1,733	1,733	1,733	--	--	--
17	GWET	17,361	17,361	17,361	--	--	--
18	GWET	1,742	1,742	1,742	--	--	--
19	GWET	1,234	1,234	1,234	--	--	--
20	GWET	56,945	56,945	56,945	--	--	--

Table 13. Summary of Monte Carlo Uncertainty Analysis Results for Simulations MC-1 through MC-7 (contd.)

	MC-3			MC-4		
	Median	95% LCI	95% UCI	Median	95% LCI	95% UCI
Predicted dD Values (‰)						
Cell						
1	-108.3	-109.3	-107.5	-106.0	-107.0	-105.0
2	-110.6	-110.9	-109.5	-108.2	-109.5	-104.3
3	-107.0	-108.4	-105.6	-104.9	-106.4	-103.6
4	-109.7	-110.7	-108.6	-108.0	-109.7	-106.8
5	-113.9	-115.0	-113.1	-115.0	-115.1	-114.9
6	-121.0	-122.3	-119.6	-121.5	-122.9	-120.6
7	-115.7	-116.8	-114.7	-118.9	-119.8	-117.9
8	-109.8	-110.7	-108.9	-107.4	-108.2	-106.6
9	-114.1	-115.4	-112.6	-113.9	-115.4	-112.6
10	-118.9	-120.5	-117.6	-121.1	-122.1	-120.1
11	-117.0	-118.5	-115.6	-118.0	-119.4	-116.6
12	-122.1	-123.2	-121.1	-122.0	-123.2	-120.6
13	-122.0	-123.4	-120.6	-122.0	-123.4	-120.6
14	-113.3	-114.2	-112.8	-112.5	-112.7	-112.3
15	-118.5	-119.7	-117.2	-118.2	-119.6	-117.0
16	-120.9	-122.4	-119.6	-121.0	-122.4	-119.6
17	-113.7	-114.5	-113.1	-113.0	-113.1	-112.9
18	-121.5	-122.0	-120.1	-121.0	-122.0	-119.6
19	-123.0	-124.4	-121.7	-122.1	-123.4	-120.8
20	-122.9	-124.4	-121.7	-122.2	-123.4	-120.9
Objective Function Values (unitless)						
wRMSEc	--	--	--	1.38	1.19	1.60
wRMSEo	--	--	--	--	--	--
wRMSEo*	0.71	0.68	0.66	--	--	--

Table 13. Summary of Monte Carlo Uncertainty Analysis Results for Simulations MC-1 through MC-7 (contd.)

		MC-5			MC-6		
		Median	95% LCI	95% UCI	Median	95% LCI	95% UCI
Recharge (afy)							
Recharge	To cell						
R	1	65,215	46,930	87,571	69,865	52,720	85,480
R	2	24,089	17,124	33,627	28,350	17,050	40,510
R	3	13,974	9,443	20,213	15,330	11,460	19,690
R	4	30,039	23,267	37,353	27,985	19,530	36,760
R	5	18,169	13,172	24,265	21,035	16,360	26,070
R	6	8,327	5,054	12,753	9,392	5,798	12,750
R	7	24,672	17,664	33,559	28,770	21,350	35,420
R	8	44,930	26,074	60,264	45,165	31,330	58,720
R	9	18,101	11,714	25,537	26,670	16,630	36,500
R	10	13,724	8,122	21,006	27,395	16,340	37,990
R	11	46,764	30,930	64,989	51,025	34,960	67,730
R	12	29,480	20,195	39,915	36,000	23,650	47,970
R	13	29,263	20,136	39,501	48,915	27,550	67,920
R	14	31,164	20,748	43,706	33,995	23,960	42,600
R	15	63,277	36,794	94,497	64,520	37,680	90,670
R	16	6,864	4,800	9,214	6,583	4,256	8,963
R	17	18,086	7,714	33,678	23,115	13,940	32,020
R	18	9,282	6,164	13,103	11,030	7,495	14,570
R	19	22,988	15,897	32,806	32,550	31,350	33,780
R	20	36,315	20,606	59,778	53,405	31,100	73,500
Cell to Cell Fluxes (afy)							
From cell	To cell						
1	8	77,245	46,470	116,800	101,400	59,900	152,400
2	3	0	0	21,240	0	0	45,840
2	4	34,720	0	50,240	33,520	0	68,210
3	5	1,551	1	8,899	10,007	741	38,590
4	1	40,965	20,410	64,930	59,405	21,430	95,740
6	12	1,581	0	6,959	0	0	7,803
7	5	49,400	33,900	69,660	64,790	38,040	120,700
8	14	85,565	52,820	138,400	140,500	96,870	199,200
9	2	14,350	3,378	22,000	18,915	1,242	35,870
9	3	0	0	0	0	0	0
9	4	1	0	11,810	0	0	20,430
9	11	0	0	0	0	0	0
9	15	0	0	0	0	0	0
10	7	34,430	21,840	52,180	80,175	42,540	123,400
10	19	0	0	0	0	0	0
11	7	1,725	0	22,380	16	1	48,660
11	10	0	0	0	15	0	6,432
11	20	1	0	6	0	0	2
12	6	0	0	16,930	23,245	0	58,600
13	19	0	0	0	28,890	0	66,550
13	20	17,145	1	30,230	2	0	47,260
14	17	99,075	39,290	203,400	233,650	162,100	317,100
15	14	25,790	1,983	58,930	53,095	22,170	92,820
15	18	2	0	1,134	1,960	0	7,579
16	15	5,177	3,255	7,605	5,574	2,575	8,902
18	14	7,917	4,682	11,950	9,125	2	19,760
19	10	21,645	14,150	31,820	57,200	33,070	62,940
19	12	3	0	3,818	150	2	9,300

Table 13. Summary of Monte Carlo Uncertainty Analysis Results for Simulations MC-1 through MC-7 (contd.)

		MC-5			MC-6		
		Median	95% LCI	95% UCI	Median	95% LCI	95% UCI
Outflow from Model Domain (afy)							
From cell	To						
1	OUT	25,660	15,120	61,330	616	1	79,680
2	OUT	3,851	2	19,870	2	0	52,930
3	OUT	12,240	3,339	35,080	4,226	199	43,040
4	OUT	21,890	11,940	34,970	1	0	11
5	OUT	70,332	50,650	94,791	94,762	57,214	179,630
6	OUT	6,363	3,456	25,980	31,610	88	67,220
7	OUT	13,135	8,816	33,070	40,085	1,397	109,300
8	OUT	34,020	20,700	50,330	29	1	1,085
9	OUT	3,411	2,759	4,068	0	0	0
10	OUT	832	678	1,006	14	0	3,653
11	OUT	41,090	29,380	59,010	42,075	3	67,140
12	OUT	29,515	15,450	41,950	1,875	1	51,700
13	OUT	10,925	2,785	34,920	5	0	40,770
14	OUT	47,985	30,190	68,940	16	1	105
15	OUT	42,310	28,840	58,050	12	0	40,900
16	OUT	1,667	1,233	2,144	0	0	3
17	OUT	118,000	50,756	232,320	252,835	178,220	340,500
18	OUT	1,386	527	3,091	16	0	17,410
19	OUT	895	20	3,413	5	0	3
20	OUT	51,419	31,596	81,042	52,167	17,671	103,800
Target Groundwater ET Discharge Rate (afy)							
From cell	To						
1	GWET	19,220	12,899	26,787	--	--	--
2	GWET	6,780	4,703	15,819	--	--	--
3	GWET	1,643	1,105	3,368	--	--	--
4	GWET	23,263	12,288	38,466	--	--	--
5	GWET	57,820	33,159	87,504	--	--	--
6	GWET	3,727	2,890	4,669	--	--	--
7	GWET	10,710	7,919	14,441	--	--	--
8	GWET	34,214	20,771	51,380	--	--	--
9	GWET	3,471	2,803	4,155	--	--	--
10	GWET	829	677	1,007	--	--	--
11	GWET	39,671	29,967	48,799	--	--	--
12	GWET	24,460	14,170	39,657	--	--	--
13	GWET	7,573	2,588	26,732	--	--	--
14	GWET	48,785	30,344	71,964	--	--	--
15	GWET	43,431	29,032	59,747	--	--	--
16	GWET	1,668	1,234	2,146	--	--	--
17	GWET	16,781	8,976	32,295	--	--	--
18	GWET	1,385	525	3,019	--	--	--
19	GWET	936	17	4,667	--	--	--
20	GWET	50,657	25,646	76,982	--	--	--

Table 13. Summary of Monte Carlo Uncertainty Analysis Results for Simulations MC-1 through MC-7 (contd.)

	MC-5			MC-6		
	Median	95% LCI	95% UCI	Median	95% LCI	95% UCI
Predicted dD Values (‰)						
Cell						
1	-105.4	-106.4	-104.3	-107.5	-108.4	-105.8
2	-107.7	-109.1	-104.4	-108.0	-109.7	-104.8
3	-104.9	-106.4	-103.6	-105.3	-106.3	-104.3
4	-107.5	-108.8	-106.4	-109.3	-110.1	-107.8
5	-115.0	-115.1	-113.4	-115.0	-115.0	-114.9
6	-121.8	-123.2	-120.6	-119.8	-120.0	-118.7
7	-118.0	-119.0	-117.0	-119.0	-119.6	-117.9
8	-107.1	-108.0	-106.1	-108.4	-109.1	-107.1
9	-114.0	-115.4	-112.6	-112.7	-114.2	-111.1
10	-120.8	-122.0	-119.7	-121.2	-121.8	-119.9
11	-118.0	-119.4	-116.6	-116.9	-118.0	-115.8
12	-122.1	-123.3	-120.6	-120.6	-121.6	-119.1
13	-122.0	-123.4	-120.6	-123.0	-124.4	-121.6
14	-112.0	-112.6	-111.3	-112.4	-112.6	-111.8
15	-118.3	-119.5	-116.9	-117.3	-118.2	-116.1
16	-121.0	-122.4	-119.6	-122.4	-123.6	-121.1
17	-113.1	-114.2	-112.9	-113.0	-113.3	-112.9
18	-120.9	-122.0	-119.6	-122.0	-122.0	-121.5
19	-122.0	-123.4	-120.6	-123.0	-123.8	-121.8
20	-122.2	-123.4	-120.8	-124.0	-125.0	-122.6
Objective Function Values (unitless)						
wRMSEc	--	--	--	1.09	0.95	1.41
wRMSEo	1.09	0.93	1.26	--	--	--
wRMSEo*	--	--	--	--	--	--

Table 13. Summary of Monte Carlo Uncertainty Analysis Results for Simulations MC-1 through MC-7 (contd.)

		MC-7		
		Median	95% LCI	95% UCI
Recharge (afy)				
Recharge	To cell			
R	1	63,090	39,590	84,660
R	2	25,725	9,664	40,520
R	3	13,800	8,230	19,620
R	4	24,450	12,720	36,520
R	5	19,280	13,030	25,900
R	6	8,064	3,275	12,670
R	7	25,805	16,690	34,940
R	8	39,370	21,090	58,690
R	9	22,745	9,000	36,330
R	10	22,975	8,692	37,580
R	11	46,030	22,650	67,670
R	12	31,370	13,800	48,310
R	13	40,175	13,330	67,840
R	14	30,545	18,070	42,640
R	15	56,770	20,740	89,510
R	16	5,794	2,604	8,941
R	17	19,685	7,236	31,450
R	18	9,924	5,324	14,510
R	19	32,090	30,470	33,780
R	20	45,345	16,740	73,070
Cell to Cell Fluxes (afy)				
From cell	To cell			
1	8	71,895	38,230	111,400
2	3	0	0	20,940
2	4	35,470	2	60,360
3	5	14	0	12,650
4	1	33,370	1,337	64,210
6	12	0	0	9,094
7	5	62,970	40,630	90,040
8	14	74,630	38,930	120,000
9	2	16,455	2,181	31,850
9	3	0	0	0
9	4	1	0	12,840
9	11	0	0	9,657
9	15	0	0	1
10	7	43,820	21,400	63,400
10	19	0	0	1
11	7	42	0	28,710
11	10	0	0	0
11	20	0	0	9
12	6	1,155	0	26,460
13	19	0	0	20,640
13	20	12,180	0	50,760
14	17	73,600	37,740	136,900
15	14	10,960	0	49,190
15	18	937	0	5,815
16	15	4,067	818	7,253
18	14	6,565	1	16,320
19	10	23,900	0	31,660
19	12	4,856	0	45,980

Table 13. Summary of Monte Carlo Uncertainty Analysis Results for Simulations MC-1 through MC-7 (contd.)

		MC-7		
		Median	95% LCI	95% UCI
Outflow from Model Domain (afy)				
From cell	To			
1	OUT	22,005	13,610	42,500
2	OUT	5,428	0	32,070
3	OUT	12,535	2,171	33,410
4	OUT	26,600	12,950	40,220
5	OUT	84,990	59,601	112,430
6	OUT	7,506	2,211	34,470
7	OUT	11,765	7,343	26,910
8	OUT	37,225	22,090	52,090
9	OUT	3,559	2,865	4,206
10	OUT	818	618	1,017
11	OUT	38,855	27,030	63,620
12	OUT	37,955	16,080	55,340
13	OUT	20,950	2,748	63,040
14	OUT	51,565	31,570	72,580
15	OUT	42,670	24,570	64,550
16	OUT	1,732	1,287	2,157
17	OUT	93,580	49,172	160,420
18	OUT	3,073	132	16,490
19	OUT	2,781	6	7,266
20	OUT	60,166	31,122	99,286
Target Groundwater ET Discharge Rate (afy)				
From cell	To			
1	GWET	21,733	13,677	29,138
2	GWET	14,071	5,272	23,528
3	GWET	2,409	150	4,875
4	GWET	28,615	13,390	44,261
5	GWET	66,619	31,970	102,220
6	GWET	3,989	2,016	5,890
7	GWET	11,113	7,282	14,899
8	GWET	39,769	22,612	56,407
9	GWET	3,605	2,891	4,262
10	GWET	817	613	1,013
11	GWET	40,720	31,158	51,920
12	GWET	38,062	15,699	59,329
13	GWET	23,805	3,976	43,228
14	GWET	55,016	32,228	77,767
15	GWET	48,607	30,529	67,400
16	GWET	1,736	1,287	2,167
17	GWET	21,809	9,589	32,840
18	GWET	1,830	90	3,606
19	GWET	5,519	256	10,695
20	GWET	57,685	29,105	90,926

Table 13. Summary of Monte Carlo Uncertainty Analysis Results for Simulations MC-1 through MC-7 (contd.)

		MC-7		
		Median	95% LCI	95% UCI
Predicted dD Values (‰)				
	Cell			
	1	-107.0	-108.6	-105.1
	2	-108.3	-110.8	-104.8
	3	-105.7	-107.2	-104.3
	4	-108.7	-110.5	-106.9
	5	-114.5	-115.0	-112.4
	6	-118.6	-121.6	-114.7
	7	-117.2	-118.8	-115.2
	8	-108.4	-110.2	-106.6
	9	-113.2	-115.4	-111.1
	10	-120.0	-122.2	-117.0
	11	-117.2	-118.7	-115.6
	12	-120.9	-122.7	-118.8
	13	-123.5	-125.4	-121.6
	14	-112.6	-114.4	-110.6
	15	-117.4	-118.9	-116.0
	16	-122.8	-124.4	-121.1
	17	-114.3	-116.6	-112.8
	18	-122.0	-123.8	-121.6
	19	-123.0	-122.5	-123.6
	20	-124.2	-125.8	-122.6
Objective Function Values (unitless)				
	wRMSEc	--	--	--
	wRMSEo	0.93	0.71	1.21
	wRMSEo*	--	--	--

Notes:
afy = acre-feet/year
LCI = lower confidence interval
UCI = upper confidence iterval
wRMSE = weighted root mean square error

Table 14. Summary of Monte Carlo Uncertainty Analysis Results for Simulation MC-8

		MC-8		
		Median	95% LCI	95% UCI
Cell to Cell Fluxes (afy)				
From cell	To cell			
1	8	77,490	77,420	77,560
2	3	0	0	1
2	4	41,710	40,600	43,260
3	5	6,975	4,160	9,100
4	1	49,310	49,240	49,370
6	12	767	212	1,432
7	5	58,215	51,090	63,760
8	14	73,175	73,080	73,270
9	2	28,620	27,640	30,100
9	3	0	0	0
9	4	2,964	1,485	3,943
9	11	0	0	0
9	15	0	0	0
10	7	47,770	47,750	47,780
10	19	0	0	0
11	7	6	0	20
11	10	0	0	0
11	20	0	0	1
12	6	0	0	0
13	19	0	0	0
13	20	2	0	7
14	17	70,380	70,040	70,710
15	14	5,840	5,557	6,137
15	18	48	7	92
16	15	11,020	11,020	11,020
18	14	4	0	25
19	10	30,930	30,920	30,950
19	12	1	0	4
Outflow from Model Domain (afy)				
From cell	To			
1	OUT	20,900	20,860	20,930
2	OUT	4,799	4,740	4,847
3	OUT	8,577	6,451	11,390
4	OUT	25,950	25,920	25,990
5	OUT	80,866	70,761	88,528
6	OUT	5,795	5,130	6,350
7	OUT	21,685	16,150	28,820
8	OUT	38,490	38,420	38,550
9	OUT	3,553	3,550	3,556
10	OUT	859	857	865
11	OUT	64,080	64,070	64,090
12	OUT	27,760	27,220	28,420
13	OUT	40,430	40,420	40,430
14	OUT	54,430	54,270	54,610
15	OUT	65,110	64,800	65,400
16	OUT	1,732	1,730	1,735
17	OUT	74,175	73,809	74,606
18	OUT	13,800	13,760	13,860
19	OUT	1,195	1,184	1,207
20	OUT	69,454	69,449	69,463
Objective Function Values (unitless)				
	wRMSEo	0.662	0.662	0.662

Notes:
afy = acre-feet/year
LCI = lower confidence interval
UCI = upper confidence iterval
wRMSE = weighted root mean square error

Appendix A. Deuterium Data for Recharge Samples

NWIS Site Number	Site Name	Latititude (NAD83)	Longitude (NAD83)	Site Type	Sample Date	Deuterium, δD (‰)
9415515	WATER CANYON CREEK NEAR PRESTON, NV	38.98772	-114.95835	SW	10/24/2003	-109.5
					10/24/2003	-112.7
10243740	MCCOY CREEK NEAR MCGILL, NV	39.37411	-114.52834	SW	5/28/1992	-118
373255114102301	204 S05 E70 04BA 1	37.54858	-114.17387	GW	6/3/1985	-95
373953113400801	(C-36-16)20abb- 2	37.66470	-113.66969	GW	1/1/1981	-94.5
374441114252801	203 S02 E67 25DABB1	37.74469	-114.42527	GW	6/4/1985	-101
374607114242501	203 S02 E68 18DD 1	37.76858	-114.40777	GW	6/4/1985	-101
374934114555201	181 S01 E63 33 1 RATTLESNAKE SPRING	37.82608	-114.93111	Spring	3/24/2004	-97.3
375136114192001	198 S01 E68 13DB 1 Spring	37.85996	-114.32304	Spring	4/8/1985	-98
					4/8/1985	-104
375140114191801	198 S01 E68 13 1 MVW above Delmue Spring	37.86107	-114.32249	SW	4/8/1985	-98
375140115115601	171 S01 E60 13 1 SEAMAN SPRING	37.86119	-115.19878	Spring	6/25/2004	-99
375310114181701	198 S01 E69 06DB 1	37.88607	-114.30554	GW	6/5/1985	-92
375406114333701	202 N01 E66 34 1 CONNOR SPRING	37.90164	-114.56022	Spring	6/24/2004	-100.6
375410114333801	202 N01 E66 34ACD 1 BIG TREES SPRING	37.90274	-114.56139	Spring	6/24/2004	-102.3
375429114325601	202 N01 E66 35BB 1 PINE SPRING	37.90802	-114.54972	Spring	4/7/1985	-99
					6/24/2004	-99
375443114550501	181 N01 E63 28CC 1 BLACK ROCK SPRING	37.91190	-114.91890	Spring	3/22/1988	-94
					3/23/2004	-93.6
375452114322501	203 S01 E66 26 1 LIME SPRING	37.91441	-114.54111	Spring	6/24/2004	-99.9
375501114550701	181 N1 E63 28 1 UNNAMED SPRING--NR BLACKROC	37.91694	-114.91861	Spring	3/23/2004	-94.3
375507114322901	202 N01 E66 26AD 1 DEADMAN SPRING	37.91857	-114.54222	Spring	3/23/2004	-86.9
					3/23/2004	-88.7
375516114325601	202 N01 E66 26BAC 1 HIGHLAND SPRING	37.92107	-114.54972	Spring	6/24/2004	-99.6
					5/1/2005	-99.3
375609114531601	181 N01 E63 22 1 HAMILTON SPRING	37.93572	-114.88764	Spring	3/23/2004	-93.1
380022114052301	201 N02 E70 25 1 TOBE SPRING	38.00608	-114.08981	Spring	5/20/2004	-98.6
380024114052301	201 N02 E70 25 1 TOBE SPRING 2	38.00675	-114.08969	Spring	5/20/2004	-89.4
380136114144201	200 N02 E69 15 1 HORSETHIEF SPRING	38.02675	-114.24503	Spring	5/20/2004	-93.7
					5/1/2005	-97.6
380140114110901	201 N02 E70 18C 1 MVW above Eagle Canyon R	38.02774	-114.18665	SW	4/9/1985	-93
380155114514401	181 N02 E63 13 1 COYOTE SPRING	38.03186	-114.86219	Spring	5/1/2005	-95.2
380300115364201	172 N02 E57 07 1 Spring	38.04994	-115.61253	Spring	7/31/1985	-95
380324115395301	172 N02 E56 10 1 UNNAMED SPRING 8	38.05667	-115.66472	Spring	7/2/2005	-104.4
380714114200001	202 N03 E68 14 1 UPPER TOWER SPRING	38.12050	-114.33344	Spring	4/28/2004	-111.8
380731114035601	201 N03 E71 18A 1 SPRING BELOW REED SUMMIT	38.12524	-114.06637	Spring	5/21/2004	-92.2
380752114031801	196 N03 E71 08 1 BARREL SPRING	38.13106	-114.05506	Spring	5/21/2004	-99
380805115355801	172 N03 E57 08 1 Spring above Adaven	38.13467	-115.60031	Spring	7/31/1985	-103
380858114154501	201 N03 E69 04BCC 1 Parsnip Spring	38.14940	-114.26332	Spring	6/5/1985	-93.5
380912114211401	202 N03 E68 03 1 BLUE ROCK SPRING	38.15344	-114.35400	Spring	4/28/2004	-90.5
380941115383001	172 N04 E56 35 1 UNNAMED SPRING 7	38.16139	-115.64167	Spring	7/2/2005	-105.9
380946114390101	181 N04 E65 35 1 FOX CABIN	38.16267	-114.65033	Spring	6/29/2004	-103.5
380953114410101	181 N04 E65 33 1 SCOTTY SPRING	38.16478	-114.68375	Spring	6/26/2004	-98.9
381002115391201	172 N04 E56 35 1 Lower Little Cherry Cr Sp	38.16716	-115.65420	Spring	7/31/1985	-103
381033114392001	181 N04 E65 26 1 LOWER FAIRVIEW	38.17572	-114.65550	Spring	6/29/2004	-97.5
381033114434201	181 N04 E65 30 1 BAILEY SPRING	38.17594	-114.72828	Spring	6/29/2004	-98.5
					5/1/2005	-97.9
381047114425701	181 N04 E65 29 1 FENCE SPRING	38.17978	-114.71594	Spring	6/29/2004	-97.4
381112114395801	181 N04 E65 22 1 UPPER FAIRVIEW	38.18658	-114.66619	Spring	6/29/2004	-97.7
381117113515901	(C-30-18)21abc-S1	38.18806	-113.86639	Spring	11/19/2005	-102.3
381150114363101	202 N04 E66 20BB 1 Wildhorse Spring	38.19718	-114.60944	Spring	4/6/1985	-92.5
381246114422301	181 N04 E65 17 1 ROBINSON SPRING	38.21272	-114.70636	Spring	6/29/2004	-97.9
381358114412201	181 N04 E65 04DBD 1 LITTLE FIELD SPRING	38.23274	-114.69028	Spring	6/26/2004	-98.5
381437114150801	201 N05 E69 33D 1 Camp Creek	38.24357	-114.25304	SW	4/9/1985	-102
381453114022301	(c-29-20)36bbb-S1	38.24806	-114.03972	Spring	11/19/2005	-105.1
381506114421801	181 N05 E65 32AD 1 MELOY SPRING	38.25162	-114.70583	Spring	6/26/2004	-99.8
381517114070201	201 N05 E70 35 1 SOUTH MONUMENT SPRING	38.25481	-114.11711	Spring	5/21/2004	-102.3
381531114074901	201 N05 E70 27 1 LION SPRING	38.25864	-114.13033	Spring	5/21/2004	-104.2
381722114123201	201 N05 E69 14DDAD1 Burnt Canyon Spring	38.28940	-114.20971	Spring	6/5/1985	-93
381838114390101	183 N05 E65 11AD 1 Spring	38.31051	-114.65111	Spring	4/5/1985	-102

Appendix A. Deuterium Data for Recharge Samples

NWIS Site Number	Site Name	Latititude (NAD83)	Longitude (NAD83)	Site Type	Sample Date	Deuterium, δD (‰)
381840114380501	183 N05 E65 12 1 COTTONWOOD SPRING	38.31103	-114.63461	Spring	6/29/2004	-102.2
381905114241201	183 N05 E68 06C 2 Wilson Creek	38.31801	-114.40416	SW	4/5/1985	-97.5
381911114362601	183 N05 E66 05CBCC1 Lower Pony Spring	38.31968	-114.60805	Spring	7/23/1981	-101
381911114362901	183 N05 E66 05CCB 1 Lower Pony Spring	38.31968	-114.60889	Spring	4/5/1985	-101
381917114383201	183 N05 E65 01BDC 1 Upper Pony Spring	38.32135	-114.64305	Spring	7/23/1981	-99
381917114383501	183 N05 E65 01BC 1 Creek near Upper Pony Sp	38.32135	-114.64389	SW	4/5/1985	-99.5
381939114143801	196 N05 E69 03 1 UNNAMED SPR IN MILLER CAN	38.32739	-114.24383	Spring	5/19/2004	-111.8
381939115283001	172 N05 E58 05 1 BRADY SPRING	38.32747	-115.47508	Spring	10/28/2003	-108.5
					10/28/2003	-110.4
381946115230901	207 N06 E59 31 1 HORSE SPRING	38.32944	-115.38583	Spring	6/30/2005	-99.5
381951113554601	(C-28-19)36bcc-S1	38.33083	-113.92944	Spring	11/19/2005	-103.8
381955115213801	207 N06 E59 32 1 LITTLE SPRING	38.33194	-115.36056	Spring	6/30/2005	-99.4
381958114583301	207 N06 E62 35 1 PERRY SPRING D37	38.33286	-114.97586	Spring	10/28/2005	-103
382023115265801	207 N06 E58 34 1 MURPHY SPRING	38.33972	-115.44944	Spring	7/2/2005	-114.5
382042115244301	207 N06 E58 25 1 TEASPOON SPRING	38.34500	-115.41194	Spring	6/30/2005	-100
382108115253701	207 N06 E58 26 1 WIREGRASS SPRING	38.35222	-115.42694	Spring	6/30/2005	-101.4
382111114220201	183 N06 E68 29 1 BAILEY SPRING	38.35294	-114.36719	Spring	5/18/2004	-101.1
382157114191001	201 N06 E68 23 1 HEADWATERS SPRING WR5	38.36575	-114.31936	Spring	5/19/2004	-107.4
					7/18/2004	-90
					8/18/2004	-108.7
					9/23/2004	-108.8
					7/27/2005	-110.4
					8/13/2005	-109.6
					11/7/2005	-107.8
382212114574701	207 N06 E62 24 1 TROUGH SPRING	38.37000	-114.96306	Spring	10/28/2005	-103.6
382214115285201	207 N06 E58 20 1 Big Spring - Grant Range	38.37050	-115.48197	Spring	7/24/1985	-112
382239115223101	207 N06 E59 18DAA 1 Forest Home Spring	38.37744	-115.37613	Spring	7/24/1985	-108
382458114474301	180 S07 E64 33 1 SIDEHILL SPRING (D19)	38.41606	-114.79612	Spring	7/23/1986	-99
					8/1/2005	-100.5
383107114443301	180 N08 E64 25 1 UNNAMED SPRING 3 (D14)	38.51850	-114.74242	Spring	10/29/2003	-108.1
					10/29/2003	-105.8
					7/30/2005	-106.6
383223114560501	207 N08 E63 191 1 Shingle Spring	38.53967	-114.93557	Spring	8/3/1985	-104
383231113591101	(C-26-19)17ddd-S1	38.54194	-113.98639	Spring	7/28/2005	-103.7
383406115214201	173B N08 E59 08 1 Spring	38.56827	-115.36252	Spring	7/24/1985	-107
383528114432001	183 N09 E65 30D 1 PATTERSON PASS SPRING WR3	38.60939	-114.71750	Spring	10/30/2003	-106.5
					10/30/2003	-109.2
					3/24/2004	-106.2
					6/23/2004	-109.1
					9/23/2004	-107.9
					1/23/2005	-108.3
					5/20/2005	-106.8
					8/15/2005	-107.6
					11/7/2005	-107.5
383556114545901	180 N09 E63 33 1 BIG SPRINGS EGAN RNG D18	38.59884	-114.91723	Spring	10/14/2003	-104.2
					7/31/2005	-106.3
383744114160901	196 N09 E69 19ADDA1 THE TROUGHS OUTLET 1	38.62893	-114.26924	Spring	8/6/2003	-104
383744114322801	183 N09 E66 23BDBB1 USBLM North Gouge Eye Well	38.62869	-114.54183	GW	10/18/2005	-111.6
383828114474501	180 N09 E64 16ACB 1 Cave Spring	38.64106	-114.79667	Spring	8/2/1985	-100
					7/23/1986	-98
					12/14/2005	-103
383830114265801	184 N09 E67 15 1 INDIAN SPRINGS (D12)	38.64161	-114.44958	Spring	7/29/2005	-105.6
384009114541701	180 N09 E63 04 1 HAGGERTY SPRING (D17)	38.66931	-114.90481	Spring	7/31/2005	-108.5
384034114463601	180 N10 E64 34 1 Sheep Spring	38.67606	-114.77751	Spring	8/2/1985	-99.5
384201114271301	184 N10 E67 27BC 1	38.70025	-114.45363	Spring	8/30/2005	-105.6
384238114435001	183 N10 E65 19 1 North Creek Spring	38.71050	-114.73140	Spring	4/3/1985	-105
384400114200001	184 N10 E68 15 1 UNNAMED SPRING #3 (D3)	38.73322	-114.33336	Spring	7/13/2005	-109.8
384518115030701	207 N10 E62 06 1	38.75500	-115.05194	Spring	5/20/1992	-114
384614114470001	180 N11 E64 33 1 ROBBERS ROOST SPRING (D16)	38.77050	-114.78331	Spring	7/31/2005	-109.3
384714114175001	184 N11 E68 25 1 UNNAMED SPRING #1(D1)	38.78733	-114.29725	Spring	7/13/2005	-106.9
384733114173101	184 N11 E68 25 1 UNNAMED SPRING #2 (D2)	38.79242	-114.29203	Spring	7/13/2005	-108.2
384745114224401	184 N11 E68 19DCDC1 USGS-MX (Spring Valley)	38.79467	-114.37944	GW	12/13/2005	-105
384749114132401	196 N11 E69 27 1 CEDAR CABIN SPRING (D4)	38.79689	-114.22339	Spring	7/13/2005	-105.9

Appendix A. Deuterium Data for Recharge Samples

NWIS Site Number	Site Name	Latititude (NAD83)	Longitude (NAD83)	Site Type	Sample Date	Deuterium, δD (‰)
384815114103301	195 N11 E69 24 1 SOUTH SPRING (D7)	38.80406	-114.17589	Spring	7/14/2005	-107.4
384827114164401	196 N11 E69 19 1 DECATHON SPRING (D5)	38.80739	-114.27883	Spring	7/14/2005	-106.9
384839114525201	180 N11 E63 15 1 SILVER SPRING (D13)	38.81086	-114.88122	Spring	7/29/2005	-111.5
385000114114701	195 N11 E69 11 1 UNNAMED SPRING #1 (D9)	38.83339	-114.19639	Spring	7/28/2005	-106.7
385004115212901	173B N11 E59 08A 1 LITTLE CURRANT CK	38.83438	-115.35891	SW	8/23/1983	-113
385007114530301	180 N11 E63 10BA 1 Chimney Rock Spring	38.83522	-114.88501	Spring	8/1/1985	-109
385020115172301	207 N11 E59 1CDAA1 Secret Spring	38.83883	-115.29058	Spring	6/16/1983	-110
385030114205901	184 N11 E68 0 SWALLOW CANYON, BELOW	38.84162	-114.35055	SW	6/14/1983	-112
385033114205201	184 N11 E68 0 SWALLOW CANYON, ABOVE	38.84245	-114.34861	SW	6/14/1983	-110
385040114213901	184 N11 E68 5DBAB1 Little Swallow Spring	38.84439	-114.36166	Spring	6/14/1983	-110
385057114534401	179 N11 E63 04 1 HOLE IN THE BANK SPR (D15)	38.84914	-114.89567	Spring	7/31/2005	-114.9
385105114101301	195 N11 E69 01 1 UNNAMED SPRING #2 (D10)	38.85147	-114.17036	Spring	7/28/2005	-105.4
385141114241301	184 N12 E67 36 1	38.86139	-114.40361	Spring	5/27/1992	-121
385145114161801	196 N12 E69 31 1 MUSTANG SPRING (D6)	38.86258	-114.27178	Spring	7/14/2005	-111.3
385233114535501	179 N12 E63 28 1 Second Sawmill Spring	38.87578	-114.89946	Spring	8/1/1985	-110
385339115225801	173B N12 E59 18 1 Spring below Currant Mtn	38.89410	-115.38364	Spring	6/15/1983	-107
					10/12/2003	-113.6
385344114535801	207 N12 E63 1 LONE PINE SPRING	38.89550	-114.90029	Spring	10/13/2003	-109.2
385402115225701	173B N12 E59 18 2 Snwmlt Sp blw Duckwater Pk	38.90049	-115.38336	Spring	6/15/1983	-105
385434114063901	195 N12 E70 15CB 1 SPRING CREEK SPRING (D8)	38.90939	-114.11166	Spring	7/16/2005	-112.5
385436115231101	173B N12 E59 07 1 Saddle Spring	38.90994	-115.38725	Spring	6/15/1983	-116
385635114175401	195 N13 E68 36 1	38.94306	-114.29833	SW	9/1/1990	-96
					10/1/1990	-110
					6/1/1991	-109
					7/1/1991	-111
					8/1/1991	-108
					9/1/1991	-109
385636114175601	195 N13 E68 36 2	38.94333	-114.29889	SW	9/1/1990	-100
385657115243601	207 N13 E58 35 1 MONITORING SPRING WR1	38.94903	-115.41008	Spring	10/12/2003	-111.2
					3/23/2004	-113.3
					6/21/2004	-114
					9/22/2004	-115.7
					1/21/2005	-115.1
					5/21/2005	-112.3
					8/14/2005	-113.2
					11/5/2005	-113.8
385706114180901	195 N13 E68 35 1	38.95167	-114.30250	SW	9/1/1990	-90
					10/1/1990	-88
					5/1/1991	-108
					6/1/1991	-105
					7/1/1991	-103
					8/1/1991	-96
					9/1/1991	-90
385752115184101	207 N13 E59 26 1 HALFWAY SPRING	38.96444	-115.31139	Spring	6/29/2005	-108.4
385804115235601	207 N13 E58 24 1 UNNAMED SPRING 1	38.96778	-115.39889	Spring	6/28/2005	-114.8
385805114170601	195 N13 E68 25 1	38.96806	-114.28500	SW	9/3/1916	-113
					8/1/1990	-108
					9/1/1990	-104
					10/1/1990	-110
					7/1/1991	-112
					8/1/1991	-108
					9/1/1991	-102
385811114164601	195 N13 E69 30 2	38.96972	-114.27944	SW	8/1/1990	-93
					9/1/1990	-101
					10/1/1990	-104
					6/1/1991	-112
					8/1/1991	-105
					9/1/1991	-99
385823114221301	184 N13 E68 20 1 RAISED SPRING D36	38.97264	-114.37042	Spring	10/27/2005	-107.6
385831115240101	207 N13 E58 24 1 SADDLE SPRING	38.97542	-115.40022	Spring	10/12/2003	-115.7
					6/28/2005	-118.6

Appendix A. Deuterium Data for Recharge Samples

NWIS Site Number	Site Name	Latititude (NAD83)	Longitude (NAD83)	Site Type	Sample Date	Deuterium, δD (‰)
385832114162901	195 N13 E69 30 1	38.97556	-114.27472	SW	8/1/1990	-106
					9/1/1990	-105
					10/1/1990	-106
					5/1/1991	-111
					6/1/1991	-111
					7/1/1991	-106
					8/1/1991	-103
					9/1/1991	-102
385837115240201	207 N13 E58 24 1 UNNAMED SPRING 2	38.97694	-115.40056	Spring	6/28/2005	-114.9
385902114572401	207 N13 E62 03D 1 WATER CANYON	38.98383	-114.95752	SW	6/14/1983	-115
					8/23/1983	-117
385903115232501	207 N13 E59 18 1 UNNAMED SPRING 3	38.98417	-115.39028	Spring	6/28/2005	-113.1
385911114093101	195 N13 E70 19 1	38.98639	-114.15861	Spring	6/19/1992	-110
385935115223101	207 N13 E59 18 1 UNNAMED SPRING 6	38.99306	-115.37528	Spring	6/29/2005	-115.1
385942115232901	207 N13 E58 13 1 DEER SPRING	38.99494	-115.39131	Spring	10/12/2003	-118.9
					6/28/2005	-119.6
390010114184001	195 N13 E68 11CAC 1 Theresa Lake Feeder Spring	39.00272	-114.31194	Spring	8/1/1990	-104
					9/1/1990	-103
					10/1/1990	-106
					6/1/1991	-112
					7/1/1991	-107
					8/1/1991	-105
					9/1/1991	-102
390023115232601	207 N13 E59 7 1 UNNAMED SPRING 5	39.00639	-115.39056	Spring	6/29/2005	-120.4
390025114543801	207 N13 E63 08 1 WATER CANYON SPRING	39.00692	-114.91064	Spring	10/14/2003	-114.4
390032114185501	195 N13 E68 11 2	39.00889	-114.31528	SW	8/1/1990	-105
					9/1/1990	-108
					10/1/1990	-109
					6/1/1991	-110
					7/1/1991	-113
390044114181301	195 N13 E68 11 1	39.01222	-114.30361	SW	8/1/1990	-111
					9/1/1990	-113
					6/1/1991	-114
					7/1/1991	-115
					8/1/1991	-113
					9/1/1991	-114
390049114174501	195 N13 E68 01 2	39.01361	-114.29583	SW	8/1/1990	-111
					9/1/1990	-112
					1/1/1991	-115
					6/1/1991	-115
					7/1/1991	-113
					8/1/1991	-113
					9/1/1991	-115
390055114141101	195 N13 E69 09 2	39.01528	-114.23639	SW	8/1/1990	-116
					9/1/1990	-106
					10/1/1990	-116
					5/1/1991	-117
390055114141401	195 N13 E69 09 1	39.01528	-114.23722	SW	8/1/1990	-115
					9/1/1990	-116
					10/1/1990	-119
					1/1/1991	-119
					5/1/1991	-118
					6/1/1991	-116
					7/1/1991	-118
					8/1/1991	-105
					9/1/1991	-118
390056114141001	195 N13 E69 09 3	39.01556	-114.23611	SW	8/1/1991	-117
					9/1/1991	-118
390112114165501	195 N13 E68 01 1	39.02000	-114.28194	SW	8/1/1990	-113
					9/1/1990	-110
					10/1/1990	-114
					1/1/1991	-110
					5/1/1991	-113
					6/1/1991	-115
					7/1/1991	-114
					8/1/1991	-114
					9/1/1991	-115
390211115233601	207 N14 E58 36 1 UNNAMED SPRING 4	39.03639	-115.39333	Spring	6/29/2005	-116.3
390223114514801	179 N14 E63 35A 1 WILLOW CREEK	39.03966	-114.86418	SW	8/22/1983	-119
					6/12/1984	-116
390228115205601	207 N14 E59 28 1 EASTER SPRING	39.04111	-115.34889	Spring	6/29/2005	-119.4

Appendix A. Deuterium Data for Recharge Samples

NWIS Site Number	Site Name	Latititude (NAD83)	Longitude (NAD83)	Site Type	Sample Date	Deuterium, δD (‰)
390451115221701	207 N14 E59 17 1 LITTLE TOM PLAIN SPRING	39.08092	-115.37153	Spring	6/6/2005	-121.84
390512114553201	207 N14 E63 08 1 UPR TERRACE SPR FLTRD WR2	39.08664	-114.92564	Spring	10/13/2003	-111.3
					10/15/2003	-114.9
					4/26/2004	-89.9
					6/23/2004	-115.6
					9/22/2004	-114.4
					2/9/2005	-114.6
					5/21/2005	-113.7
					8/11/2005	-113.4
					11/6/2005	-113.7
390513115223901	207 N14 E59 07 1 BIG TOM PLAIN SPRING	39.08700	-115.37736	Spring	6/6/2005	-121.1
390542115214901	207 N14 E59 08 1 STOVE SPRING	39.09486	-115.36358	Spring	6/6/2005	-114.5
390543114081801	195 N14 E70 08DC 1 USGS-MX (Snake Valley S.)	39.09522	-114.13916	GW	7/16/2005	-113.2
390655115233201	173B N15 E58 36 1 SAGE HEN SPRING	39.11533	-115.39211	Spring	6/6/2005	-112.44
390718115220901	174 N15 E59 32 1 CIRCLE WASH SPRING	39.12169	-115.36928	Spring	6/6/2005	-114.5
390755115230401	174 N15 E59 30 1 SHELLBACK SPRING	39.13197	-115.38436	Spring	6/7/2005	-123.6
390802114574101	207 N15 E62 25CBBC1 Spring	39.13383	-114.96224	Spring	6/16/1983	-111
390818114025501	195 N15 E71 30CDDD1 CAINE SPRING	39.13839	-114.04864	Spring	12/12/2005	-114
390825115232201	174 N15 E58 25 1 UNNAMED SHELLBACK RIDGE SP	39.14039	-115.38953	Spring	6/7/2005	-123.59
390844114581201	207 N15 E62 23DCBD1 South Spring	39.14550	-114.97085	Spring	6/17/1983	-111
390905115233401	174 N15 E58 24 1 UNNAMED HAYDEN CANYON SPR	39.15147	-115.39264	Spring	6/7/2005	-120.9
390922114574701	207 N15 E62 23AAAD1 North Spring	39.15605	-114.96391	Spring	6/17/1983	-113
390933115235601	174 N15 E58 13 1 UNNAMED STONE CABIN SPR	39.15911	-115.39892	Spring	6/7/2005	-114.16
391041114170601	195 N15 E68 12 1 ROCK SPRING D35	39.17783	-114.28686	Spring	10/26/2005	-113.7
391054114222801	184 N15 E68 08BCCB1 ROCK SPRING	39.18153	-114.37431	Spring	12/12/2005	-114
391101114162501	195 N15 E69 7 1 RABBIT BRUSH SPRING	39.18361	-114.27361	Spring	10/26/2005	-117.1
391135114414401	179 N15 E65 05A 1 STEPTOE CREEK	39.19300	-114.69640	SW	6/14/1983	-117
391212114274501	184 N16 E67 32 1 UNNAMED SPRING 14 D41	39.20342	-114.46261	Spring	12/13/2005	-121
391259115235301	174 N16 E58 36 1 ASPEN SPRINGS(SOUTH)	39.21628	-115.39800	Spring	6/7/2005	-120.89
391316115235701	174 N16 E58 25 1 UNMARKED ASPEN SPR NORTH	39.22100	-115.39906	Spring	6/7/2005	-119.29
391345114535501	179 N16 E63 29AAAA1 City of Ely - Spring	39.22911	-114.89946	Spring	6/14/1983	-120
					8/5/2003	-117
391348114153901	195 N16 E69 19 1 UNNAMED SPRING	39.23000	-114.26083	Spring	10/26/2005	-115.7
391420115232001	174 N16 E58 24 1 CHICKEN SPRING	39.23886	-115.38886	Spring	6/7/2005	-122.02
391446114285801	184 N16 E66 34B 1 CLEVE CREEK	39.24605	-114.48362	SW	6/15/1983	-117
					8/22/1983	-119
391609114514601	179 N16 E63 10ADAC1 City of Ely	39.26911	-114.86363	GW	7/6/1983	-120
391654115232401	174 N16 E58 01D 1 UPPER ILLIPAH CREEK	39.28160	-115.39087	SW	6/13/1983	-124
					8/23/1983	-123
391810114232101	184 N17 E67 25 1	39.30278	-114.38917	Spring	6/18/1992	-116
391828114125901	195 N17 E69 28 1 UNNAMED SPRING 12 D33	39.30753	-114.21608	Spring	10/25/2005	-117.8
391932114160201	195 N17 E68 24 1 MUD SPRING D34	39.32575	-114.26714	Spring	10/25/2005	-115.6
391949114290401	184 N17 E67 19 1 UNNAMED SPRING 17 D44	39.33028	-114.48450	Spring	12/14/2005	-117.6
391950115271801	174 N17 E58 21BAC 1 Sand Spring	39.33049	-115.45587	Spring	7/14/1981	-123
392001115263601	174 N17 E58 2AAB 1 Wild-Horse Spring	39.33354	-115.44420	Spring	7/14/1981	-129
392105115265901	174 N17 E58 9 1 TUNNEL SPRING	39.35139	-115.44972	Spring	7/1/2005	-118.3
392118115201201	174 N17 E59 09D 1 LOWER ILLIPAH CREEK	39.35493	-115.33753	SW	6/13/1983	-114
392212114481001	179 N17 E64 05BC 1	39.36994	-114.80363	GW	6/13/1984	-120
392300115493001	154 N18 E55 31CABC1 U.S. FERA	39.38604	-115.82727	GW	7/31/1987	-129
392318114170401	184 N18 E68 26 1 EIGHT MILE SPRING (D32)	39.38836	-114.28433	Spring	8/26/2005	-116.1
392609115192801	174 N18 E59 10 1 SAMMY SPRING	39.43597	-115.32453	Spring	5/24/2005	-117.6
392625115190801	174 N18 E59 10 1 INDIAN SPRING	39.44039	-115.31883	Spring	6/5/2005	-119.11
392634115482101	154 N18 E55 08CADA1	39.44271	-115.80672	GW	7/31/1987	-123
392721115494901	154 N18 E55 06 1	39.45583	-115.83028	Spring	7/31/1987	-125
392724115562001	155A N18 E54 06 1	39.45667	-115.93889	Spring	7/31/1987	-117
392740114361501	184 N18 E65 01 1	39.46111	-114.60417	SW	5/28/1992	-116
392842114303301	184 N19 E66 26 1 UNNAMED SPRING 16 D43	39.47853	-114.50900	Spring	12/14/2005	-122.9
392847114513601	179 N19 E63 26CCB 1	39.47966	-114.86085	GW	7/26/1983	-125
392905114183701	184 N19 E68 27 1 UNNAMED SPRING #5 (D31)	39.48483	-114.31031	Spring	8/26/2005	-116.9
392913115163201	174 N19 E59 25 1 DEER SPRING	39.48683	-115.27558	Spring	6/4/2005	-114.11
392920114294301	184 N19 E66 25 1	39.48889	-114.49528	SW	6/18/1992	-111

Appendix A. Deuterium Data for Recharge Samples

NWIS Site Number	Site Name	Latititude (NAD83)	Longitude (NAD83)	Site Type	Sample Date	Deuterium, δD (‰)
392945115165001	175 N19 E59 24 1 ROBBERS ROOST NO 2 SPRING	39.49597	-115.28047	Spring	6/4/2005	-112.01
393033114593501	178B N19 E62 16 1 UNNAMED SPRING 1	39.50919	-114.99297	Spring	5/24/2005	-118.9
393304115134801	178B N19 E60 04 1 SUMMIT SPRING	39.55108	-115.23000	Spring	6/4/2005	-120.8
393320115130501	178A N20 E60 33C 1 Thirty Mile Spring	39.55549	-115.21892	Spring	8/23/1983	-126
393347114361801	184 N20 E66 30DCC 1 KALAMAZOO CREEK SPRING WR6	39.56383	-114.59251	Spring	7/20/2004	-121.6
					9/21/2004	-118.5
					1/23/2005	-121.6
					5/23/2005	-118.6
					8/12/2005	-119.2
					10/5/2005	-120.6
					11/8/2005	-121
					12/13/2005	-120.1
393417114314101	184 N20 E66 27C 1 KALAMAZOO CREEK	39.57133	-114.52890	SW	6/14/1983	-124
					8/24/1983	-121
393759115471001	154 N20 E55 04 1	39.63306	-115.78611	Spring	7/31/1987	-120
393838114121801	184 N20 E69 34 1 MIKES SPRING (D20)	39.64375	-114.20489	Spring	8/23/2005	-122.5
394045115385701	154 N21 E56 22 1	39.67917	-115.64917	Spring	7/31/1987	-124
394051114112701	184 N21 E69 21 1 UNNAMED SPRING #1 (D21)	39.68078	-114.19089	Spring	8/23/2005	-122.7
394248114135901	185 N21 E68 12 1 GRASS VALLEY SPRINGS (D22)	39.71325	-114.23300	Spring	8/23/2005	-124.3
394320115363601	175 N21 E56 01 1 UNNAMED NR LITTLE WILLOW	39.72236	-115.60986	Spring	6/5/2005	-125.9
394328115342301	175 N21 E57 05 1 WOODCHUCK SPRING	39.72453	-115.57297	Spring	6/5/2005	-119.56
394409115341301	175 N22 E57 33 1 MUD SPRING	39.73586	-115.57036	Spring	6/5/2005	-117.55
394528115162101	175 N22 E59 24 1 CABIN SPRING	39.75789	-115.27244	Spring	6/5/2005	-124.42
394529115143301	178B N60 E22 1 BUTTE SPRING	39.75817	-115.24247	Spring	5/24/2005	-120.4
394623114124101	185 N22 E69 19 1 CEDAR SPRING (D23)	39.77314	-114.21142	Spring	8/23/2005	-120.6
394631114283001	184 N22 E66 23 1 DIPPING TANK SPRING (D28)	39.77525	-114.47511	Spring	8/25/2005	-121.5
395135114282201	184 N23 E66 24 1 ROCK SPRINGS (D29)	39.85983	-114.47278	Spring	8/25/2005	-119.1
395152114552601	179 N23 E62 13B 1 EGAN CREEK	39.86438	-114.92475	SW	8/24/1983	-126
					6/14/1984	-123
395523114592101	178B N24 E62 29 1 JOHNSON SPRING	39.92319	-114.98922	Spring	5/24/2005	-123.4
395617114213901	185 N24 E67 23 1 UNNAMED SPRING #4 (D27)	39.93803	-114.36075	Spring	8/25/2005	-121.9
395916114260001	184 N24 E67 05 1 UNNAMED SPRING #2 (D25)	39.98783	-114.43342	Spring	8/24/2005	-121
395937114251501	185 N25 E67 32 1 UNNAMED SPRING #3 (D26)	39.99367	-114.42072	Spring	8/25/2005	-122.8
400054114480001	179 N25 E63 18D 1 GOSHUTE CREEK	40.01493	-114.80086	SW	6/15/1983	-122
					8/24/1983	-124
400243114580301	178B N25 E62 03D 1 SNOW CREEK	40.04521	-114.96836	SW	6/15/1983	-122
					8/24/1983	-125
400255115293801	176 N25 E57 13AD 1 STATION SPRING AT ORIFICE	40.04846	-115.49490	Spring	5/23/2000	-128
400339115095001	175 N25 E60 12 1 WHITE ROCK SPRING	40.06083	-115.16389	Spring	5/24/2005	-119.2
400405115314901	176 N25 E57 11BBBC1 FORT RUBY RANCH 1	40.06799	-115.53111	GW	5/2/2002	-129
400442114544101	178B N25 E62 01 1 LOWER SNOW CREEK SPRING	40.07836	-114.91139	Spring	5/24/2005	-120.9
					5/24/2005	-120.7
401105115292801	176 N27 E57 36AA 1 NINO SP AT FISH HATCHERY	40.18469	-115.49187	Spring	5/23/2000	-125
401205115301101	176 N27 E57 24DC 1 Cave Creek Spring	40.20179	-115.49608	Spring	5/23/2000	-124
					1/11/2001	-122
					5/1/2002	-125
401412115285601	176 N27 E58 07BD 1 SP 0.89MI N BRESSMAN CABIN	40.23671	-115.48324	Spring	5/25/2000	-122
401515115284901	176 N27 E58 06BADD1	40.25406	-115.48110	GW	5/25/2000	-125
401813115255201	176 N28 E58 15CCBB1 RUBY LAKE ESTATES 1	40.30359	-115.43188	GW	4/30/2002	-129
401822115274001	HARRISON PASS CR AT BEDROCK/ALLUVIAL CONTACT	40.30609	-115.46202	SW	9/19/2000	-122
401913115265701	176 N28 E58 09CBDB1 RUBY VALLEY STORE	40.32023	-115.44909	GW	10/8/2002	-124
402010115265001	176 N28 E58 04CBAC1	40.33604	-115.44810	GW	5/25/2000	-127
402343115125801	176 N29 E60 16BDBD1 BASQUE WELL NO 2	40.39521	-115.21620	GW	4/30/2002	-137
402360115190101	176 N29 E59 15BBBC1	40.39983	-115.31770	GW	5/25/2000	-139
					10/10/2002	-137
402555114591801	178A N30 E62 33CAC 1 USBLM	40.43187	-114.98920	GW	10/9/2002	-128
403334115155101	176 N31 E59 24ABBC1	40.55948	-115.26499	GW	10/9/2002	-127
403958115121101	176 N32 E60 09DBDA1	40.66615	-115.20393	GW	5/1/2002	-122
404335115123801	176 N33 E60 21BDCD1	40.72658	-115.21139	GW	10/10/2002	-127

Notes:
GW = groundwater other than spring (e.g. well)
SW = surface water

Appendix B. Deuterium Data for Regional / Deep-Intermediate Groundwater Samples

NWIS Site Number	Site Name	Latitude (NAD83)	Longitude (NAD83)	Site Type	Sample Date	Deuterium, δD (‰)
375346114133301	198 N01 E69 35CC 1 Spring	37.89607	-114.22665	Spring	4/8/1985	-101
380531114534201	181 N03 E63 27CAA 1 USGS-MX (N. Dry Lake)	38.09190	-114.89584	GW	6/19/2003	-107
380758115204601	172 N03 E59 10BD 1 USGS-MX (Coal Valley Well)	38.13745	-115.33975	GW	1/15/1981	-110
					6/25/2003	-108
380845114533601	181 N03 E63 03DCC 1	38.14579	-114.89418	GW	12/10/1980	-108
381440114323301	202 N05 E66 35DC 1 Dodge Well	38.24440	-114.54333	GW	6/7/1985	-107
381626114540801	180 N05 E63 20CC 1 SILVER KING WELL	38.27394	-114.90211	GW	9/2/2005	-89.3
381943114562201	180 N06 E63 31DCAC1 LEWIS WELL	38.32872	-114.93948	GW	9/2/2005	-98.2
382105115104801	207 N06 E60 25BDAD1 Moon River Springs	38.35162	-115.18169	Spring	4/27/1982	-120
382120114352101	183 N06 E66 29ABC 1 Lake Valley Well	38.35551	-114.59000	GW	6/7/1985	-111
382259115090801	207 N06 E61 18AADA1 NDW - HOT CREEK SPRING	38.38300	-115.15335	Spring	5/20/1992	-119
					9/25/2004	-120.5
					1/24/2005	-119
					5/18/2005	-118.6
					8/14/2005	-117.4
					11/6/2005	-119.1
382318115075801	207 N06 E61 09CCBB1 Hot Creek Campground Well	38.38828	-115.13363	GW	7/19/1981	-118
382513114312001	183 N07 E66 36C 1 USBLM - Mustang Well	38.42023	-114.52305	GW	11/8/2005	-114.6
382517115012001	207 N07 E62 33BCCC1 Flag Spring 3	38.42134	-115.02307	Spring	1/17/1984	-105
382620115340801	173B N07 E57 28ACBD1 Bullwhacker Spring	38.43883	-115.56975	Spring	6/15/1983	-114
382624115004001	207 N07 E62 28ABDC1 Butterfield Spring	38.43967	-115.01168	Spring	7/19/1981	-105
382807114521001	180 N07 E63 14BADD1 USGS-MX (Cave Valley)	38.46856	-114.87029	GW	7/10/2003	-105
383114115123401	207 N08 E60 27D 1 USBLM	38.52050	-115.21030	GW	7/23/1986	-118.5
383116115324601	173B N08 E57 27DACC2 Bitterfield Spring	38.52105	-115.54697	Spring	6/15/1983	-116
383307114471001	180 N08 E64 15BCBC1 USBLM	38.55190	-114.78695	GW	11/8/2005	-104.6
					11/8/2005	-103.9
383325114134901	196 N08 E69 15B 1	38.55718	-114.22471	GW	8/31/2005	-114
383346115313801	173B N08 E57 11DDB 1 Blue Eagle Springs	38.56299	-115.52836	Spring	7/17/1981	-114
383458114473601	180 N08 E64 04ABDD1 USBLM	38.58301	-114.79334	GW	7/23/1986	-102
383533114102901	196 N08 E70 06B 1 USBLM - Monument Well	38.59162	-114.16832	GW	10/5/2005	-113.4
383540115081801	207 N09 E61 32DABC1 Moorman Spring	38.59467	-115.13918	Spring	7/18/1981	-119
383607115023801	207 N12 E62 31D 1	38.85578	-115.04613	GW	7/23/1986	-112
383730115025201	207 N09 E62 19A 1 Emigrant Springs	38.62495	-115.04863	Spring	7/18/1981	-108
383813114380901	183 N09 E65 13CBAA1	38.63686	-114.63575	GW	5/20/1992	-112
					10/19/2005	-111.1
383826114051201	196 N09 E70 14DABD1 20A	38.64042	-114.08678	GW	10/5/2005	-112.7
383915114375901	183 N09 E65 12CA 1 South Big Spring	38.65412	-114.63389	Spring	4/4/1985	-111
383922114375901	183 N09 E65 12BD 1 North Big Spring	38.65606	-114.63389	Spring	4/4/1985	-112
384152114075001	195 N10 E70 33ACBB1 Big Spring	38.69773	-114.13138	Spring	6/19/1992	-111
					1/22/2005	-112.2
					5/20/2005	-109.8
					7/13/2005	-112.2
					8/13/2005	-112.2
					11/8/2005	-110.3
384226114050601	195 N10 E70 25CBC 1 BARCASS 3A	38.70723	-114.08596	GW	7/14/2005	-111.1
384245115101601	207 N10 E61 19	38.71250	-115.17111	GW	7/23/1986	-120
384309115045901	207 N11 E61 23AA 1	38.71911	-115.08390	GW	7/23/1986	-111
384331114043401	195 N10 E70 24BC 1 BARCASS 2A	38.72526	-114.07699	GW	7/14/2005	-120.8
384454115101701	207 N10 E61 07	38.74833	-115.17139	GW	7/23/1986	-119
384521114043801	195 N10 E70 12	38.75583	-114.07722	GW	9/1/2005	-109.8
384534114495301	180 N10 E64 06BDA 1 ROBBERS ROOST WELL	38.75928	-114.83237	GW	7/18/2005	-107.5
384620114313601	184 N11 E66 35DBAC1 (S. Fox flowing well)	38.77217	-114.52750	GW	7/6/1983	-113
					8/30/2005	-111.8
384640114280101	184 N11 E67 32AADA1 SPET1W	38.77767	-114.46706	GW	9/3/2005	-113
384702114034101	195 N11 E70 36BD 1 USGS-MX	38.78384	-114.06221	GW	9/1/2005	-108.7
384803115133001	207 N13 E60 33A 1 William Hot Spring	38.94772	-115.22891	Spring	4/29/1982	-118
385158115000401	207 N11 E62 04AABA1 Lund Spring	38.84994	-115.00335	Spring	4/27/1982	-113
385516114502101	179 N12 E63 12BDAB1	38.91994	-114.84612	GW	1/19/1981	-117
385521114503601	179 N12 E63 12AB 1 USGS - S Steptoe MX Well	38.92244	-114.84418	GW	7/16/2003	-115
385530115044601	207 N12 E61 12DBDD1 Nicholas Spring	38.91244	-115.06113	Spring	4/27/1982	-124

Appendix B. Deuterium Data for Regional / Deep-Intermediate Groundwater Samples

NWIS Site Number	Site Name	Latitude (NAD83)	Longitude (NAD83)	Site Type	Sample Date	Deuterium, δD (‰)
385538115045701	207 N12 E61 02AC 1 Cold Springs - Preston	38.92716	-115.08335	Spring	7/16/1981	-121
					6/16/1983	-126
385540115045701	207 N12 E61 02ACAB1 Preston Big Spring	38.93355	-115.08141	Spring	9/25/2004	-122.6
					1/24/2005	-122.4
					5/21/2005	-120
					8/14/2005	-121.2
					11/6/2005	-120.4
385546114250501	184 N12 E67 02 1 CEDAR SPRINGS	38.92939	-114.41817	Spring	7/12/2005	-107.4
385613114250401	184 N12 E67 02ACBA1 USBLM (Shoshone pond well)	38.93634	-114.41889	GW	7/6/1983	-109
					5/27/1992	-108
					1/22/2005	-110.3
					5/20/2005	-108.1
					7/12/2005	-108.6
					8/12/2005	-108.6
					11/8/2005	-108.2
390352114305401	184 N14 E66 24BDDD1 USGS-MX (Spring Valley N.)	39.06439	-114.51584	GW	12/12/2005	-83
390457116323401	140A N14 E47 02A 1 Spring	39.08243	-116.54369	Spring	1/1/1974	-128
390541114471301	179 N20 E64 17DD 1	39.09466	-114.78779	GW	6/14/1984	-121
390753116051701	155A N15 E52 35C 1	39.13132	-116.08895	GW	7/31/1987	-119
390754114303001	184 N15 E66 25DCAD1 LAP&W Spring Vly Well 1	39.13161	-114.50917	GW	9/16/1982	-125
390807114282501	184 N15 E67 29	39.13528	-114.47361	GW	6/18/1992	-121
391410116032101	155A N16 E53 30B 1	39.23076	-116.05672	GW	7/31/1987	-123
391637116021801	155A N16 E53 08BCBB1 Fish Creek Springs	39.27687	-116.03922	Spring	7/17/1981	-121
391755115555401	155A N17 E54 31	39.29861	-115.93167	GW	7/31/1987	-118
392411113514301	(C-16-18)22cab-S1	39.40300	-113.86277	Spring	8/26/1981	-109
392527113290901	(C-16-15)13bab-S1	39.42411	-113.48665	Spring	8/25/1981	-111
392731114382801	179 N18 E65 03DA 1 McGill Spring	39.45855	-114.64196	Spring	7/15/1981	-122
392737114021201	(C-15-19)31cbd-S1	39.46014	-114.03763	Spring	5/28/2003	-120
					9/24/2004	-119.6
					1/22/2005	-120
					5/23/2005	-119.4
					7/17/2005	-119.7
					8/12/2005	-119.8
					11/8/2005	-122.8
392815113593001	(C-15-19)31bc -S1	39.47078	-113.99249	Spring	8/26/1981	-121
393212114545001	179 N19 E63 05 1 Spring	39.53660	-114.91475	Spring	7/15/1981	-123
393442114231801	184 N20 E67 26ABBD1 USBLM	39.57633	-114.40029	GW	11/9/2005	-124.3
393946114482301	179 N21 E63 24 1 Spring	39.66271	-114.80724	Spring	1/1/1974	-128
394001114482600	179 N21 E63 24 2 Spring	39.66688	-114.80808	Spring	5/28/1992	-125
394031114465601	179 N21 E64 19BDAD1	39.67521	-114.78308	GW	6/14/1984	-125
394149114302201	184 N21 E66 15DBDD1 WILLOW SPRING	39.69682	-114.50607	Spring	10/20/2005	-122.7
394427115304301	175 N22 E57 25CCCC1 Well at Alligator Ridge	39.74076	-115.51282	GW	4/24/1984	-127
394436115270401	175 N22 E58 28CCCA1 Ram. Res. Wtr Supply Well	39.74326	-115.45198	GW	7/19/1985	-130
394859115363701	154 N23 E56 36DD 1	39.81632	-115.61116	GW	7/31/1987	-122
394949114331802	184 N23 E66 31AB 2	39.83021	-114.55585	GW	7/27/1983	-126
395027113234001	(C-11-14)23dcd-S1	39.84072	-113.39520	Spring	5/29/2003	-111
395029113233601	(C-11-14)23ddc-S1	39.84133	-113.39415	Spring	8/27/1981	-111
395116114451301	179 N23 E64 20AA 1 LAP&W Steptoe Well 1	39.85438	-114.75447	GW	9/16/1982	-124
395226114215401	185 N23 E67 14BA 1 TIPPET SPRING (D24)	39.87383	-114.36585	Spring	8/24/2005	-123.3
395342114532701	179 N23 E63 06 1 Hot Sp, Cherry Creek	39.89493	-114.89169	Spring	1/1/1974	-128
395846113591101	(C-10-19)04ddc-1	39.97944	-113.98639	GW	10/4/2005	-121.6
395935113584601	(C- 9-19)34CCD- 1	39.99299	-113.98000	GW	10/4/2005	-121.7
400119115274801	176 N25 E58 29ABDC2 RV-1 SHALLOW	40.02194	-115.46333	GW	8/20/2002	-121
400119115274802	176 N25 E58 29ABDC3 RV-1 DEEP	40.02194	-115.46333	GW	8/20/2002	-127
					9/10/2003	-127
400131115254501	176 N25 E58 27BAAA1 RV-2	40.02528	-115.42917	GW	8/20/2002	-127
					8/21/2002	-123
400458114371401	179 N26 E65 34DABA2	40.08271	-114.62141	GW	7/27/1983	-129
400954114442401	179 N27 E64 34DCC 1	40.16493	-114.74086	GW	4/21/1983	-133
					6/14/1983	-132

Notes:

GW = groundwater other than spring (e.g. well)

Appendix C.

Comparison of Optimization Methods for a Discrete-State Compartment (DSC) Groundwater Accounting Model: Uniform Random Search (URS), Shuffled-Complex Evolution (SCE), and Multi-Objective Complex Evolution (MOCOM) Algorithms

Kevin Lundmark

Graduate Program of Hydrologic Sciences

University of Nevada, Reno

ABSTRACT

A discrete-state compartment (DSC) groundwater accounting model for a five-basin area in eastern Nevada was developed for demonstration of the uniform random search (URS) method and shuffled complex evolution (SCE) and multi-objective complex evolution (MOCOM) optimization algorithms. The DSC model is simple, mass balance mixing model which represents hydrographic areas as a series of interconnected cells. Model optimization is achieved by varying the fractional groundwater flows between cells and out of the model domain. A multiple objective optimization problem was posed by evaluating model performance in terms of predicted concentrations and predicted outflows from the model domain. The inclusion of target, minimum outflow rates complicated model optimization, and results suggest that target outflow rates may be better handled by modifications to the accounting model rather than during optimization. The inability of the model to match predicted concentrations to observed concentrations suggest that either concentration data are not representative or a different model is needed.

1. INTRODUCTION AND SCOPE

This paper presents the results from the optimization of a discrete-state compartment (DSC) groundwater accounting model using a variety of common parameter estimation and uncertainty analysis techniques. The model used for this exercise is a relatively simple mass-balance groundwater accounting model which represents hydrographic basins as a series of connected cells. While simple in its approach, this accounting model provides a useful framework for evaluating combinations of groundwater flow systems and uncertainties associated with predicted groundwater flows.

The groundwater accounting model is described in the section that follows. Because the model includes mass fluxes of an environmental tracer (deuterium) as well as flow rates (volume per unit time), optimization of the model may include aspects dealing with either tracer concentrations or flow rates, and these two variables (concentration and flowrate) may be used to pose an optimization problem involving multiple objective criteria. Multiple-objective optimization problems are characterized by a trade off between objective criteria, and as such, these problems have sets of solutions rather than a single parameter set. The set of solutions which defines the minimum uncertainty in the parameters that can be achieved without assigning subjective relative preference to the objective criteria is referred to as a Pareto set (Yapo *et al.* 1998).

The scope of this paper is to describe how multiple optimization approaches may be applied to hydrologic model. Optimization approaches applied to the model include the uniform random search (URS) method and the shuffled-complex evolution (SCE) and multi-objective complex evolution (MOCOM) optimization algorithms. The results of the optimization approaches will be presented and discussed with a focus on the tradeoffs between multiple objective criteria based on concentration and outflow predictions from the model.

2. GROUNDWATER ACCOUNTING MODEL

2.1 Water budgets

Water budgets (or water balances) are an application of simple mass conservation equations which may be used to establish the basic hydrologic characteristics of a geographical region (Dingman 2002). The fundamental equation for a water budget is the sum of inputs rates (Q, volume per time) minus the sum of output rates equals the change in storage of the system. If the system is assumed to be at steady-state, then the change in storage is zero and the water budget becomes:

$$\sum Q_{Inputs} = \sum Q_{Outputs}$$

For a groundwater system, inputs may include direct recharge from precipitation, indirect recharge of precipitation from surface water runoff, groundwater inflow from outside the system boundary, or recharge from anthropogenic sources. Groundwater outputs may include discharge as springs, discharge to surface water bodies, evapotranspiration (ET), groundwater outflow to outside the system boundary, and

pumping for domestic, agricultural, industrial, and mining uses. Within the Great Basin province in eastern Nevada, the primary contributors of recharge are precipitation and groundwater inflow and that discharge is principally by ET and groundwater outflow, a simplified water budget may be expressed as:

$$Recharge_{precip} + GW_{inflow} = Discharge_{GWET} + GW_{outflow}$$

where recharge from anthropogenic sources and pumping for domestic, agricultural, industrial, and mining uses are assumed to be negligible. This simplified water budget also assumes that groundwater discharged from springs recycles back into the shallow water table where subsequent evaporation or transpiration occurs.

2.2 Groundwater accounting

A groundwater accounting model is a tool which can help verify tabulated water budgets and evaluate interbasin groundwater flows. For a basic mass-balance type groundwater accounting model, simplified mass-balance mixing equations are used to account for inputs and outputs to the system, rather than the standard groundwater flow equation used in typical numerical simulations. The mass-balance model has the same fundamental equation as the water budget; the difference for the mass balance model is that the mass of a substance (or tracer) moving in and out of the system per unit time is used instead of volumes of water.

Considering that the mass flux of a tracer in water may be calculated as its concentration (mass per volume) times the volume of water and assuming this system is at steady state, the mass balance approach may be viewed as a water budget modified to include concentrations, and the general equation may be expressed as:

$$\sum_{i=1}^{N_{in}} (Q_{in\,i} \times C_{in\,i}) = \sum_{j=1}^{N_{out}} (Q_{out\,j} \times C_{out\,j})$$

where Q_{in} and C_{in} represent the flowrate (volume/time) and concentration (mass/volume) for each of N_{in} inputs and Q_{out} and C_{out} represent the flowrate and concentration for each of N_{out} outputs.

The benefit of this approach is that if tracer concentrations vary for different model inputs and between different areas within a system, then modeling the movement of the tracer within the system can provide information on magnitudes and directions of water flow. In this way, groundwater chemistry data are used to help verify the water budget and may provide information on the mixing patterns and source areas for groundwater in the carbonate aquifer system.

2.3 Discrete-State Compartment Model

A groundwater accounting model which has been recently applied to hydrographic basins in eastern Nevada is a modified Discrete-State Compartment (DSC) model. The DSC model is a mixing cell model that represents groundwater systems as a network of interconnected cells. Both water and tracer movements are governed by a set of conservation of mass equations which incorporate water budget (groundwater recharge) and environmental tracer values into iterative water and mass balance

calculations for the modeled system. The DSC model is advantageous for use in the Great Basin because it may be applied to systems lacking sufficient information on hydraulic gradients and aquifer parameters necessary to define complex groundwater models (Carroll and Pohll, 2007).

The DSC model was developed by Campana (1975) as a tool to model the mass of any groundwater tracer (ie. groundwater constituents or environmental isotopes) via mixing cell mass-balance equations. Whereas the original DSC model allowed for transient simulations and the use of non-conservative tracers, the DSC model which is applied for this study has been modified to simulate only steady-state conditions of a conservative tracer (Carroll and Pohll, 2007). Consequently, assumptions for cell volumes and source/sink rates are not necessary. Model inputs include the number of cells, rates and concentrations for recharge, and connections between cells. A schematic illustration of a DSC model is shown as Figure 1.

The steady-state assumption requires that volume and mass discharging from a cell is equal to all inputs of volume and mass. The algorithm of an instantaneously mixed cell may be expressed as:

$$C_i = \frac{\overbrace{\sum_{j=1}^{N}\left(Q_{i,j}^{r} C_{i,j}^{r}\right)}^{\text{Mass from recharge}} + \overbrace{\sum_{k=1}^{D}\left(f_{k,i} Q_k^d C_k^d\right)}^{\text{Mass from GW inflow}}}{\underbrace{\sum_{j=1}^{N}\left(Q_{i,j}^{r}\right)}_{\text{Recharge rate}} + \underbrace{\sum_{k=1}^{D}\left(f_{k,i} Q_k^d\right)}_{\text{GW inflow rate}}}$$

where C is a cell's steady-state modeled concentration. Discharge can occur to another cell (as interbasin groundwater flow within the model domain) or out of the model domain (as ET or interbasin groundwater flow out of the model domain. Therefore,

$$\sum_{h=1}^{P} f_{i,h} + f_{i,out} = 1.0$$

where P is the number of outflows to adjacent cells from cell i, $f_{i,h}$ is the fraction of flow and mass discharged from cell i and received by cell h, and $f_{i,out}$ is the fraction of flow and mass discharged from cell i out of the model domain.

During model optimization, flow fractions ($f_{i,h}$ and $f_{i,out}$) and cell ranks are adjusted until the predicted cell concentrations and/or outflows best match observed cell concentrations and/or outflows. The parameters $f_{i,h}$ and $f_{i,out}$ effectively control the volume and mass moving between each cell and out of the model domain. Optimization of the DSC model is achieved by minimizing the error between observed and predicted values for each cell in the model. The process of DSC model optimization has traditionally been performed by manually adjusting cell-to-cell and boundary fluxes until modeled tracer concentrations in each cell most closely match observed values. An example of an objective function for concentration is the weighted root mean squared error for concentration, wRMSE C:

$$wRMSE_C = \left(\frac{\sum_{i=1}^{N} wc_i^{\,2} (Cp_i - Co_i)^2}{N} \right)^{0.5}$$

where Co_i and Cp_i are the observed and predicted concentrations in cell *i*, respectively, *N* is the number of cells being modeled and wc_i is the weight assigned to cell *i* for the observed concentration.

DSC models have also traditionally not included assumptions relating to discharge of groundwater by ET. In order to incorporate available ET estimates and deter unrealistically low discharge rates, a second objective function was identified based on outflow criteria. Under this scenario, an iteration was penalized if a cell's outflow rate was less than the estimated groundwater ET rate. In this context, groundwater ET rates represent hypothetical minima for outflow rates from cells in the model. An objective function for targeting these minimum outflow rates is the weighted root mean square error for outflow, wRMSE Out:

$$wRMSE_{OUT} = \left(\frac{\sum_{i=1}^{nl} \begin{Bmatrix} w_{Q_i}^{\,2} (Q_{ET_i} - Q_{out_i})^2 ; \text{if } Q_{out} < Q_{ET} \\ 0 \qquad\qquad\qquad ; \text{if } Q_{out} \geq Q_{ET} \end{Bmatrix}}{N} \right)^{0.5}$$

where Q_{ETi} and Q_{outi} are the target (minimum) and predicted outflows for cell *i*, respectively, *N* is the number of cells being modeled and w_{Qi} is the weight assigned to cell *i* for the target outflow rate.

3. DISCRETE-STATE COMPARTMENT MODEL OPTIMIZATION

3.1 DSC model application

The study area used for this exercise includes five hydrographic basins in eastern Nevada. These basins are a subset of a larger study area which is the subject of an ongoing groundwater study in White Pine County, Nevada, and adjacent areas in Nevada and Utah. Two hydrographic areas have been subdivided into three sub-basins each. These six sub-basins along with the two undivided hydrographic basins comprise the nine-basin study area for this exercise (Figure 2). Cell connectivity and DSC model inputs for recharge and observed deuterium values for these basins were taken from another report (Lundmark *et al.*, in press). The nine-cell network includes ten cell connections, corresponding to interbasin groundwater flowpaths. These connections plus outflows from five cells yield a DSC model with fifteen optimization parameters. Note that four cells only have one output (outflow from the model domain with no interbasin flow) therefore outflow from these cells are constant (f = 1.0) and are not optimization parameters.

The optimization of the DSC model was accomplished by developing MATLAB controllers which modified input parameters, called the FORTRAN-based DSC model,

managed model output, and linked with optimization algorithms. Output from optimization of the DSC example model include interbasin flows (between cells) and outflow from the model domain for each cell, as well as predicted concentrations (deuterium values) for each cell. Optimization results were evaluated to identify the model output associated with Pareto-optimal solutions from each optimization method.

3.2 Uniform random search (URS) optimization

The uniform random search (URS) optimization approach is a technique which relies on brute computational force to evaluate the results from many combinations of parameters. The URS approach involves 1) generation of large sets of parameters using a uniform sampling of the parameter space, 2) model runs with each set of parameter samples and calculation of associated objective measures, and 3) analysis of results in terms of parameter and objective values (Duan et al, 1992). The interpretation of results from the URS analysis may include evaluation of parameter and objective values, or the incorporation of likelihoods or weighting functions in a Bayesian framework.

The URS optimization performed for the DSC included the generation of 5,000 sets of the fifteen optimization parameters using a uniform random number generator. Uniform random distributions were generated between zero and one for each parameter. In order to satisfy the requirement that all outflow fractions for each cell sum to one, random numbers generated for each cell were summed and the fraction used in the DSC model was the random number divided by the sum.

The results from the URS optimization are presented on the plots included as an appendix. These plots show the objective measures wRMSE C and wRMSE Out versus fractional flow parameters for each cell. The plots illustrate that the constraint that all fractions sum to one results in a bias toward lower values for each the parameter sets, with the effect being most pronounced for cell number four.

The objective space plot of the results of the URS optimization of the DSC model (Figure 3) shows the distribution of results' values for wRMSE C and wRMSE Out. Of the 5,000 parameter sets evaluated, 564 sets resulted in a zero value for wRMSE Out. Of these results, only the point corresponding to the lowest wRMSE C value is considered a Pareto solution (circled). Three other Pareto solutions were identified by the URS approach. The Pareto curve illustrates the tradeoff between the best fit based on concentration (the Pareto solution point furthest to the right) and the fulfillment of the target discharge requirements (Pareto solution point to the left on the y-axis).

Results from the URS method can also be interpreted using a Bayesian Monte Carlo approach, where the results from a URS analysis are assigned a weight based on a likelihood function. In this manner, results from parameter sets with lower errors are given a greater weight that results from parameter sets which gave poor fits. The Monte Carlo analysis performed on the DSC model included a simple likelihood function, the inverse of wRMSE C. Bayesian weights for each of the 5,000 realizations were calculated as the likelihood function of the individual realization divided by the sum of the likelihood functions for all realizations. Model results (e.g. individual interbasin flows and outflows by cell from the model domain) were sorted while maintaining the associated Bayesian weights and the cumulative weights were calculated for each

realization. Finally, the 99 % confidence interval for model predictions were calculated as the predicted values associated with cumulative weights of 0.005 and 0.995. The occurrence of 0 values for wRMSE Out prevented the application of the Bayesian Monte Carlo analysis to the URS results using wRMSE Out objective function values.

Figure 4 presents a comparison of interbasin flow and outflow results from the URS analysis. Results include 99% confidence intervals calculated using wRMSE C, the results associated with the parameter set with the lowest wRMSE C, the range of results associated with parameter sets which resulted in wRMSe Out = 0, and the range of values associated with the Pareto set of solutions identified for the URS optimization approach. The results on Figure 4 show that the Bayesian 99% confidence intervals generally have the widest range of values. Relatively wide ranges of values are also associated with results with wMRSE Out values equal to zero. The result associated with the lowest wRMSE C value for interbasin flow between cells four and one is not within the associated 99% confidence intervals, indicating that there are generally similar values for wRMSE C for most realizations. The magnitudes for several Pareto set flows also extend outside the 99% confidence interval ranges (interbasin flows from cells one to three and four to one and outflow from cell three), indicating that relative to the set of ranked, weighted results of the Bayesian analysis, the Pareto set results for these parameters represent relatively extreme outcomes.

3.3 Shuffled complex evolution (SCE) optimization

The shuffled complex evolution (SCE) optimization algorithm is a robust method for identifying global minima to optimization problems. The method includes components of the simplex procedure, controlled random search, competitive evolution, and complex shuffling. The SCE method is described in detail by Duan *et al.* (1992). A summary of the SCE method is as follows: 1) a set of sample points are generated in the feasible parameter space, 2) objective function values are evaluated for each point and each point is ranked by their objective value, 3) the points are divided into complexes and each complex evolves within objective space, 4) evolved complexes exchange (shuffle) and the process is repeated until the samples converge to a specified tolerance or until a maximum number of iterations has been performed.

The SCE method is a single objective optimization method, so for models which include multiple objective criteria, such as the DSC model example, the objective functions are typically combined using weighting factors. The SCE optimization which was performed for the DSC model included the variation of weights for the wRMSE C (X_C) and wRMSE Out (X_O) where $X_C + X_O = 1$. The weight X_O was varied from 0 to 1 by 0.1 increments, resulting in a set of eleven separate SCE runs and eleven optimal parameter sets (Figure 4). The plot of SCE solutions in parameter space shows that whenever the weight for wRMSE Out was >0, the SCE algorithm found a solution satisfying conditions to generate a wRMSE Out = 0, plotted on the y-axis of Figure 5. Of the ten solutions with wRMSE Out =0, only the solution with the lowest value of wRMSE C is considered to be a Pareto solution; this point corresponds to a wRMSE Out weight of $X_O = 0.5$. The other Pareto solution resulted from no contribution of wRMSE

Out to the objective function ($X_O = 0$) and represents the global minimum based on concentration.

3.4 Multi-objective complex evolution (MOCOM) optimization

The multi-objective complex evolution (MOCOM) optimization method is a general optimization algorithm which was designed for use with models with multiple possible objective criteria. The MOCOM algorithm is described by Yapo et al. (1998) as an extension of the SCE optimization algorithm which combines the strengths of controlled random search, competitive evolution, Pareto ranking, and a multi-objective downhill simplex search. The MOCOM method includes similar aspects as SCE, most notably complex evolution in objective space; however, the MOCOM algorithm does not include exchange (shuffling) between different complexes. The output from optimization by MOCOM is the generation of a Pareto curve of a user-specified number of points.

Application of the MOCOM approach to the example DSC model was complicated by the wRMSE Out objective function. In general, the MOCOM approach resulted in a Pareto curve or a single solution depending on the initial sample population and whether the samples converged to the line decried by wRMSE Out = 0. An example of output from MOCOM when a Pareto curve was found is shown in Figure 6. The Pareto curve includes one sample (at far left) with a wRMSE Out = 0 and the rest of samples with wRMSE Out > 0 and with wRMSE C values which are less than the wRMSE C value associated with the sample at wRMSE Out = 0. The series of plots shown in Figure 7 illustrate an example of a MOCOM optimization in which the sample points converge to a single value. The convergence progresses from an early state where multiple points identify the wRMSE Out = 0 minimum, followed by the convergence of all sample points to the wRMSE Out = 0 line, and concluding when all samples converge to a single point.

Twenty samples were used for the MOCOM simulations described above and shown in Figures 5 and 6. MOCOM simulations were run with greater than twenty points, however these trials were observed to result in convergence of all points to the wRMSE Out = 0 line followed by a period of very slow convergence of samples toward a reduced number of points.

4. SUMMARY AND DISCUSSION

A comparison of results from the Pareto solution sets from each optimization approach is shown for flows in Figure 8. The flows which result from the Pareto set of the URS optimization generally displays the widest range. Ranges associated with the SCE Pareto set were also relatively large. The difference between the 20-point MOCOM Pareto set and the single-point MOCOM solution is quite large for some flows, indicating that the results for optimization of the DSC model by this method are strongly dependent on the initial population of sample points and whether these points converge to the objective-space line associated with wRMSE Out = 0. Results from the SCE optimization approach appear most useful because of their clear demonstration of the effects of subjective weights of objective functions on model predictions.

Outflow results from the Pareto solution sets from each optimization method were close to greater than the target (minimum) groundwater ET outflows; however, with the exception of the single-point MOCOM solutions, each optimization approach resulted in a Pareto solution for at least one cell where the outflow was less than the target (minimum) groundwater ET rate. This illustrates the effect of the concentration objective function (wRMSE C) on the solution set.

The ranges of observed concentrations for each cell associated with the Pareto solutions for each optimization approach are shown in Figure 9. Cells four, six, and eight are upgradient (i.e. not downgradient of any other cells); this is apparent in their constant observed concentrations. For these cells, the observed concentrations are always equal to the concentration of recharge. The remaining, downgradient-type cells displayed a relatively low degree of variability in the ranges of observed concentrations associated with the Pareto sets, and with the exception of cell three, no downgradient cell achieved a predicted concentration equal to the observed concentration. The inability for either upgradient or downgradient cells to match the observed concentrations indicates that either 1) a different or more elaborate model is needed to achieve a better match, 2) the recharge and/or observed concentrations are not representative of actual conditions, or 3) some combination of 1) and 2).

The results from the optimization of the DSC model using URS, SCE, and MOCOM optimization approaches indicate that model optimization was complicated by the outflow objective function, wRMSE Out, which could have a value of zero for many combinations of parameters. The application of the current DSC to groundwater accounting problems which include target (minimum) groundwater ET discharge rates is limited in that the current model does not allow for the input of these target rates as boundary conditions. Optimization of this type of groundwater accounting problem may be better handled by either a more complicated model or a revised DSC model which includes fixed discharge rates.

Acknowledgement

This work was originally prepared for the course GEOL701s - Parameter Estimation and Uncertainty Analysis. The approach and discussion were heavily influenced by the course material and through interaction with the course's instructor, Dr. Doug Boyle.

5. REFERENCES

Campana, M. E. Finite-state models of transport phenomena in hydrologic systems, Ph.D. Dissertation, University of Arizona, Tuscon, 1975.

Carroll, R.W.H. and G. M. Pohll. draft. A user's manual for the Discrete-state Compartment Model - Shuffled Complex Evolution (DSCM-SCE). Division of Hydrologic Sciences Publication. Desert Research Institute

Dingman, S.L. 2002. Physical Hydrology. Prentice-Hall, Inc. Upper Saddle River, New Jersey. 2nd ed.

Duan, Q., Gupta, V.K., Sorooshian, S., 1992. Effective and efficient global optimization for conceptual rainfall-runoff models. Water Resources Research 28(4): 1015-1031.

Lundmark, K.W., G.M. Pohll and R.W.H. Carroll. draft. Steady State Water Budget Accounting Model for Water Resources of the Basin and Range Carbonate Aquifer System in White Pine County, Nevada, and Adjacent Areas in Nevada and Utah. Division of Hydrologic Sciences Publication No. 412XX. Desert Research Institute.

Yapo, P.O., Gupta, H.V., Sorooshian, S. 1998. Multi-objective global optimization for hydrologic models. Journal of Hydrology 204 (1998) 83-97

Figure 1. DSC Model Components

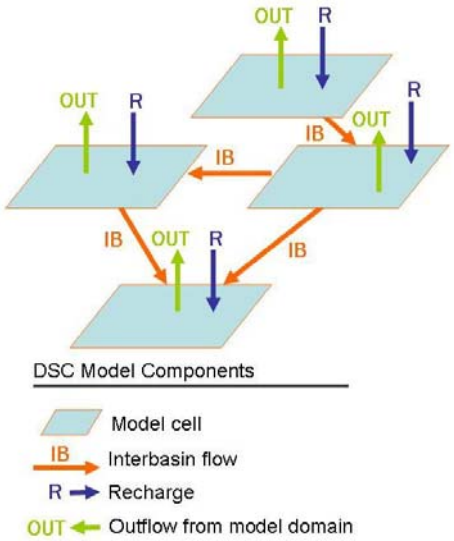

Figure 2. DSC Model Application

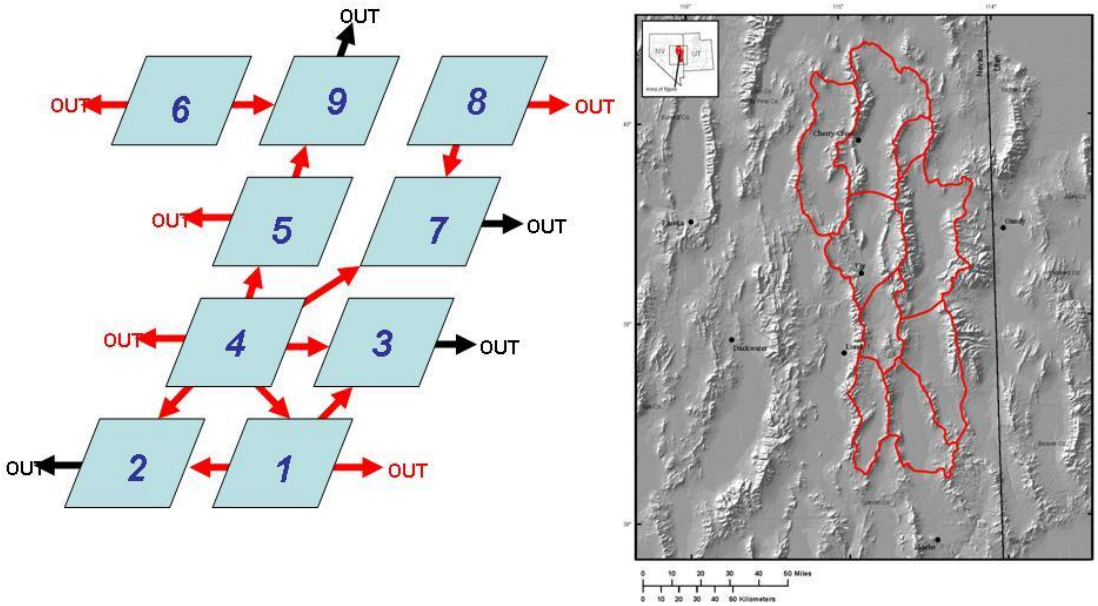

Figure 3. Results from URS optimization, shown in objective space with Pareto solutions circled

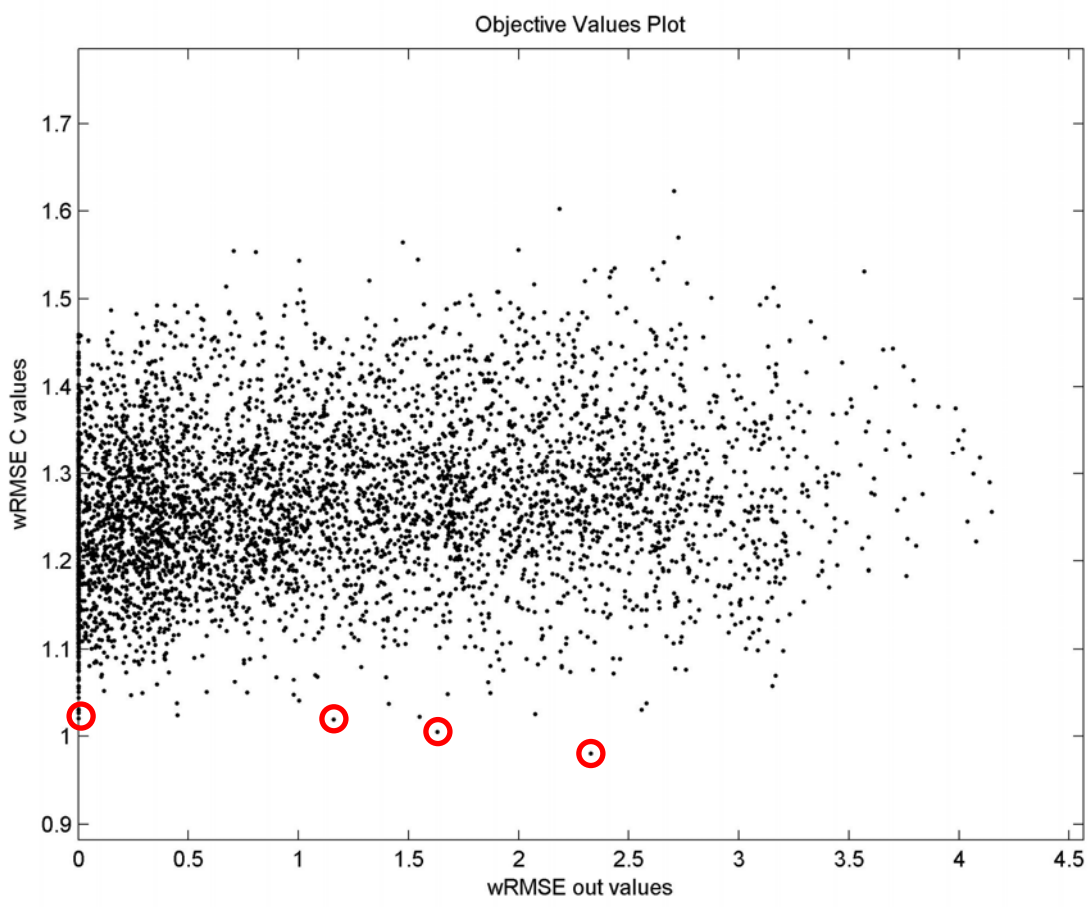

Figure 4. Comparison of results from URS optimization, including 99% Bayesian confidence intervals using wRMSE C, best objective criteria results for wRMSE C and wRMSE Out, and Pareto solutions

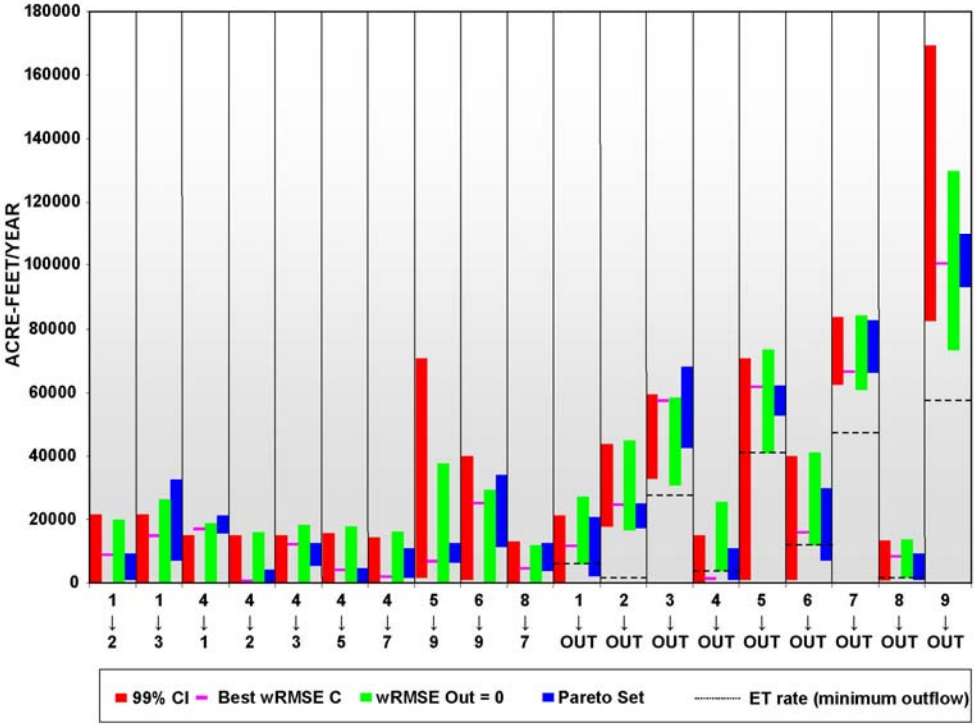

Figure 5. Results from SCE optimization, shown in objective space with Pareto solutions circled

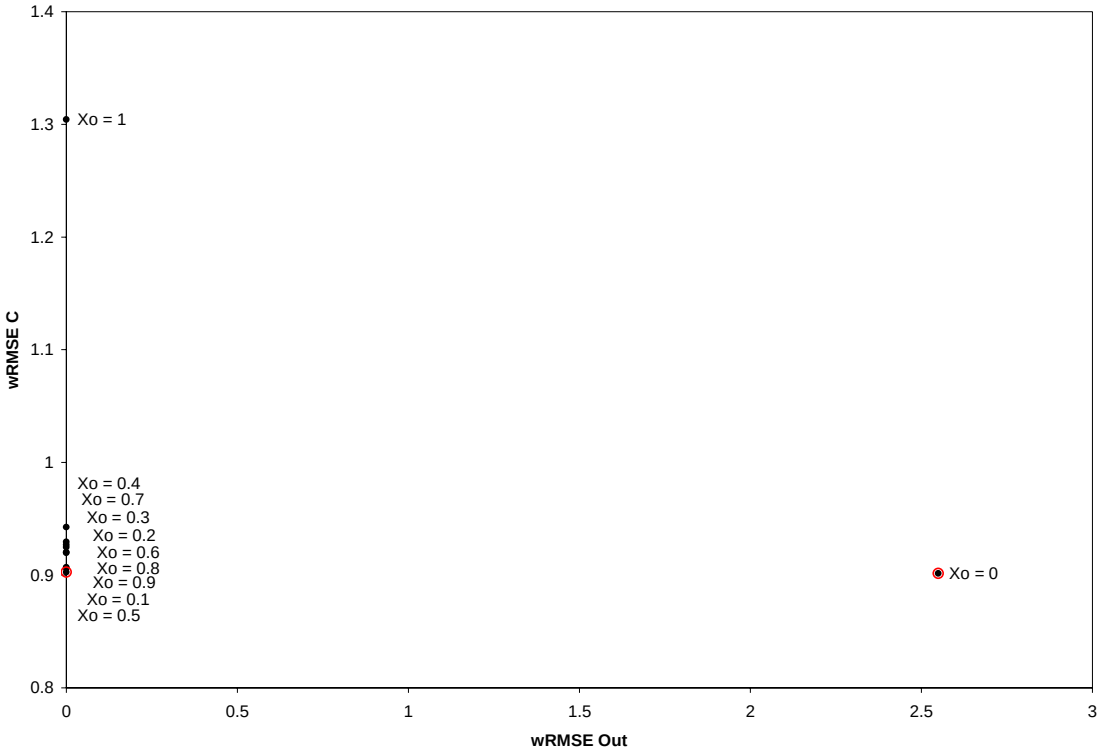

Figure 6. Results from MOCOM optimization showing Pareto curve formed when samples did not converge

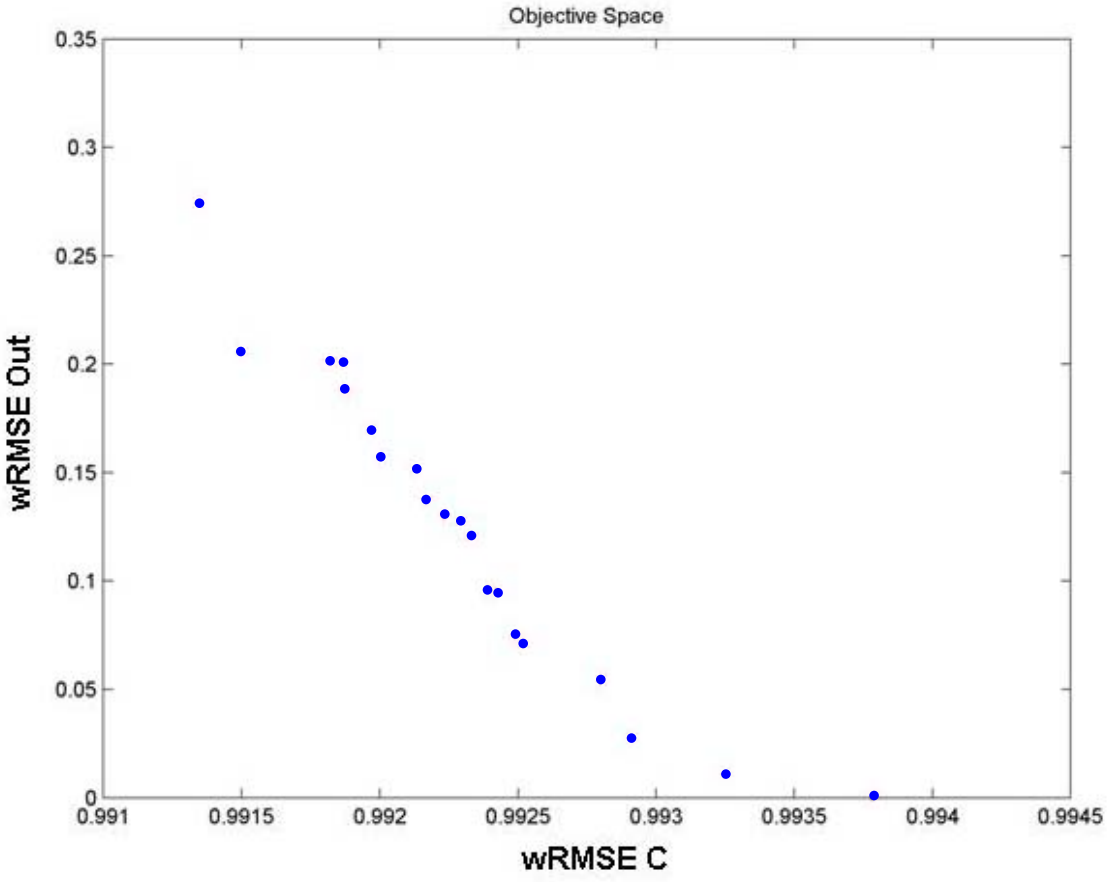

Figure 7. Results from MOCOM optimization, showing progression of sample convergence to single point

1) Sample points identify objective minimum (wRMSE Out = 0)

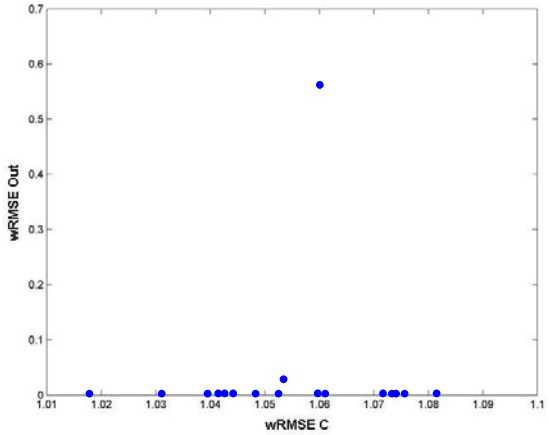

2) All sample points identify objective minimum; begin converging

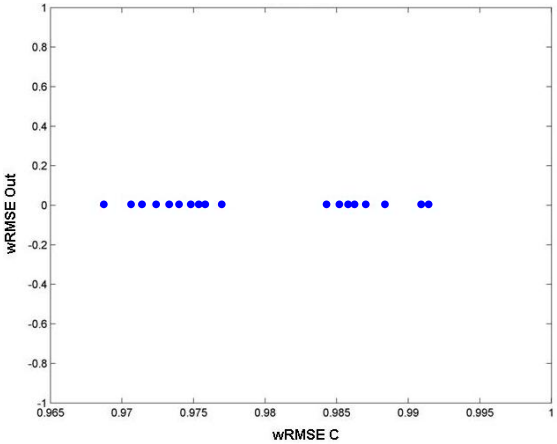

3) Sample points converge to single value

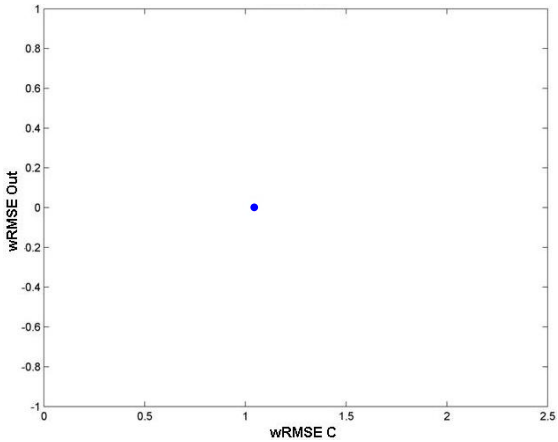

Figure 8. Results from all optimization approaches, shown as ranges of flows predicted by DSC model for Pareto optimal solutions

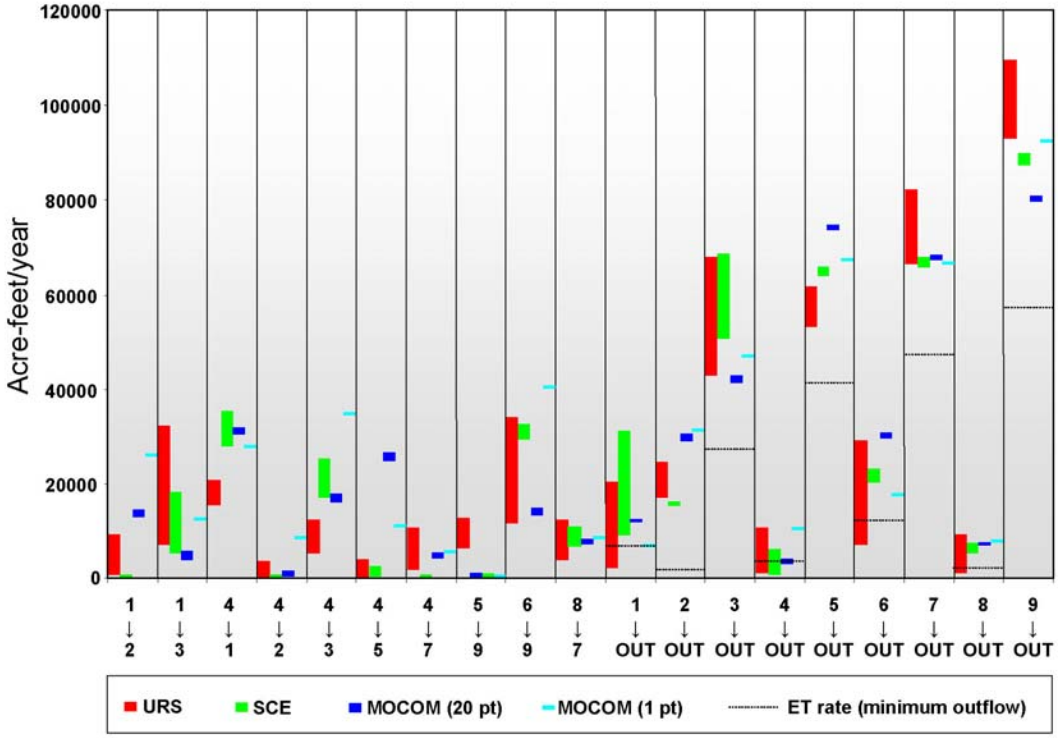

Figure 9. Results from all optimization approaches, shown as ranges of deuterium values predicted by DSC model for Pareto optimal solutions

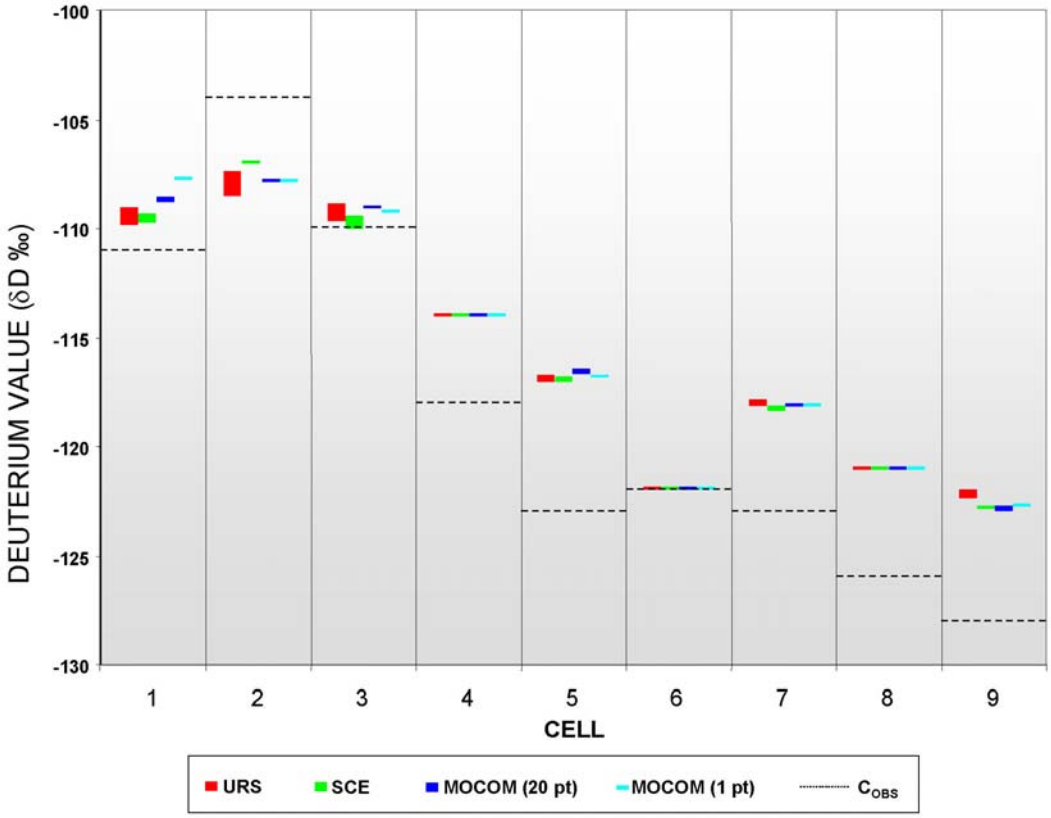

Attachment

Plots showing parameter and objective values for URS optimization

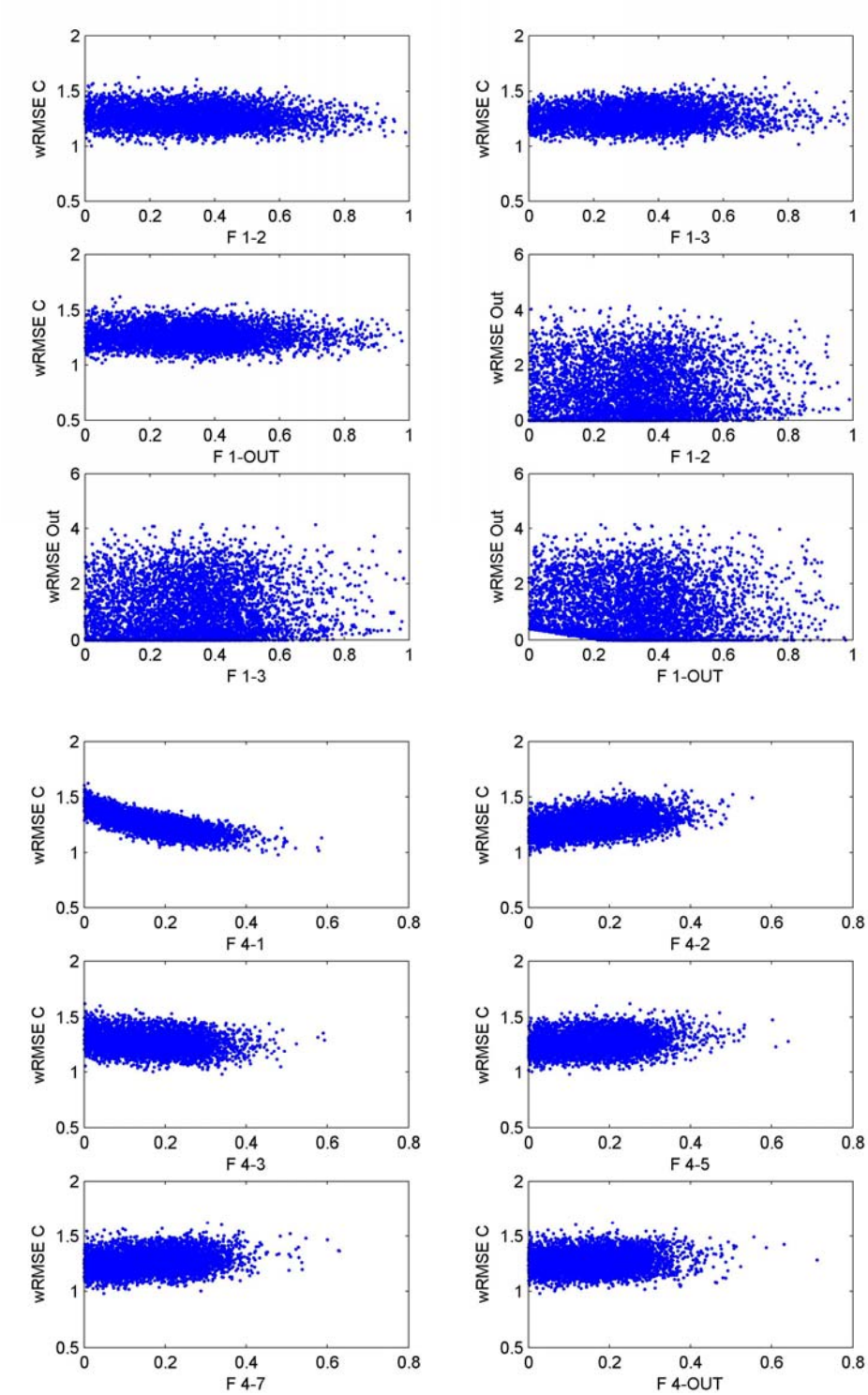

Attachment

Plots showing parameter and objective values for URS optimization

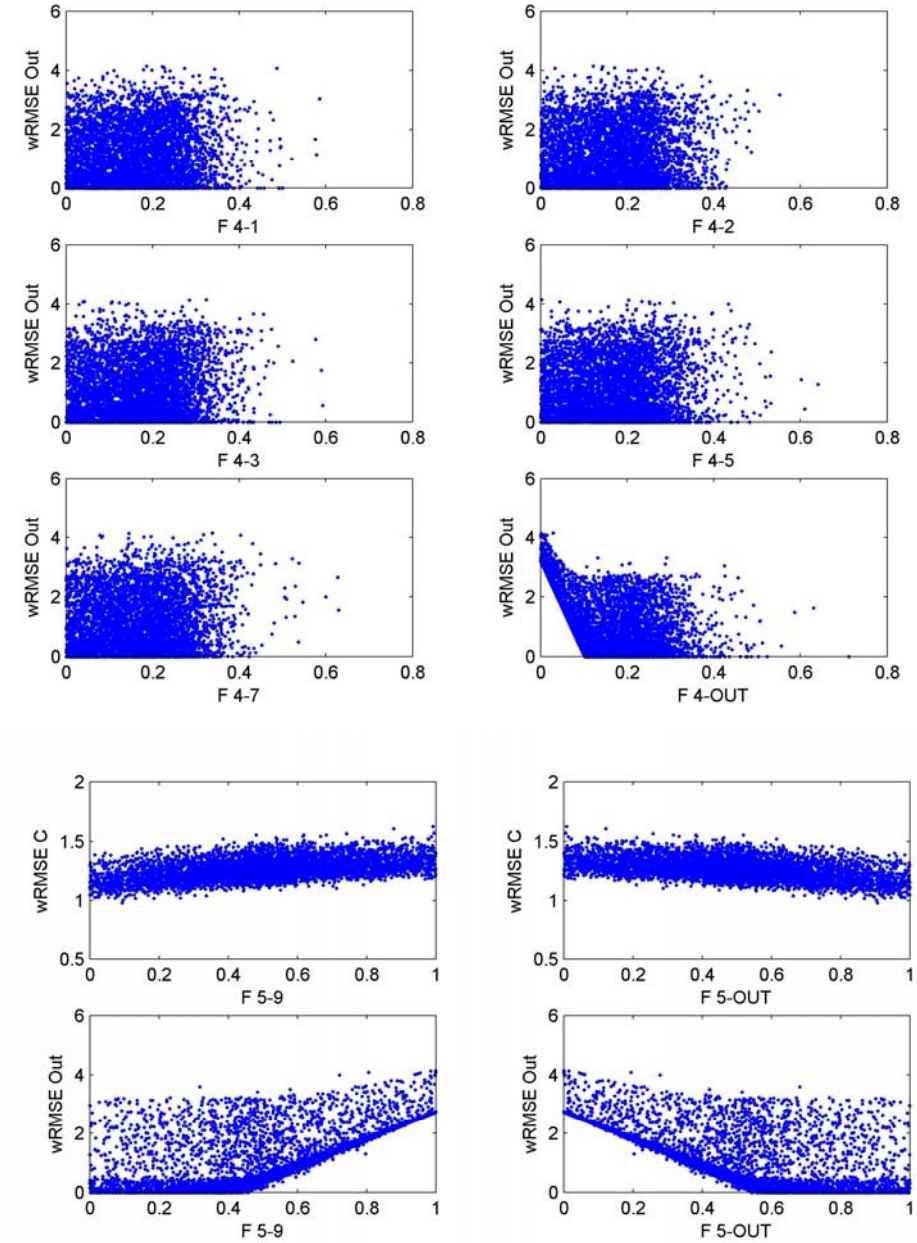

Attachment
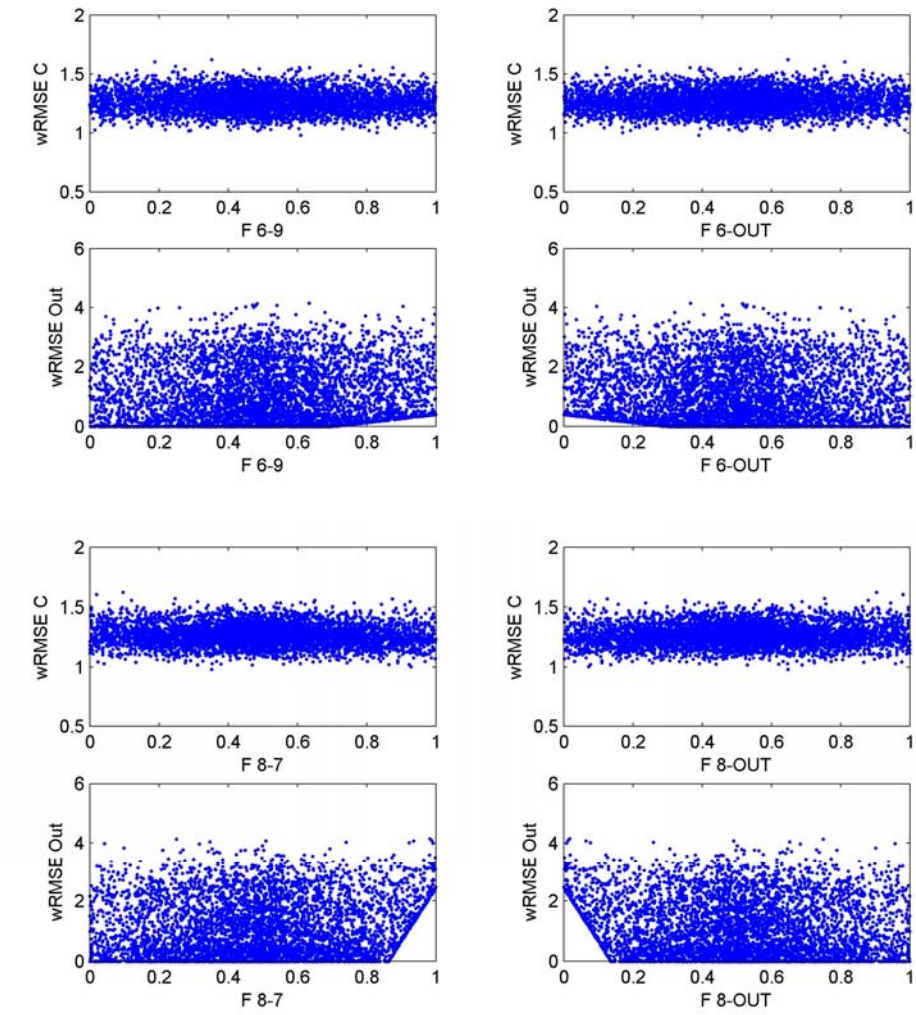
Plots showing parameter and objective values for URS optimization